Assessment of Inelastic Performance of Flat Plate and Wide Beam Frames

by

Wamea Raisa Khan

MASTER OF ENGINEERING IN CIVIL AND STRUCTURAL ENGINEERING

Department of Civil Engineering

BANGLADESH UNIVERSITY OF ENGINEERING AND TECHNOLOGY

March, 2018

Assessment of Inelastic Performance of Flat Plate and Wide Beam Frames

by

Wamea Raisa Khan

Submitted to the Department of Civil Engineering,
Bangladesh University of Engineering and Technology (BUET), Dhaka
in partial fulfilment of the requirements for the degree
of

MASTER OF ENGINEERING IN CIVIL AND STRUCTURAL ENGINEERING

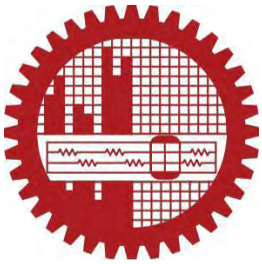

Department of Civil Engineering

BANGLADESH UNIVERSITY OF ENGINEERING AND TECHNOLOGY

March, 2018

This project titled "**ASSESSMENT OF INELASTIC PERFORMANCE OF FLAT PLATE AND WIDE BEAM FRAMES**", submitted by Wamea Raisa Khan, Roll No. 0412042306P, Session: April 2012, has been accepted as satisfactory in partial fulfillment of the requirement for the degree of **Master of Engineering in Civil and Structural Engineering** on 25 March, 2018.

BOARD OF EXAMINERS

Dr. Raquib Ahsan — **Chairman**
Professor
(Supervisor)
Department of Civil Engineering, BUET

25.3.18

Dr. Ahsanul Kabir — **Member**
Professor and Head
Department of Civil Engineering, BUET

Dr. Tahsin Reza Hossain — **Member**
Professor
Department of Civil Engineering, BUET

Dr. Mohammad Al Amin Siddique — **Member**
Associate Professor
Department of Civil Engineering, BUET

DEDICATION

This Thesis is Dedicated to My Parents

DECLARATION

It is hereby declared that, except where specific references are made, the work embodied in this project is the result of investigation carried out by the author under the supervision of Dr. Raquib Ahsan, Professor, Department of Civil Engineering, BUET.

Neither the thesis nor a part of it is concurrently submitted elsewhere for the award of any degree or diploma.

_____

(Wamea Raisa Khan)

ACKNOWLEDGEMENTS

First of all the author would like to give thanks to almighty Allah who is very kind to allow completing this research work effectively.

The author expresses her profound gratitude and heartiest thanks to her project supervisor Professor Dr. Raquib Ahsan, Department of Civil Engineering, Bangladesh University of Engineering and Technology (BUET) for his constant guidance, supervision, keen interest as well as resource management in making this project success. His helpful guidance has benefited the author greatly.

The author is grateful to the members of project defence committee Professor Dr. Ahsanul Kabir, Professor Dr. Tahsin Reza Hossain and Associate Professor Dr. Mohammad Al Amin Siddique for their advice and help in reviewing this study.

The author wants to express her appreciation to Dr. Iftekhar Anam, Professor, Department of Civil Engineering, UAP, for his continuous guidance. Without his support, it would be difficult to complete the research work.

The author is appreciative to Engineering & Research Associates Limited (ERA) for their cooperation, assistance and technical supports.

The author is very thankful to her family members and friends for their unconditional love, encouragement, blessings and co-operation.

ABSTRACT

Structural systems such as – flat plates and wide beam column frames are often preferred over conventional beam column framing systems because of architectural, functional and economic considerations. While comprehensive design guidelines are available for beam column systems, more rigorous analytical and experimental observations are required to develop comprehensive design guidelines for flat plates and wide beam column frames. As such the aim of this research is to study the nonlinear behavior of flat plates and wide beam column frames and compare their seismic performance as compared to that of beam column frames.

A 10-storied readymade garments factory building have been used in this study. Firstly linear static analysis have been performed following BNBC 1993 and three type of structures, i.e. beam column frames, flat plates and wide beam column frames have been designed. Nonlinear static analysis for maximum considered earthquake (MCE), design basis earthquake (DBE) and serviceability earthquake (SE), has been conducted for these three type of structures by using linear analysis data to understand the nonlinear behaviour for moderate seismic zone (zone 2) as per BNBC 1993. As nonlinear performances- maximum displacement, base shear capacity and hinge formation were determined according to ASCE 41 'Displacement Coefficient Method'. In nonlinear static analysis, parameters like story height, material strength have been varied for all types of structural systems for comparison of results.

While beam column frame systems perform much better than the other two systems in linear static analysis, flat plates have been found to possess much higher base shear capacity when nonlinear static analysis is employed. Wide beam column frames, though less costlier than flat plates, are structurally much less inferior compared to any other systems. As such flat plates structures should be preferred over wide beam column framing systems from architectural or functional point of view. The discrepancy in the results obtained from linear static and nonlinear static analysis calls for measuring nonlinear performance of sensitive structures.

TABLE OF CONTENTS

LIST OF FIGURES

LIST OF TABLES

CHAPTER 1
INTRODUCTION

1.1 General

Over the past few decades, intensive research in structural engineering greatly increased our knowledge of the behavior of reinforced concrete (RC) frame structures and its design. RC frame structures contain different structural elements; such as columns, beams, slabs, walls etc. By analyzing and understanding the behavior of these elements, the design principles of frame structures have been developed gradually. Over the years new analysis and design procedures have been incorporated into design codes (ASCE, ACI, FEMA, and EUROCODE etc.). At the same time advancements in computing technology have enabled structural engineers to analyze and design structures faster and more efficiently according to the new design codes. The analysis procedures are typically of two types: linear and nonlinear. Currently, there are numerous easy-to-use software programs which can perform such analyses and designs reasonably well.

Numerous researches have been conducted related to frame structures with column-beam, frame structures with flat plate, frame structures with wide beams. Each structural system behaves differently compared to the others. Depending on the purpose of use each system can have multiple advantages. In this thesis three types of models are formed and their behavior, performance and different design parameters have been assessed.

1.2 Background of the Study

Numerous papers, thesis and publications have been produced in Europe, Australia, Canada and USA related to wide beam column frame structures' seismic behavior, buckling, column joints etc. A significant number of short to mid height RC buildings with wide beams have been constructed in areas of moderate seismicity in Spain and Italy. Wide beam structural system is also common in other countries such as France, Australia, Canada and USA. The performance of wide beam structures subjected to seismic loads is not well understood since only limited experimental results are available currently, compared with those of conventional frame structures. Hence, the use of wide beam systems in seismically active regions is usually prohibited. Currently,

many codes of practice restrict the use of a wide beam-column system to resist lateral loads through limiting the maximum beam width b_w. These geometric restrictions are based on historic design practices mentioned in various codes.

Flat slab building structures possess major advantages over traditional slab-beam-column structures because of the free design of space, shorter construction time, and architectural, functional and economical aspects. On the other hand, flat plate structural system is significantly more flexible under lateral loads than traditional RC frame system and that make the system more vulnerable under seismic events. It seems necessary to study the advantages of wide beam frame structures over flat plate structures where practical use of wide beam structures are significantly increasing day by day even in Bangladesh.

1.3 Objectives of the Research

Principle objectives of the present study are:

a. To conduct pushover analysis of Flat plate structures and observe its seismic performance.
b. To conduct pushover analysis of Wide beam frame structures and observe its seismic performance.
c. To compare seismic behaviour of Wide beam frame structures and Flat plate structures.

1.4 Methodology

The methodology observed in conducting this research work can be summarized as follows:

a. Develop models of flat plate structures and wide beam frame structures by finite element methods using ETABS.
b. Input different earthquake parameter for both type of structures.
c. Perform non-linear static / pushover analysis.
d. Observe the formation of plastic hinges, their location and non-linear behavior and performance of the structure.
e. Compare structural performance of wide beam frame structures with flat plate structures.
f. Compare construction cost of wide beam frame structures with flat plate structures.

1.5 Scope of the Work

This paper shows the non-linear performance of three types of structure namely beam-column frames, wide-beam column frames and flat plate structures. Each type of structures has been investigated varying parameters such as story height (10 ft, 12ft and 15 ft) and concrete strength (3 ksi and 4 ksi). Another flat plate structure considering column sizes same as beam column frame has been incorporated in this study. All structures are considered as 10 storied. Different parameters like – base shear capacity, maximum top deflection, stiffness, plastic hinge formtion and construction cost have also presented with respect to flat plate structures and wide beam frame structures. Seismic performances of these structures analyzed here will aid researchers in carrying out the work further.

1.6 Organization of the Thesis

The thesis paper is organized in five chapters. Apart from chapter one, the following chapters are organized as follows:

Chapter 2: A literature review is presented in this chapter focusing on non-linear analysis of different structural systems with varying heights and material strengths following various codes and design guidelines.

Chapter 3: This chapter presents the numerical modeling of three types of structures. Basic design considerations for linear static analysis; modeling criteria, hinge properties and loading criteria for non-linear static / pushover analysis have been discussed in this chapter.

Chapter 4: This chapter presents the results of linear static analysis and non-linear analysis. The comparisons of results gained from the analyses of three types of structures varying parameters such as story height and material properties, are shown in this chapter.

Chapter 5: This chapter summarizes the research and lists out the conclusions based on the outcome of the numerical results and recommends scopes for further studies.

CHAPTER 2
LITERATURE REVIEW

2.1 Introduction

A summary of the literature pertaining to the various frame structures with nonlinear analysis methods for the identification and monitoring of performance of the structures based on changes in material properties, story height and specification of relevant codes is presented in this section.

2.2 Beam Column Frame Structures

Frame structures are the structures having the combination of beam, column and slab to resist the lateral and gravity loads. Beam column frame structures are most widely used structural system. Extensive investigations were carried out previously and nonlinear modeling parameters are well established for this structural system. To compare structural performance in lateral seismic force of flat plate structures and wide beam frame structures, beam column frame structures are utilized in this study.

2.3 Wide Beam Column Frame Structures

Wide beams will generally be those where the width of beam is greater than width of column. Beams that are very wide compared to the columns that they frame into are widely used in some regions of low seismicity. These types of beams are also termed as hidden beams. Wide beams are favored structural elements due to their many inherent features that characterize them; they save on floor height clearance; they also save on formwork, labor and material cost. Moreover, wide beams form an acceptable aesthetic appearance that does not hinder efficient interior space partitioning. Such beams have the added advantage of clearing the way for horizontal electromechanical ductwork.

Band beams may not be used in regions of high seismicity due to restrictions on beam width specified in various codes.

2.3.1 ACI 318 provisions for wide beam

There are some guidelines on wide beam properties and design in codes such as ACI 318 and Eurocode 2 where many of these guidelines are not directly proposed for these

beams. In fact, most of them refer to the special cases of beams or slabs, which are concert with wide beams. ACI 318-14 provisions for wide beam are given below:

I. Dimensional limits

Beams shall satisfy the conditions (a) Clear span ℓ_n shall be at least $4d$, (b) Width b_w shall be at least the lesser of $0.3h$ and 10 in, (c) Projection of the beam width beyond the width of the supporting column on each side shall not exceed the lesser of c_2 and $0.75c_1$.

Experimental evidence indicates that, under reversals of displacement into the nonlinear range, behavior of continuous members having length-to-depth ratios of less than 4 is significantly different from the behavior of relatively slender members. Design rules derived from experience with relatively slender members do not apply directly to members with length-to-depth ratios less than 4, especially with respect to shear strength. Geometric constraints indicated in (b) and (c) were derived from practice and research on reinforced concrete frames resisting earthquake-induced forces. The limits in (c) define the maximum beam width that can effectively transfer forces into the beam-column joint. An example of maximum effective beam width is shown in Figure 2.1.

II. Longitudinal beam reinforcement

Longitudinal beam reinforcement outside the column core shall be confined by transverse reinforcement passing through the column that satisfies spacing requirements of section 18.6.4.4, and requirements of sections 18.6.4.2, and 18.6.4.3 of ACI 318-14, if such confinement is not provided by a beam framing into the joint.

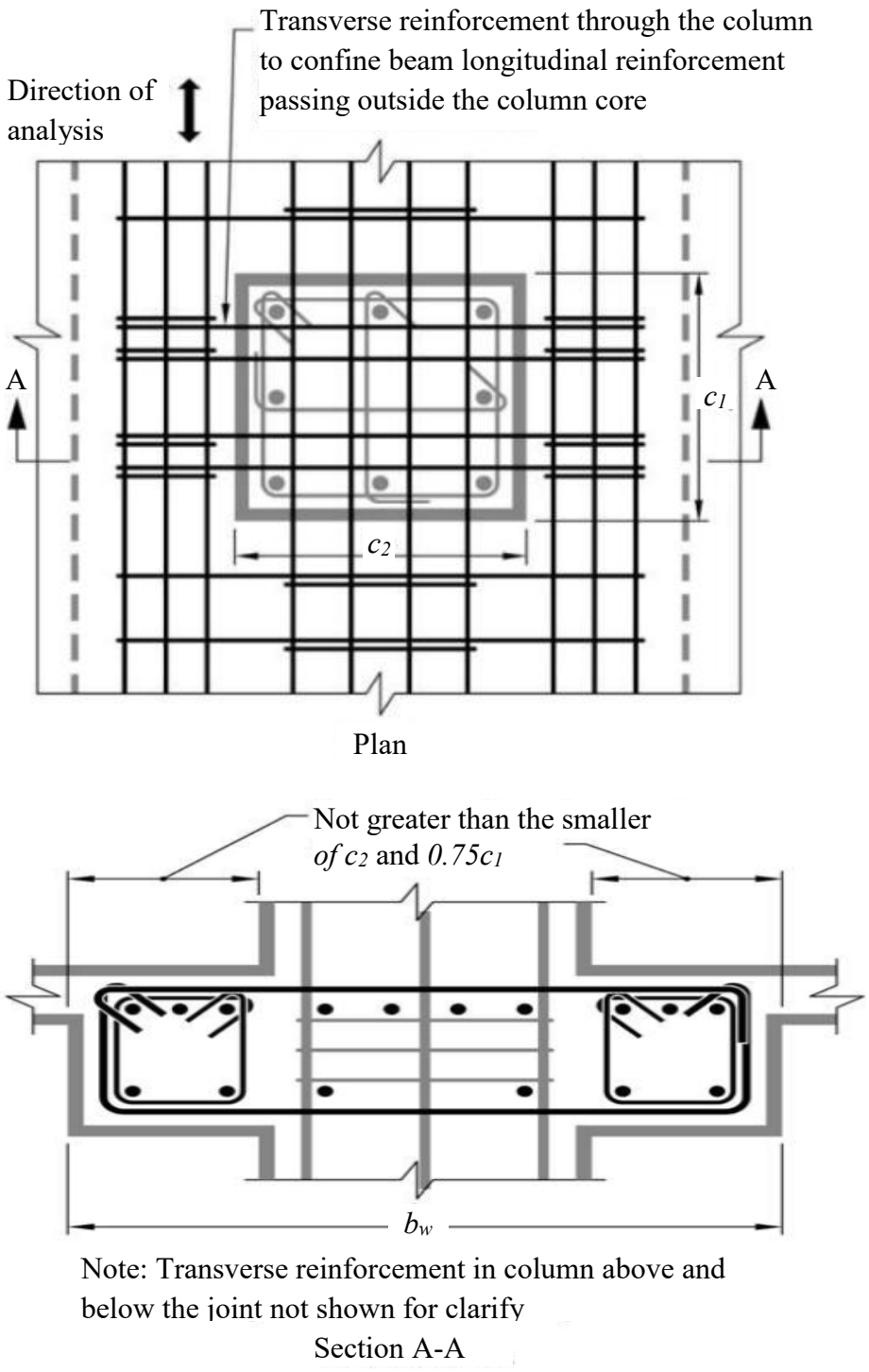

Figure 2.1: Maximum effective width of wide beam and required transverse reinforcement (Fig. R18.6.2: ACI 318-14)

III. Transverse reinforcement

The required transverse reinforcement, or transverse beam if present, is intended to confine the beam longitudinal reinforcement and improve force transfer to the beam-column joint. An example of transverse reinforcement through the column provided to

confine the beam reinforcement passing outside the column core is shown in Figure 2.1. Additional detailing guidance and design recommendations for both interior and exterior wide-beam connections with beam reinforcement passing outside the column core may be found in ACI 352R.

IV. Shear reinforcement

Shear reinforcement satisfying the conditions (a) Stirrups, ties, or hoops perpendicular to longitudinal axis of member, (b) Welded wire reinforcement with wires located perpendicular to longitudinal axis of member, (c) Spiral reinforcement. Inclined stirrups making an angle of at least 45 degrees with the longitudinal axis of the member and crossing the plane of the potential shear crack shall be permitted to be used as shear reinforcement.

V_s for shear reinforcement shall be calculated by $V_s = A_v F_{yt} d/s$ where **s** is the spiral pitch or the longitudinal spacing of the shear reinforcement. Research has shown that shear behavior of wide beams with substantial flexural reinforcement is improved if the transverse spacing of stirrup legs across the section is reduced.

2.3.2 Previous study on wide beam column frame structures

A number of researchers have investigated the performance of wide beam connections. There have been many studies on wide beam behavior. Some of the research works have been summarized in this section:

James et al. (1999) studied on reinforced concrete exterior wide beam-column-slab connections subjected to lateral earthquake loading. Experimental results from quasi-static cyclic lateral load tests of three reinforced concrete-exterior wide beam-column-slab sub-assemblages are presented. The effects of having a significant amount of wide beam flexural steel anchored outside the column core for beams more than three times as wide as columns are investigated, particularly in terms of plastic hinge development and spandrel beam torsion requirements. Slab participation in wide beam-column-slab connections is also examined.

James et al. (2001) studied on reinforced concrete wide-beam construction resisting lateral earthquake loads. Experiments and analysis were conducted to address concerns

about performance of reinforced concrete connections with shallow, wide beams subjected to lateral earthquake loading and to compare behavior of wide beam connections to that of conventional connections. Two wide beam-column-slab connections and one conventional beam-column-slab connection were subjected to cycles of reversing lateral displacements up to 5% drift. Experimentally determined wide beam connection stiffness was closer to the conventional beam connection stiffness than had been predicted. Refined models were developed, with features such as rigid end offsets for wide beam connections, to better represent observed behavior. Nonlinear models were also developed that accurately captured differences in energy dissipation as well as stiffness.

Li et al. (2010) studied on seismic behavior of reinforced concrete exterior wide beam-column joints. An experimental and numerical investigation carried out on RC wide beam-column joints when subjected to seismic loads is reported within this paper. The experimental study was conducted by subjecting three full-scale wide exterior beam-column specimens to simulated seismic loads at the Nanyang Technological University of Singapore. Seismic performance analysis of the joints were based on the results obtained from the experiment in terms of their general behavior, hysteresis response, and the strain profiles of the longitudinal reinforcement within the specimens. These experimental results were then used to validate a three-dimensional (3D) nonlinear finite-element (FE) model. The behavior of the joints under the influence of critical influencing factors like column axial load, transverse beam, and beam bar anchorage ratio were also analyzed through the parametric studies carried out.

Shuraim (2012) studied on transverse stirrup configurations in RC wide shallow beams supported on narrow columns. This paper addressed the influence of stirrup configurations in wide beams on the effectiveness of stirrups in contributing to shear resistance as a ratio of the nominal shear stirrup strength. The 16 beams were composed of: three beams without stirrups, six beams having a constant amount of stirrups with either two-leg or four-leg configuration, and seven other beams with various configurations to verify the trend. On the basis of findings of this study, guidelines for computing the stirrup contribution in shear resistance were proposed and verified by comparisons with tested beams from the present study and a previous study by Serna-Roes et al.

James (2012) studied on behavior & design of reinforced concrete beam-column connections with wide beams. The American Concrete Institute (ACI) recommendations for design of beam-column joints in monolithic reinforced concrete structures (ACI 352R-91) currently recommends that wide beam construction not be used in structures to in elastically dissipate energy from earthquake ground motions, because of concerns about wide beam flexural reinforcement anchored in transverse beams, as well as concerns about the stiffness and energy dissipation of wide beam frames. In the last ten years, much research has been conducted on wide beam construction, and as a result, changes are being introduced for the treatment of wide beam construction in the new revised ACI 352 recommendations. This paper summarizes the research results to date and presents the revised ACI 352 recommendations.

Lubell et al. (2008) studied on one-way shear in wide concrete beams with narrow supports. Wide reinforced concrete beams are frequently used as primary structural members in buildings or bridges, to support floor loads and to transfer forces from discontinuous walls or columns above. In these roles, these critical members may in turn be supported on walls extending across the full width of the beam, or on narrower columns. An experimental program on 8 large-scale shear-critical reinforced concrete beams is presented. The results show that the one-way shear strength was moderately reduced as the support width to beam width ratio decreased. This influence occurred for members without shear reinforcement and for members with a moderate shear reinforcement ratio. A capacity reduction function was developed to account for this influence on one-way shear strength, and its application demonstrated with a design example.

Helou et al. (2014) studied on performance based analysis of hidden beams in reinforced concrete structures. In the following study the structural influence of hidden beams within slabs is investigated. With the primary focus on a performance based analysis of such elements within a structure. This is investigated with due attention to shear wall contribution to the overall behavior of such structures. Conversely, shallow beams seem to render the overall seismic capacity of the structure unreliable. Since such an argument is rarely manifested within the linear analysis domain; a pushover analysis exercise is

thus mandatory for behavior prediction under strong seismic events. In such events drop beams have the edge.

Taqieddin (2014) studied on Deflection of wide hidden beams in one-way slab systems by nonlinear finite element study. The effectiveness of compression reinforcement in controlling the deflection of a wide-hidden continuous reinforced concrete beam is studied using nonlinear finite element (FE) simulations. Concrete damaged-plasticity and reinforcing steel elasto-plasticity are used in the nonlinear FE simulations of ABAQUS. Results are compared to Elastic FE simulations as well as to conventional code procedures.

Donmez (2015) studied on seismic performance of wide-beam infill-joist block RC frames in Turkey. The purpose of this study is to review the history and current practice of infill-joist frames in Turkey and to conduct a performance evaluation of infill-joist frames designed per the current earthquake code (2007). Regulations for this building subtype (wide-beam, infill-joist block reinforced-concrete frames) are critically reviewed, and the designer's response to code regulations is discussed. Results indicate that the force-based design approach used in the current code is not always adequate to satisfy the displacement demands. In addition, it is observed that layout, proportioning, and detailing requirements of beam-end regions and beam-column connections do not always warrant ductile behavior as targeted.

Zaidee et al. (2017) studied on validation of finite element modeling for wide & shallow reinforced concrete beams. This paper aims to validate ABAQUS finite element model for analysis of wide and shallow reinforced concrete beams. The validation has been achieved through comparison of load deflection curves of the finite element model with those obtained from experimental works of another researcher. After reviewing of related literature and the experimental work, the finite element model has been prepared in a step-by-step approach. Comparison between load-deflection curves obtained from finite element model with those of experimental works indicates good agreement such that the proposed model can be adopted in future for further studies.

2.4 Flat Plate Structures

Reinforced concrete flat plate is a type of structural system containing slabs with uniform thickness supported directly on columns without using beams. Flat plates are commonly used in buildings where relatively low gravity loads are applied. A major concern for flat plates is punching failure of slab in the vicinity columns due to high stress concentration. Flat Plate system has an advantage of introducing an edge beam at the periphery of the panel to reduce the deflection of the exterior panel of the plate. The main disadvantage in Flat plates is their lack of resistance to lateral loads, hence special features like shear walls, structural Walls are to be provided if they are to be used in high rise constructions.

The slab beam columns system behaves integrally as a three dimensional system, with the involvement of all the floors of the building, to resist not only gravity loads, but also lateral loads. However a rigorous three dimensional analysis of the structure is complex. Unlike the planer frames, in which beam moments are transferred directly to columns, slab moments are transferred indirectly, due to flexibility of the slab. Also slab moments from gravity can leak from loaded to unloaded spans; this must be accounted for, in the analysis.

2.4.1 Previous study on flat plate structures

Early 1854, early Patents were issued for RC Slabs based on the concept of the concrete forming an arch with reinforcement acting as the tie, and In 1867, based on the reinforcement acting as a catenary with the concrete used as a filler.

In 1903, the first patent for a recognizable RC Slab was given to Turner. He described a “mush-room” slab supported directly by columns with flared tops and reinforced both parallel to the column lines and along the diagonals. By 1913 over 1000 “flat” slabs had been built. Each builder had to develop his own design procedures and then verify the design by conducting a performance load test or by posting a performance bond.

In 1910, by requiring six design methods, McMillan compared the quantity of reinforcement for a 20ftX20ft interior panel carrying 200 psf live load, and found that they varied by a factor of 4.

Nichols (1914) established a simple criterion for the minimum total moment that must exist across the critical sections of a panel to satisfy equilibrium. His paper was not well received because he indicated total moments considerably greater than those used many of the “successful” slab designers.

All other designer turned to classical plate theory. In 1811, Lagrange formulated the governing differential equation for elastic plate bending. This is called *classical plate theory.* Solutions of this equation for rectangular panels bounded by combinations of simply supported and fixed edges had been developed. However, because these solutions were based on non-deflecting panel boundaries, the slab bending moments obtained are valid only when stiff beams are present on all four sides of each panel.

In 1921, the first slab “code provisions” appeared and were two parts. The first part was placed in the body of the code and presented design coefficients for the slab obtained from solutions based on classical theory and were applicable only for “two-way” slabs with stiff beams between all columns. The second part was placed in an appendix to the code and covered “flat” slabs. It was long recognized that neither procedure was satisfactory.

In the late 1950s, University of Illinois primarily resolves the problem by initiated comprehensive study. As a result Direct Design Method (DDM) and Equivalent Frame Method (EFM) were developed. These procedures were incorporated in the code.

Pan and Moehle (1992) investigated the ductility, drift capacity, and seismic performance of FSC connections with different gravity shear ratios ($V_u / \phi V_c$). Based on this study, the model proposed by banchik is good enough to model structure two dimensionally. However, this model cannot give a comprehensive understanding of behavior of structure. By using nonlinear procedure in three-dimension analysis, inelastic behavior of structure can be examined. In order to simplify the analysis, including in nonlinear procedure, the grid model is proposed. In grid model, the slab is replaced by arrangement of equivalent beam with certain width.

Extensive research has been carried out to find out the behavior of slab-column connection. The failure mode depends upon the type and extent of loading. Punching

shear strength of slab-column connection is of importance which very much depends on the gravity shear ratio. The mechanism of transfer of moments from slab to column is very complex when subjected to lateral loading and unbalance moments. These unbalanced moments produce additional shear and torsion at the connections and then get transferred into the column which results in excessive cracking of slab leading to further reduction in the stiffness of the slab.

Erberik et al. (2004) studied on seismic vulnerability of flat-slab structures. The vulnerability study generally focuses on the generic types of construction due to the enormous size of the problem. Hence simplified structural models with random properties to account for the uncertainties in the structural parameters are employed for all representative building types. The study has three main objectives. The first objective is to investigate the fragility of flat-slab reinforced concrete systems. Developing the fragility information of flat-slab construction will be a novel achievement since the issue has not been the concern of any research in the literature. The second objective is to assess HAZUS as an open-source, nationally accepted earthquake loss estimation software environment. It is important to understand the potentials and the limitations of the methodology, the relationship between the hazard, damage and the loss modules, and the plausibility of the results before using it for the purposes of hazard mitigation, preparedness or recovery. The last objective is to implement the fragility information obtained for the flat-slab structural system into HAZUS. The methodology involves many built-in specific building types, but does not include flat-slab structures. Hence it will be extra achievement to develop HAZUS compatible fragility curves to be used within the methodology.

Kim et al. (2008) studied on seismic performance evaluation of non-seismic designed flat-plate structures. In this study the seismic performance of flat plate system structures designed without considering seismic load was investigated. Both the capacity spectrum method provided in ATC-40 in 1996 and nonlinear dynamic analyses were carried out to obtain maximum inter story drifts for earthquake loads. Also, a seismic performance evaluation procedure presented in FEMA-355F in 2000 was applied to evaluate the seismic safety of the model structures. The analysis results showed that the maximum inter story drifts of the non-seismic designed flat-plate structures computed by the capacity spectrum method and the nonlinear dynamic analysis were smaller than the limit

state for the collapse prevention performance level. However, the results of the FEMA procedure showed that the model structures did not have enough strength to ensure seismic safety.

Wang et al. (2008) studied on Finite-element analysis of reinforced concrete flat plate structures by layered shell element. A finite-element model for nonlinear analysis of reinforced concrete flat plate structures is presented. A flexible layering scheme incorporating the transverse shear deformation is formulated in shell element environment. Each node of the layered shell element can be specified as either a normal node or a node with shear correction. A three-dimensional hypo-elastic material model is implemented to model reinforced concrete. The cracking effects of tension softening, aggregate interlock, tension stiffening, and compression softening in multidirectional cracked reinforced concrete are incorporated explicitly and efficiently. A flat plate, a flat slab with drop panel, and a large size flat plate with irregular column layout have been analyzed. The influence of the distribution of transverse shear strain on the punching shear failure mode has been identified in the numerical studies. The proposed finite-element model has been proved to be capable of simulating the localized punching shear behavior of slab–column connections and to be suitable for global analysis of structural performance of flat plate structures.

Kang et al. (2009) studied on nonlinear modeling of flat-plate systems. Analytical and experimental studies were undertaken to assess and improve modeling techniques for capturing the nonlinear behavior of flat-plate systems using results from shake table tests of two, approximately one-third scale, two-story reinforced concrete and posttensioned concrete slab–column frames. The modeling approach selected accounts for slab flexural yielding, slab flexural yielding due to unbalanced moment transfer, and loss of slab-to-column moment transfer capacity due to punching shear failure. For punching shear failure, a limit state model based on gravity shear ratio and lateral inter story drift was implemented into a computational platform (Open Sees). Comparisons of measured and predicted responses indicate that the proposed model was capable of reproducing the experimental results well for an isolated connection test, as well as the two shake table test specimens.

Harras et al. (2015) studied on a numerical model of flat-plate to column connection behavior. In this paper, a simple procedure is described for predicting the nonlinear moment-rotation behavior of flat-plate-to-column connections. That behavior is expressed by standardized moment-rotation functions. These functions were derived using a modified Rambert-Osgood function and all available experimental data. The influence of the most significant connection parameters such as the steel ratio, concrete strength, gravity loading, etc., on the connection behavior is incorporated into the functions. The computer analysis program is also described and an example is considered to compare results obtained from the program with those published in the literature.

Ying et al. (2009) studied on nonlinear modeling of slab-column connections under cyclic loading. Based on a beam analogy concept, a two-dimensional (2D) nonlinear model for interior slab-column connections was developed for use in pushover analyses of flat-plate structures. The slab lateral resistance from flexure and shear acting on the connection was modeled by an equivalent beam element and the resistance from torsion by a rotational spring element. The parameters defining connection lateral stiffness were calibrated from the tests presented in this study and were validated using experimental data reported in other studies.

Erberik et al. (2004) studied on vulnerability analysis of flat slab structures. Flat-slab RC buildings exhibit several advantages over conventional moment-resisting frames. However the structural effectiveness of flat-slab construction is hindered by its alleged inferior performance under earthquake loading. This is a possible reason for the observation that no fragility analysis has been undertaken for this widely-used structural system. This study focuses on the derivation of fragility curves using medium-rise flat-slab buildings with masonry infill walls. The developed curves were compared with those in the literature, derived for moment-resisting RC frames. The study concluded that earthquake losses for flat-slab structures are in the same range as for moment-resisting frames for low limit states, and considerably different at high damage levels. Observed differences are justifiable on the grounds of structural response characteristics of the two structural forms.

Song et al. (2012) studied on seismic performance of flat plate system with shear reinforcements. In this study, the results of experimental study about three isolated

interior flat slab-column connections were applied to input data of slab-column connections for non-linear pushover analysis to investigate the system level seismic capacity for 45 shear-reinforced flat plate systems. And the over strength factor and a response modification factor are used as major parameters to define the seismic capacity of the system, both of which are design factors of the seismic resistance system in the IBC 2012(ICC, 2012) as an index. Analysis results showed that the flat plate system reinforced with shear band showed the efficiency of an RC intermediate moment resistance frame except for the 5-story case. Also in this study, the effective response modification factor was evaluated for flat plate structures without walls. Through a comparative analysis of the results, we defined the seismic force-resisting system applicable to flat plate systems.

2.4.2 Provisions of flat plate as per various design codes

A flat slab is a highly indeterminate structure and its exact analysis is difficult. An approximate analysis can be made by considering an interior panel of slab. BNBC 2015 provides an empirical approach Direct Design Method and Equivalent Frame Analysis for the analysis of flat slab. Via Direct Design Method this it's easy to calculate bending moment and shear force in flat slab without use of computer. But the Equivalent Frame Analysis gives more exact results.

Table 2.1: Methods of analysis of flat plate structure followed by different codes

Methods	BNBC 2015	BNBC 1993	ACI 318 14	Eurocode	Canadian Standards	Indian Standards
Direct Design Method (DDM)	√	√	√	√	√	√
Equivalent Frame Method (EFM)	√	√	√			√
ACI Coefficient Method		√				
Limit State Method				√		

2.5 Nonlinear Static Analysis (NLSA) Procedure

In 1970, the nonlinear static analysis (pushover analysis) came in to practice, but the potential use of the pushover analysis has been recognized for last 10-15 years. Time

history analysis (THA) is another method of nonlinear analysis. This method (THA) of analysis is more accurate although to evaluate seismic demand. The application of NLSA procedure is generally considered to be more appropriate for seismic design due to its simplicity and ease to use. This method of analysis (THA) is based on assumption that the response of the multi-degree of freedom (MDOF) structure can be related to the response of an equivalent single degree of freedom (SDOF). For this reason, the NLSA procedure is known as the most useful tool in the engineering practice for evaluation and assessment of seismic behavior of structures Some guidelines and standards such as ATC-40, FEMA-356, and FEMA-440 and standards such as ASCE 41-13 currently has provided.

Nonlinear static analysis is executed by applying the gravity loads as well as lateral load. Lateral load is gradually increased along a direction under consideration. The inspected building is pushed according to predefined lateral load pattern. A plot of the total base shear versus top displacement in a structure is obtained by this analysis. The plot would indicate any premature failure or weakness. The analysis is carried out up to failure, thus it enables determination of collapse load and ductility capacity. On a building frame, plastic rotation is monitored. A lateral inelastic force versus displacement response for the complete structure is analytically computed. This type of analysis enables weakness in the structure to be identified.

2.5.1 Capacity spectrum method

In 1996, ATC 40 is published by Sigmud Freeman and by Applied Technology Council afterwards. Performance based analysis by capacity spectrum method is improved in ATC 40. Here, it is stated that horizontal displacement demands and load carrying capacities are related each other. In 2005, FEMA 440 published this enhanced method. Determination of performance point in ATC-40 and FEMA 440 is discussed below.

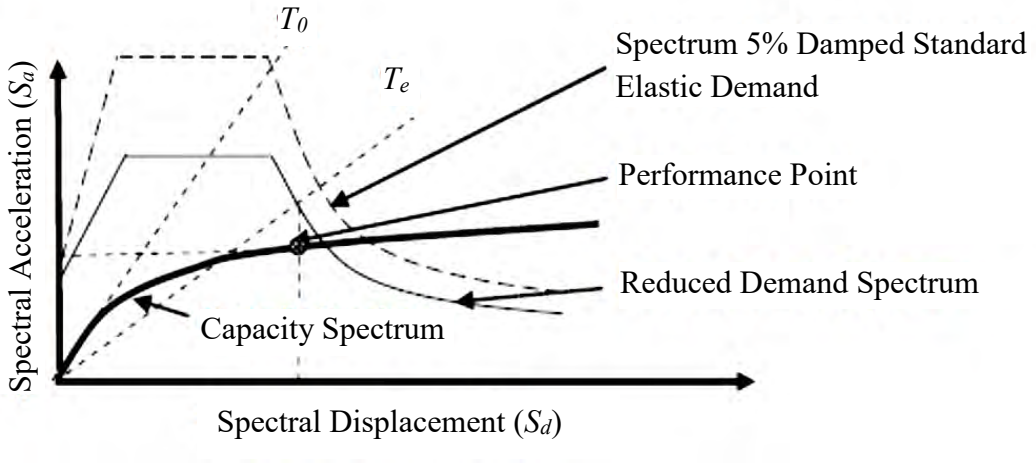

Figure 2.2: Determination of performance point according to capacity spectrum method.

Determination of performance point as per capacity spectrum curve by ATC 40

- Any point V_i, δ_i on the multiple degree of freedom capacity curve is converted to corresponding point S_{ai}, S_{di} on the equilibrium single degree of freedom capacity spectrum using the modal mass coefficient and participation factors equations.
- A point on capacity spectrum curve is estimated as performance point and spectrum curve is idealized with two linear lines.
- Equivalent viscous damping is obtained as, $\beta_0 = 63.7(a_y d_{pi} - d_y a_{pi})/(a_{pi} d_{pi})$
  Existing structures which don't have enough ductility, cannot make perfect hysteresis loops all the time. Effective viscous damping can be calculated by using damping modification factor is defined by, $\beta_{eff} = \kappa\beta_0 + 5$
- Spectral reduction factors are given by

$$SR_A = \{3.21 - 0.68\ ln(\beta_{eff})\}/2.12$$

$$SR_V = \{2.31 - 0.41\ ln(\beta_{eff})\}/1.65$$

- When the displacement at the intersection of the demand spectrum and the capacity spectrum, d_i, is within 5 percent ($0.95d_{pi} \leq d_i \leq 1.05d_{pi}$) of the displacement of the trial performance point, a_{pi}, d_{pi}, d_{pi} becomes the performance point. If the intersection of the demand spectrum and the capacity spectrum is not within the acceptable tolerance, then a new a_{pi}, d_{pi} point is selected and the process is repeated.

Determination of performance point as per capacity spectrum curve by FEMA 440

- Any point V_i, δ_t on the multiple degree of freedom capacity curve is converted to corresponding point S_{ai}, S_{di} on the equilibrium single degree of freedom capacity spectrum using the modal mass coefficient and participation factors equations.
- A point on capacity spectrum curve is estimated as performance point and spectrum curve is idealized with two linear lines.
- Values of post-elastic stiffness α and ductility μ is calculated as follows,

$$\alpha = \{(a_{pi}-a_y)/(d_{pi}-d_y)\}/(a_y/d_y) \text{ and } \mu = d_{pi}/d_y$$

- Corresponding effective damping, β_{eff} and corresponding effective period, T_{eff} are calculated according to the coefficients of FEMA 440.
- Spectral Reduction for Effective Damping is calculated

$$B = 4/\{5.6 - \ln(\beta_{eff})\%\};\ (S_a)\ \beta = (S_a)_{\%5}\ /B(\beta_{eff})$$

The use of the effective period and damping equations generate a maximum displacement *di* that coincides with the intersection of the radial effective period line and the ADRS demand for the effective damping. Max acceleration a_i is determined on the capacity curve corresponding to the maximum displacement, d_i. If it is within acceptable tolerance, the performance point corresponds to a_i and d_i. If it is not within acceptable tolerance, then a new a_{pi}, d_{pi} point is selected and the process is repeated.

2.5.2 Displacement coefficient method

In FEMA-356, Displacement Coefficient Method is defined base on capacity curve, which is obtained from pushover analysis. In this method, the biggest displacement demand is determined with specific coefficients. In 2005, FEMA 440 published this enhanced method. Target displacement is symbolized with δ_t. Determination of performance point in FEMA-356 and FEMA-440 is discussed below.

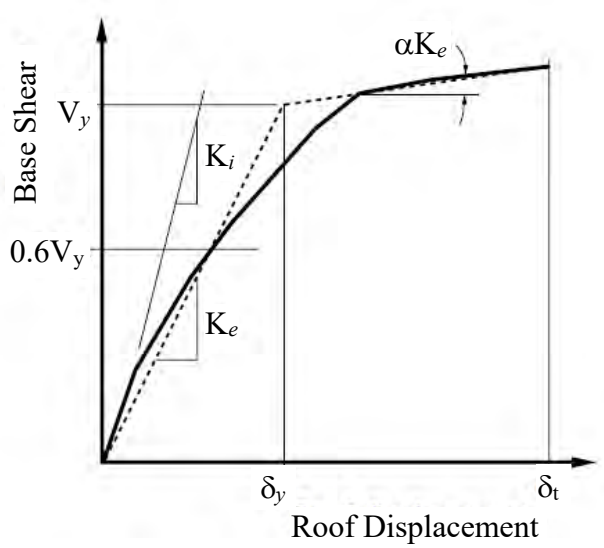

$T_e = T_i \sqrt{(K_i/K_e)}$
Where,
T_e = *Effective fundamental period*
T_i = *Elastic fundamental period*
K_i = *El astic lateral stiffness*
K_e = *Effective lateral stiffness*

Figure 2.3: Determination of performance point by displacement coefficient method

Determination of performance point as per displacement coefficient method by FEMA 356

- C_0 - The first modal participation factor at the level of the displacement control node;
  - The modal participation factor at the level of the control node calculated using a shape vector corresponding to the deflected shape of the structure at the target displacement.
  - It is explained according to framing system and story number at the table 3.2 of FEMA 356.

- C_1 - $C_1 = 1.0$ for $T_e \geq T_0$
  $C_1 = \{1 + (T_0 - 1)T_0/T_e\}/R_0$ for $T_e < T_0$

- C_2 - Values of C_2 for different framing systems and Structural Performance Levels shall be obtained from Table 3-3 of FEMA 356.

- C_3 - $C_3 = 1.0$ for $\alpha > 0$
  $= 1.0\ \{abs(\alpha)(R_0 - 1)^{3/2}\}/T_e$ for $\alpha \leq 0$

Determination of performance point as per displacement coefficient method by FEMA 440

- C_0 - The first modal participation factor at the level of the displacement control node;

- The modal participation factor at the level of the control node calculated using a shape vector corresponding to the deflected shape of the structure at the target displacement.
- It is explained according to framing system and story number at the table 3.2 of FEMA 356.

- C_1 - $C1 = 1 + (R - 1)/ (aT_e^2)$ *for* $T<0.2$ *sec*
  $C1 = 1.0$ for $T>1.0$ *sec*

- C_2 - $C2 = 1 + 1/800\{(R - 1)/T\}^2$ *for* $T<0.2$ *sec*
  $C2 = 1.0$ for $T > 0.7$ *sec*

- C_3 - C_3 coefficient is not taken into consideration

2.5.3 Nonlinear static procedures (NSP) adopted by ASCE 41-13

I. Lateral load pattern

There are three lateral load pattern proposed in FEMA-356 also adopted by ASCE 41-13, namely (a) inverted triangular distribution, (b) uniform distribution, (c) distribution of forces proportional to fundamental mode (mode 1). Ghaffarzadeh et al. studied response seismic demand of RC frames using NSP. The results show that push (a) pattern and push (c) pattern yielded similar results and reasonably accurate estimates of the maximum displacement. Although, slightly overestimate in the upper stories, while push (b) pattern overestimate demands at the lower stories. Moreover, the applicability lateral load pattern on evaluation of seismic deformation demands using NSP were investigated by Kunnath and Kalkan. It was found that in all cases, push (a) pattern provided closest results to the mean time history analysis, and other two load patterns tend to overestimate demands at the lower stories.

II. Structural performance level

The seismic performance of a building structure is measured by the stage of damage under a certain seismic hazard in which is quantified by roof displacement and deformation of the structural members. Figure 2.4 shows force-deformation relation for plastic hinge in pushover analysis. This guidelines and standards previously mentioned define force-deformation criteria for potential locations of plastic hinge. There are five points labelled A, B, C, D, and E are used to define the force-deformation behavior of the plastic hinge, and three points labelled IO (immediate occupancy), LS (life safety), and CP (collapse prevention) are used to define acceptance criteria for the hinge. There are six levels of structural performance in ASCE 41-13, i.e., Immediate occupancy (S-1), Damage control range (S-2), Life safety (S-3), Limited safety range (S-4), Collapse prevention (S-5), and Not considered (S-6). Two levels of seismic hazard are commonly defined for buildings, namely (a) design basic earthquake (DBE): an earthquake with a 10% probability in 50 years of being exceeded. This is an earthquake with a 500 years reoccurrence period, and (b) maximum considered earthquake (MCE): an earthquake with a 2% probability in 50 years of being exceeded. This is an earthquake with a 2500 years reoccurrence period.

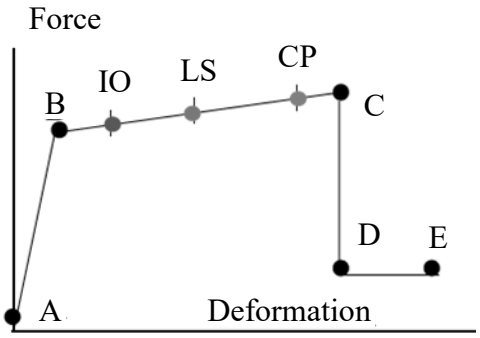

Figure 2.4: Force-deformation relation for plastic hinge

III. Procedures to determine target displacement

The displacement coefficient method documented in FEMA-440 and modified to consider effects of strength and stiffness degradation on seismic response in FEMA 440a and adopted in the ASCE-41-13 standard. This method is accomplished by modifying the elastic response of equivalent SDOF system with coefficient C_0, C_1 and C_2 is expressed as: $\delta_t = C_0 C_1 C_2 S_a (T_e^2/4\pi^2)\, g$ where S_a is response spectrum acceleration at the effective fundamental period and damping ratio of the building, g is acceleration due to gravity, T_e is the effective fundamental period computed from $T_e = T_i \sqrt{(K_i/K_e)}$ in which K_i and K_e are the elastic and effective stiffness of the building respectively in the direction under consideration obtained by idealizing the pushover curve as a bilinear relationship.

C_0 is modification factor to relate spectral displacement of an equivalent SDOF system to the roof displacement of the building MDOF system obtained from table 2.4.

C_1 is modification factor to relate expected maximum inelastic displacement to displacement calculated for linear elastic response computed from

$C_1 = \quad 1.0$	$T_e > 1.0$ sec
$1 + (R - 1)/(aT_e^2)$	0.2 sec $< Te \leq 1.0$ sec
$1 + 1/800\{(R - 1)/T_e\}2$	$T_e < 0.2$ sec

Table 2.2: Values of modification factor C_0 (Table 7-5: ASCE 41-13)

Number of stories	Shear buildings[a]		Other buildings
	Triangular load pattern	Uniform load pattern	Any load pattern
1	1.0	1.0	1.0
2	1.2	1.15	1.2
3	1.2	1.2	1.3
5	1.3	1.2	1.5
10+	1.3	1.2	1.5
Note: Linear interpolation shall be used to calculate intermediate values.			
[a] Buildings in which, for all stories, story drift decreases with increasing height.			

where a is equal to 130 for soil site class A and B, 90 for soil site class C, and 60 for soil site classes. D, E, and F, and R is the ratio of elastic and yield strengths is given as follows: $R = S_aC_m/(V_y/W)$ in which V_y is the yield strength estimated from pushover curve, W is the effective seismic weight, and C_m is the effective modal mass factor at the fundamental mode of the building.

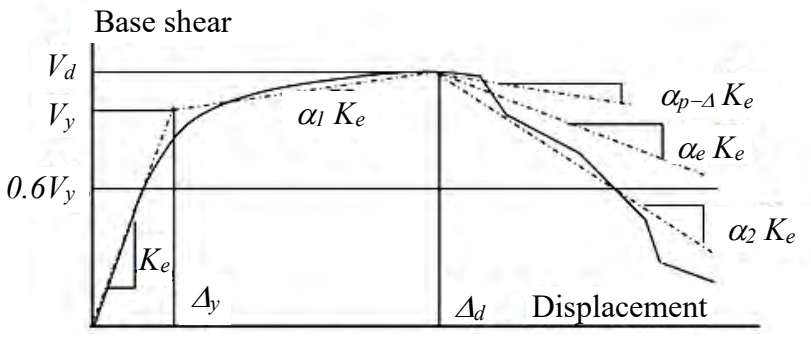

Figure 2.5: Idealized force-deformation curves (Figure 7-3: ASCE 41-13)

C_2 is modification factor to represent the effect of pinched hysteretic shape, stiffness degradation, and strength deterioration on maximum displacement response computed from

$C_2 = \quad 1.0 \qquad\qquad T_e > 0.7\ sec$

$1 + 1/800\{(R-1)/T_e\}^2 \qquad T_e \leq 0.7\ sec$

To avoid dynamic instability, ASCE 41-13 limit the R value as $R \leq R_{max} = \Delta_d/\Delta_y + abs(\alpha_e)^{-h}/4;\ h = 1.0 + 0.15\ ln(T_e)$ in which Δ_d is the deformation corresponding to peak strength, Δ_y is the yield deformation, and α_e is the effective negative post yield slope given by $\alpha_e = \alpha_{p\text{-}\Delta} + \lambda(\alpha_2 - \alpha_{p\text{-}\Delta})$ where α_2 is the negative post yield slope ratio and $\alpha_{p\text{-}\Delta}$ is the negative slope ratio caused by p-Δ effects defined in Figure 2.5, and λ is the near-field effect factor given as 0.8 for $S_1 \geq 0.6$ and 0.2 for $S_1 < 0.6$ [S_1 is defined as the 1 second spectral acceleration for the maximum considered earthquake].

2.6 Conclusion Drawn from the Literature Review

The two most recent, refined and reformed methods to conduct pushover analysis are Capacity Spectrum Method (FEMA 440EL) and Displacement Coefficient Method (ASCE 41-13). Both methods are employed to assess nonlinear performance of structures in this study.

CHAPTER 3
NUMERICAL MODELING

3.1 Introduction

This chapter presents numerical modeling of three types of building structures namely Beam column frame structures, flat plate structures and wide beam frame structures. A readymade garments (RMG) factory building situated at Narayanganj, Bangladesh have been used in this research. Firstly structural design of this building have been worked out using linear static analysis (LSA) as per BNBC 1993. Using LSA design data, non-linear static analysis (NLSA) have been performed for numerous configurations of the above mentioned three types of structural systems. Basic design consideration for LSA and modeling criteria, hinge properties and loading criteria for NLSA/pushover analysis have been discuss in this chapter.

3.2 Linear Static Analysis

In this Section basic design considerations (material properties, loading, boundary conditions etc.) and design outputs of linear static analysis have been discussed in this section.

3.2.1 Design considerations for linear static analysis

The Structural performance of above mentioned building has been analysis and design according to Bangladesh National Building Code (BNBC) 1993. Other Specifications, Codes, Standards have been utilized as required in structural design.

I. Structural geometry considerations

Firstly, three types of structural system adopted with same shape, size, story height and number of story of the above mentioned building. These three types of buildings have been considered as per design requirement and checked as per BNBC 1993 weather it is regular or irregular structure. Typical Column location and layout plan, beam location and layout plan and slab outline layout are shown in the following layouts accordingly (figure 3.1 – figure 3.3). Those are 10 (ten) storied buildings with story height of 10 ft and floor area per floor is (174ft×96ft)16704ft^2.

II. Material specifications

The grade of steel and concrete strength considered is as follows:

Table 3.1: Material specification

Material Properties	cylinder strength
Grade of concrete (For Footing, column & beam, slab and others)	3000 psi
Grade of Steel (all members)	60000 psi

III. Loading criteria

The above mentioned buildings have been analyzed for possible load actions such as Gravity Loads and Lateral Loads. Gravity Loads, such as dead and live loads applied at the floors or roofs of the building according to the provision of Chapter 2, Part 6 of BNBC 1993 are as follows:

Table 3.2: Dead and live loads

Dead Loads	
Self-Weight of Concrete	150 pcf
Self-Weight of Brick	120 pcf
FF (Floor finish) on floors	25 psf
FF (Floor finish) on Roof	40 psf
FF60 (Floor finish) on Stair	60 psf
RPW (Random Partition Wall) on floors	25 psf
Fixed Partition Wall (FPW) on floor beams	900 plf
Parapet Wall (PW) on roof beams	120 plf
Live Loads	
LL63 (Floor Live Load)	63 psf
LL42 (Roof Live Load)	42 psf
LL100 (Stair Case Live Load)	100 psf

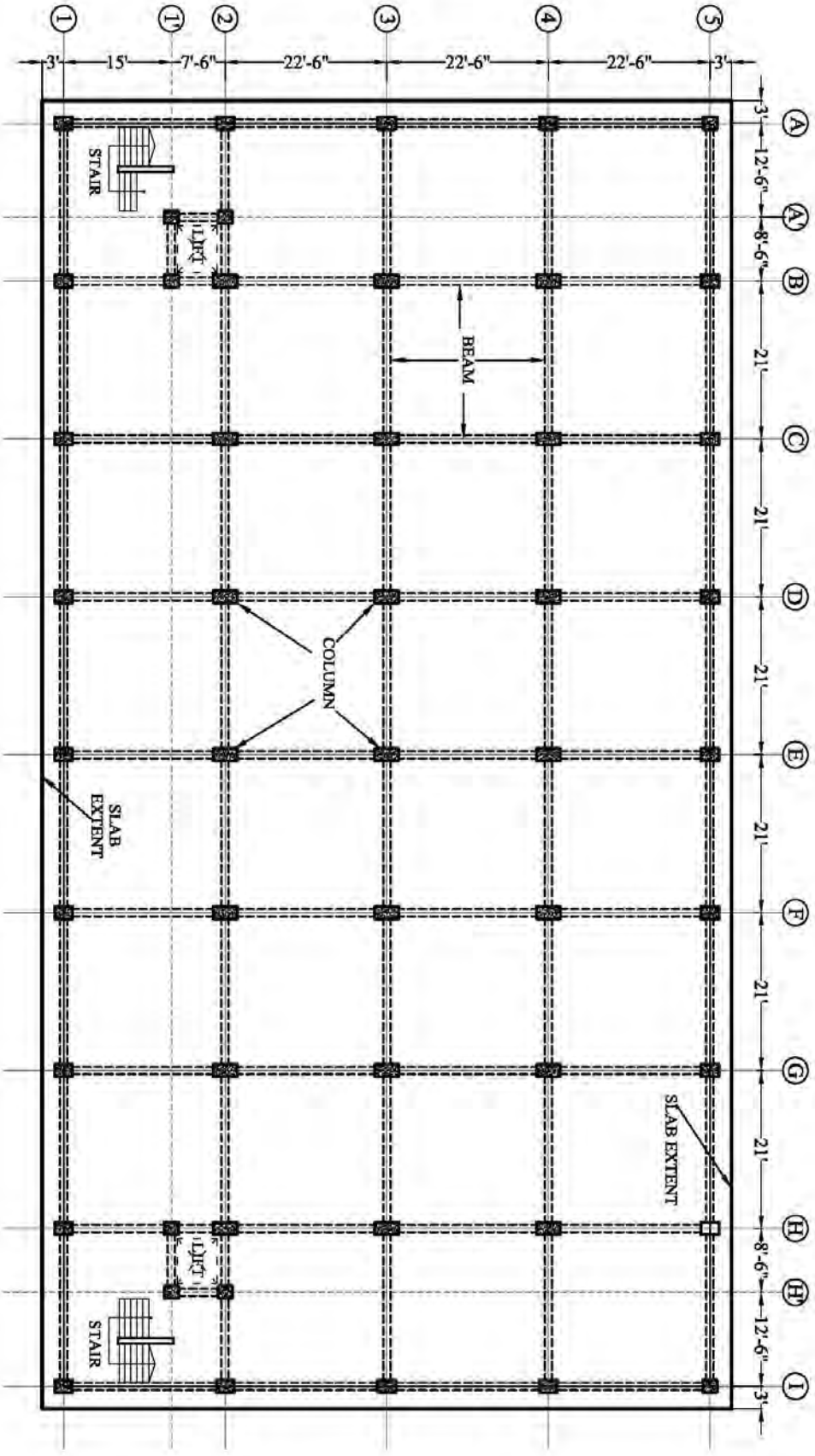

Figure 3.1: Typical floor layout of beam column frame structure

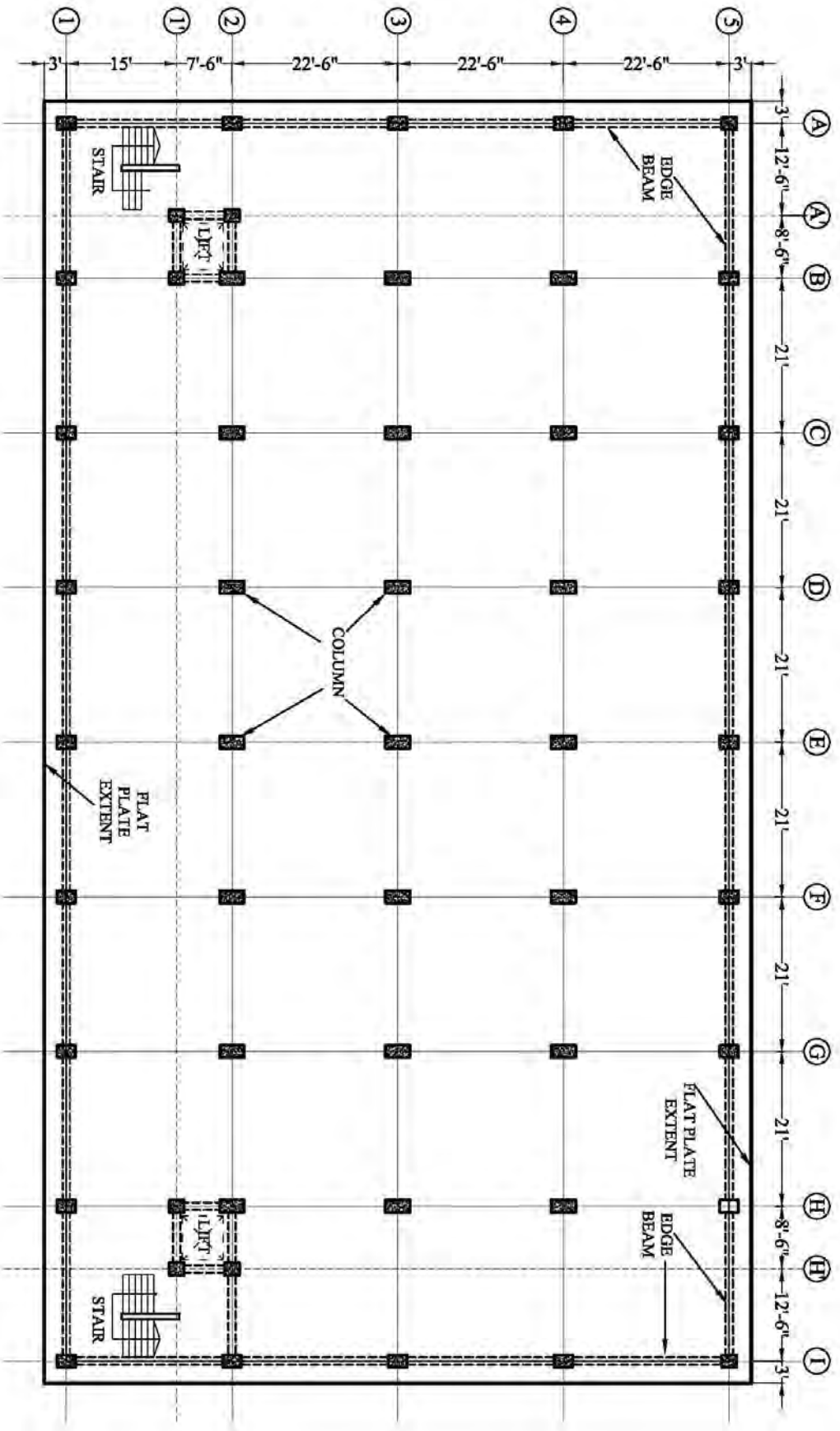

Figure 3.2: Typical floor layout of flat plate structure

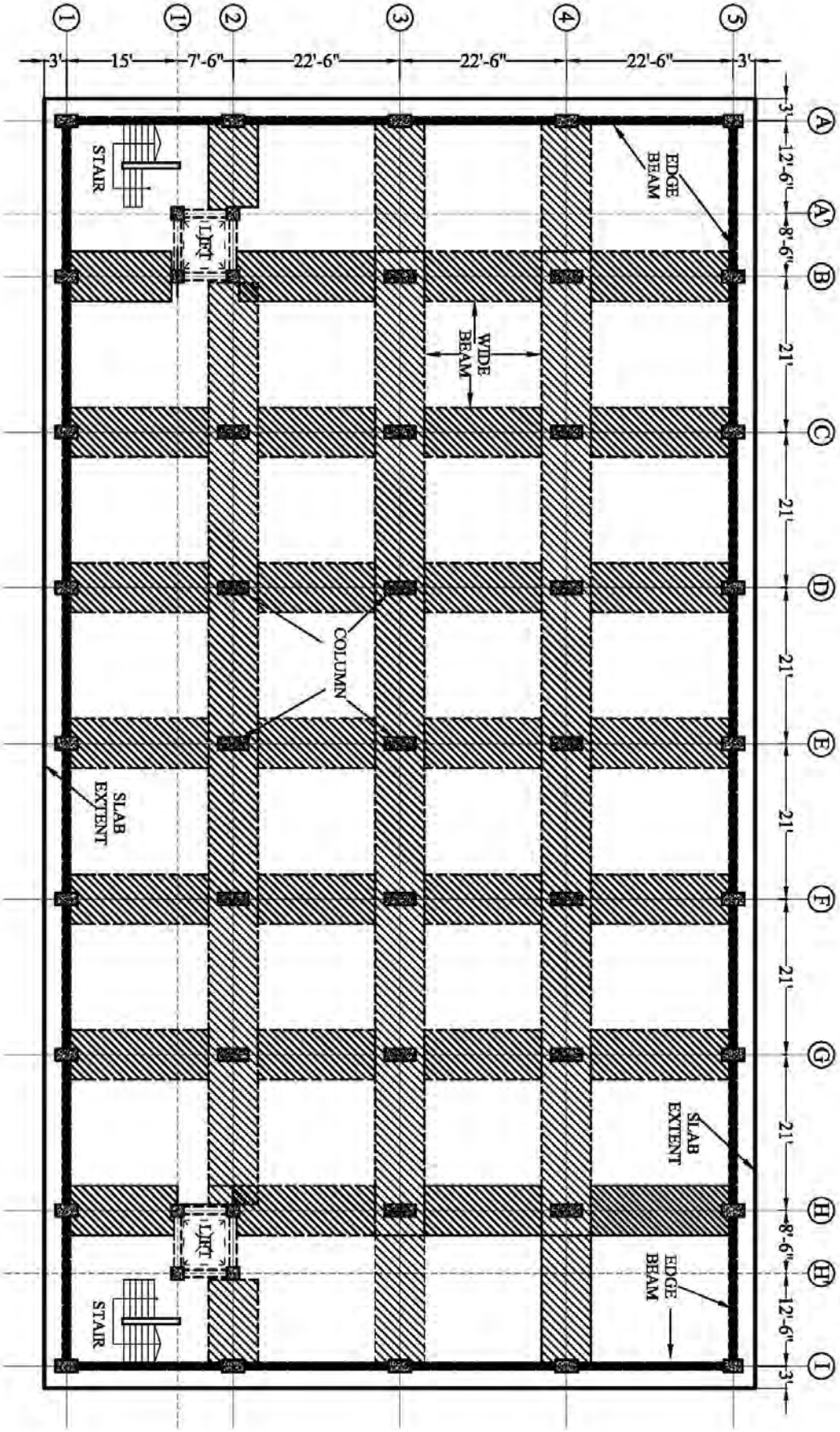

Figure 3.3: Typical floor layout of wide beam frame structure

Lateral Loads, such as Wind Load and Seismic Load applied at the building in accordance with the provision of Chapter 2, Part 6 of BNBC 1993 is as follows:

Table 3.3: Wind load parameters

Basic Wind Speed, V_b	195 km/h(Narayanganj, Bangladesh)
Structural Importance Coefficient (C_I)	1.0
Exposure Category	A
Overall Pressure Coefficient, C_p	1.4(X-direction) 1.59 (Y- direction)

Table 3.4: Earthquake parameters

Seismic Zone	Zone II (Narayanganj)	
Seismic Zone Coefficient (Z)	0.15	[Table 6.2.22]
Response Modification Coefficient (R)	8	[Table 6.2.24]
Structural Importance Factor (I)	1.0	[Table 6.2.23]
Site Coefficient (S)	1.5	[Table 6.2.25]
Numerical coefficient (C_t)	0.03 (for 'h' in 'ft')	
Fundamental period of vibration, (T)	1.09 sec	

IV. Boundary conditions (support conditions)

Column base supports have been considered as fixed supports in 3D model of super structure to simulate structural behavior.

V. Design method and load combinations

Ultimate Strength Design (USD) method and various loads have been applied to the structures in combination with factors listed below in reviewing the quantity of reinforcement of all structural members.

Factored load combinations for RCC design

$U = 1.4D$

$U = 1.4D + 1.7L$

$U = 0.9D \pm 1.3W_{x/y}$

$U = 0.9D \pm 1.43E_{x/y}$

$U = 1.05D \pm 1.275W_{x/y}$

$U = 1.05D \pm 1.4\ E_{x/y}$

$U = 1.05D + 1.275L \pm 1.275W_{x/y}$

$U = 1.05D + 1.275L \pm 1.4E_{x/y}$

VI. Analysis type selection

By using the equivalent linear static analysis method and Finite Element method, structural analysis has been performed in a single step.

3.2.2 Design outputs

Structural analysis and design of beam column frame structure, flat plate structure and wide beam frame structure have been performed using LSA procedure and USD method as per BNBC 1993. In super structure, number of columns, number of grade beams, number of floor beams of three types of structures are showed in the following Table.

Table 3.5: List of columns, grade beams & floor beams of structures in linear static analysis

Type of Structure	No. of Columns (at each story level)	No. of Grade Beams (at ground floor level)	No. of Floor Beams (at each story level)
Beam-column frame structure	51 nos.	84 nos.	84 nos.
Flat plate structure	51 nos.	63 nos.	32 nos. of Edge beam
Wide beam-column frame structure	51 nos.	84 nos.	32 nos. of Edge beam, 52 nos. of Wide beam

Location, orientation, size and reinforcement details of each structural members of each story levels are summarized in Appendix-A of beam column frame structures, flat plate structures and wide beam frame structures accordingly.

3.3 Non-linear Static Analysis (Pushover Analysis)

Non-linear static analysis (NLSA) have been performed for above mentioned three structural systems varying parameters like material strength and Story height to evaluate and compare performance and applicability in practice. In addition to those

three structural systems, another flat plate structure is analyzed witch is converted from beam column frame structure without any change in beam and column size and reinforcement. Several models are analyzed is listed in ***Table 3.6.*** Typical layouts for Model 1, Model 2, Model 3 and Model 4 are shown in Appendix B.

Table 3.6: Model types and their ID

Structural System	Story Height (feet)	Model ID	
		f'_c= 3 ksi f_y= 60 ksi	f'_c= 4 ksi f_y= 60 ksi
Beam-Column Frame structure (Model-1)	10	M-1.1	M-1.3
	12	M-1.2	M-1.4
Flat Plate Structure (Model-2)	10	M-2.1	M-2.3
	12	M-2.2	M-2.4
Frame Structure with Wide beam (Model-3)	10	M-3.1	M-3.3
	12	M-3.2	M-3.4

3.3.1 Modeling criteria and hinge properties

In this section, modeling criteria and properties of structural members of beam-column frame, flat plat and wide beam-column frame structure are considered and discussed.

I. Beam-column moment frame:

Beam-column frame elements are considered as line elements with properties concentrated at component centerlines in analytical model. The beam–column joint is considered monolithic rigid joint as shown in figure 3.4. Beams and columns are modeled using concentrated plastic hinge models. Nonlinear modeling parameters and acceptance criteria for beams, columns, and beam–column joints are provided in Appendix B respectively.

II. Slab–column moment frames

Effective beam width model is considered where columns and slabs are represented by line elements rigidly interconnected at the slab–column connection and the slab width included in the model is adjusted to account for flexibility of the slab–column connection. Slab (shell) element width is reduced to adjust the elastic stiffness to more closely match measured values. Column behavior and slab–column moment and shear

transfer are modeled separately. Effective beam width layout and details are summarized in Appendix B.

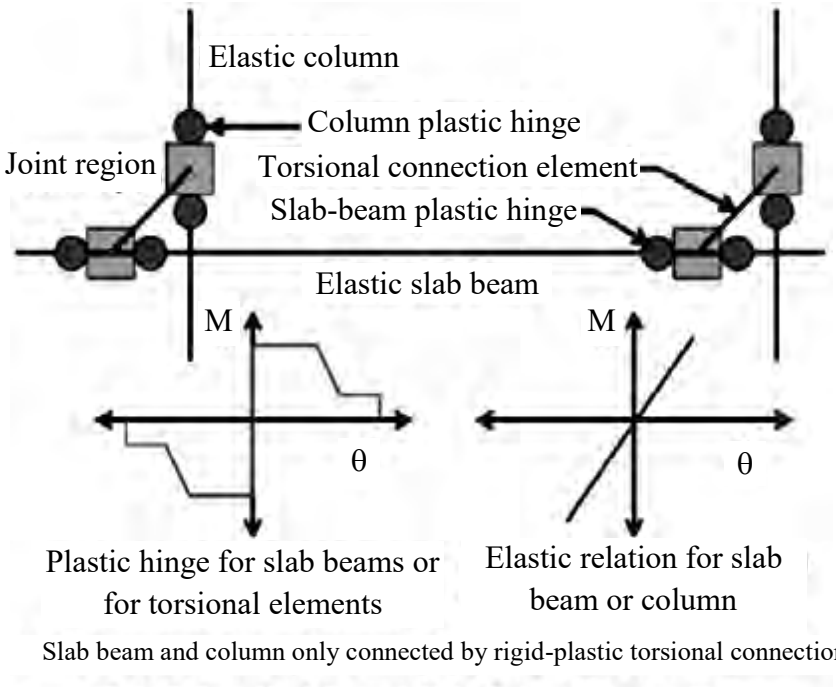

Figure 3.4: Modeling of slab-column connection (Figure C10-2: ASCE 41-13)

The beam–column joint is considered monolithic and slab beams and columns are modeled using concentrated plastic hinge models. Nonlinear modeling parameters and acceptance criteria for slab columns connections are provided in Appendix B.

3.3.2 Loading criteria and response spectra

There are three lateral load pattern proposed in FEMA-356 also adopted by ASCE 41-13, namely (a) inverted triangular distribution, (b) uniform distribution, (c) distribution of forces proportional to fundamental mode (mode 1). Third one has been utilized in this research. The generalized load-deformation relation is shown in Figure 3.6.

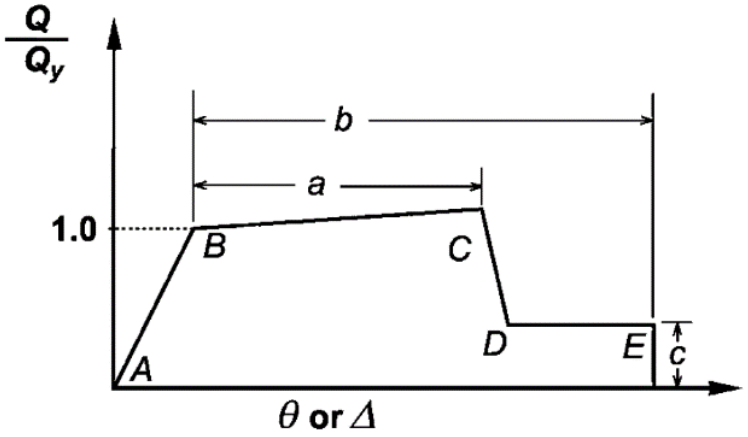

Figure 3.5: Load-deformation relationship (Figure 10-1.a: ASCE 41-13)

For earthquake load consideration, BNBC 2015 response spectra curve have been used (figure 3.7) for the nonlinear static analysis (NLSA).

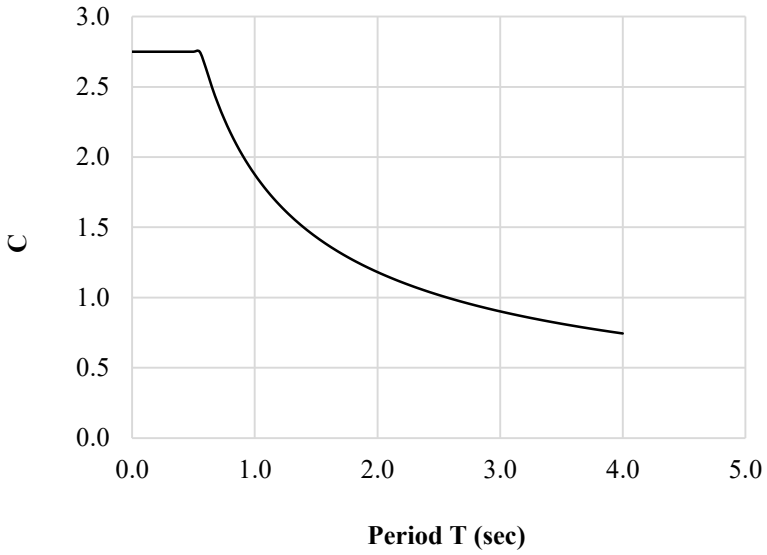

Figure 3.6: BNBC 1993 response spectrum curve

3.3.3 Effective stiffness for crack section model

Beam, column and shear wall sections are considered as cracked sections in nonlinear static procedure as per ASCE 41-13. Effective stiffness for cracked sections are summarized in ***Table 3.2.***

Table 3.7: Effective stiffness values as per ASCE 41-13 (Table 10.5)

Components	Flexural Rigidity	Shear Rigidity
Beams	0.3 E_cI_g	0.4 E_cA_g
Columns	0.7 E_cI_g	0.4 E_cA_g
Flat slabs	0.33 E_cI_g	0.4 E_cA_g

CHAPTER 4
RESULTS

4.1 Introduction

Structural performance under linear static analysis (LSA) and nonlinear static analysis or pushover analysis (NLSA) have been discussed in this chapter. Results from LSA for Model-1 (Beam Column Frame System), Model-2 (Flat Plate Structure) and Model-3 (Wide Beam Column Frame System), mentioned in chapter three along with the cost of superstructures have been compared. Nonlinear behavior of Model-1 to Model-4 has been discussed and compared with one another and parametric study has been conducted varying story height and material property for each of the models.

4.2 Structural Performance from Linear Static Analysis

Four sets of data from linear static analysis have been presented graphically. Maximum story displacement, story drift, story shear, base shear and story stiffness among three structural systems have been compared. For linear static analysis BNBC 1993 has been followed in design as well as for comparison of results.

a) Maximum story displacement

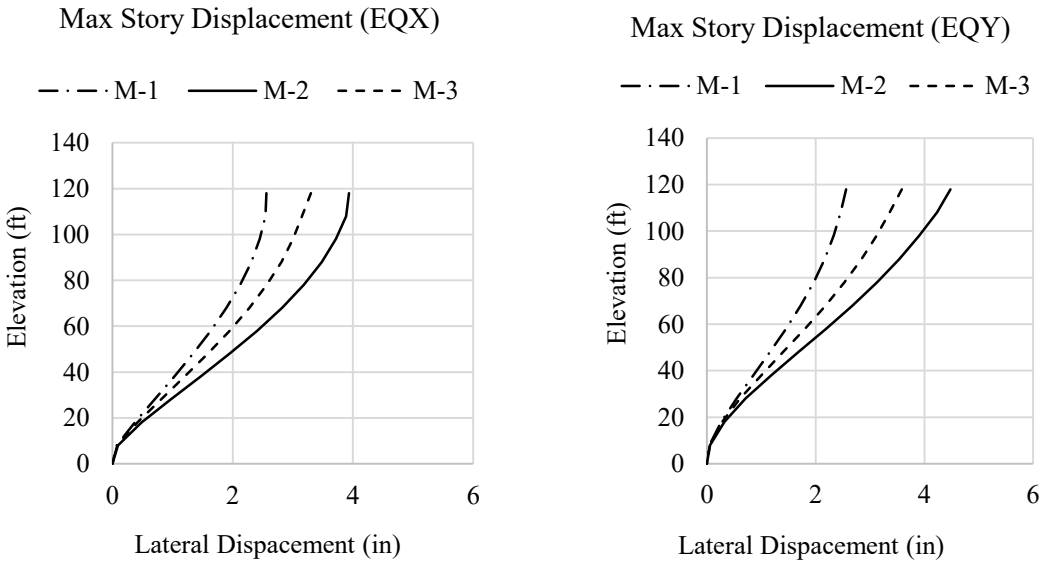

Figure 4.1: Maximum story displacement under earthquake loading

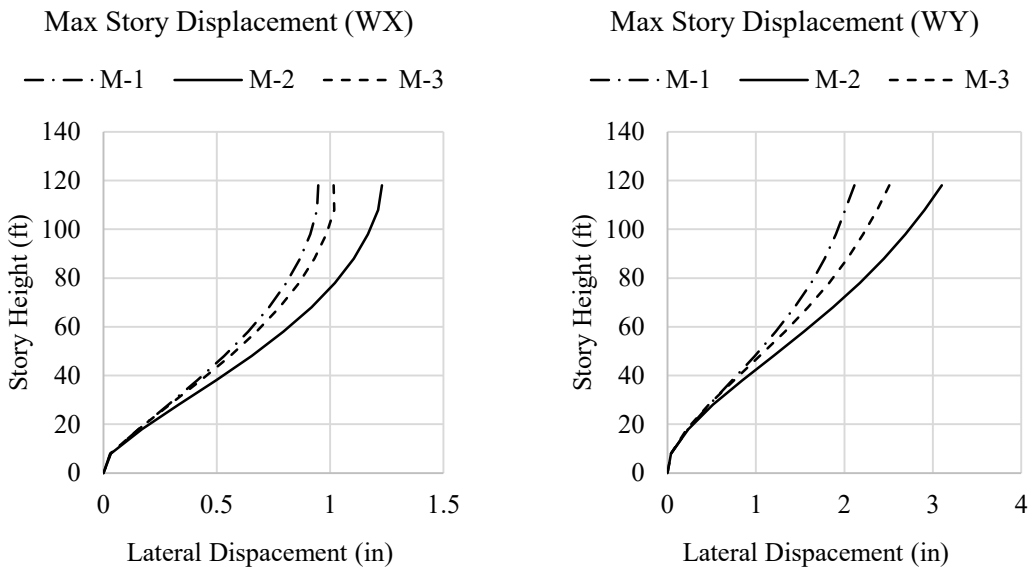

Figure 4.2: Maximum story displacement due to wind

It is apparent from the Story Height vs. Lateral Displacement curves (figure 4.1to figure 4.2) that flat plate structures (M-2) undergo the largest displacement at the top followed by wide beam column structures (M-3). Since the exposed area for wind load is larger along the y-direction, the displacement at top is understandably larger (2.5 times larger compared to x-direction). Beam column frames perform well under lateral loads because of the transfer of moments and shear forces of the rigid diaphragms to the beams. As a result deflections under lateral load are smaller for beam column frames (M-1).

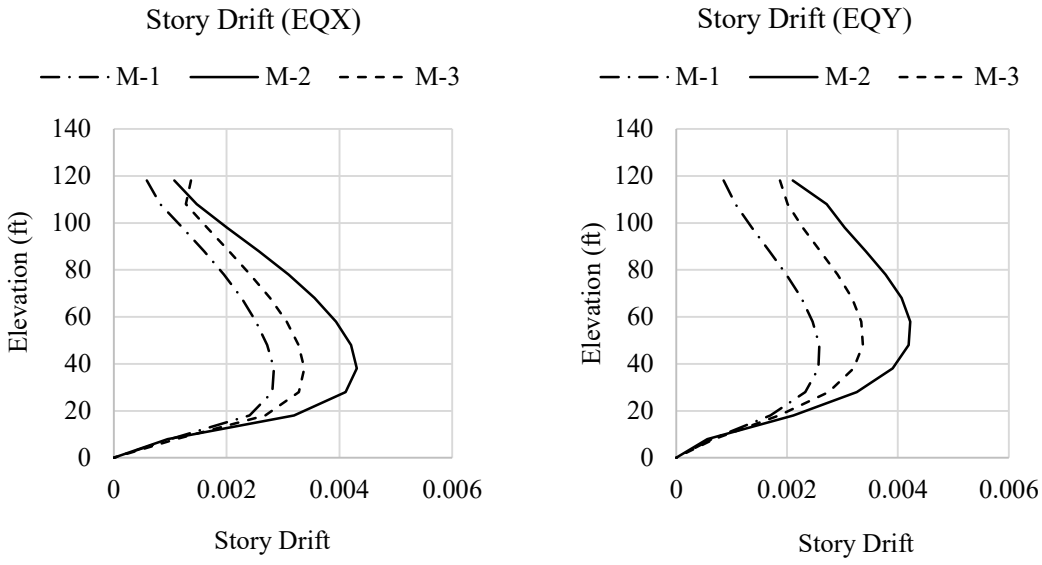

Figure 4.3: Story drift under earthquake loading

According to BNBC 1993 the allowable displacement is $\Delta \leq 0.03\ h\ /\ R \leq 0.004\ h$ for time period $T \geq 0.7$ seconds. So for the building, $\Delta = 0.03\ (110/8) \times 12 = 4.95$ inches. The maximum displacement observed is 4.23 inches, which is well below the allowable limit.

b) Story drift

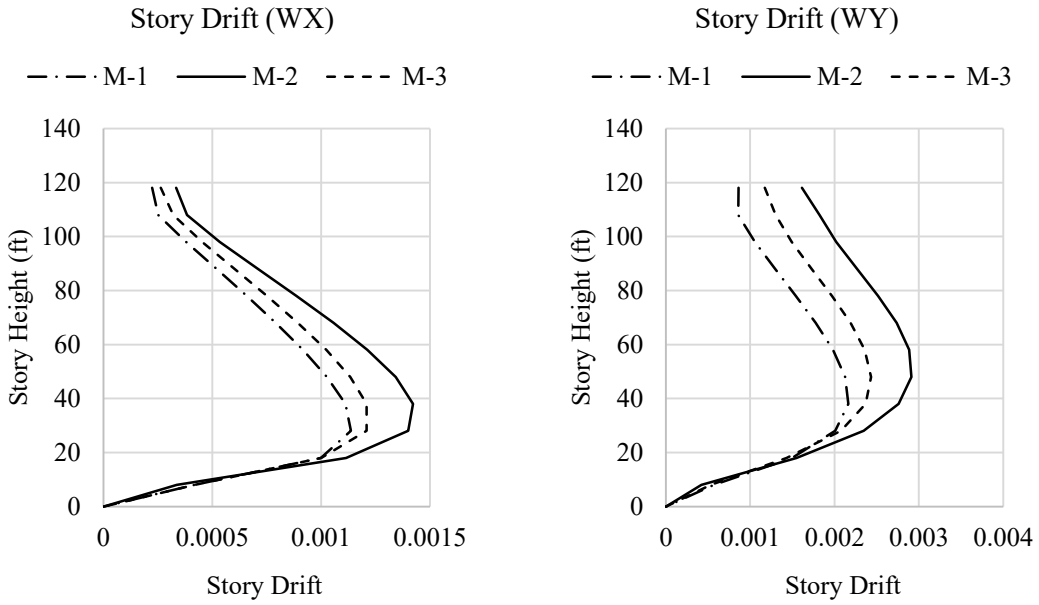

Figure 4.4: Story drift due to wind

Story drifts (figure 4.3 to figure 4.4) are also smaller in beam column frames (M-1) compared to the other forms. This indicates that the changes in displacement between two successive stories are larger in flat plates (M-2). Since change in displacement between two successive stories are larger in the lower floors compared to the upper floors, story drift gradually decreases along the height of a building.

The allowable limit for story drift according to BNBC 1993 has been calculated to be 0.045, which is much higher than the observed maximum value of 0.0043.

c) Story shear

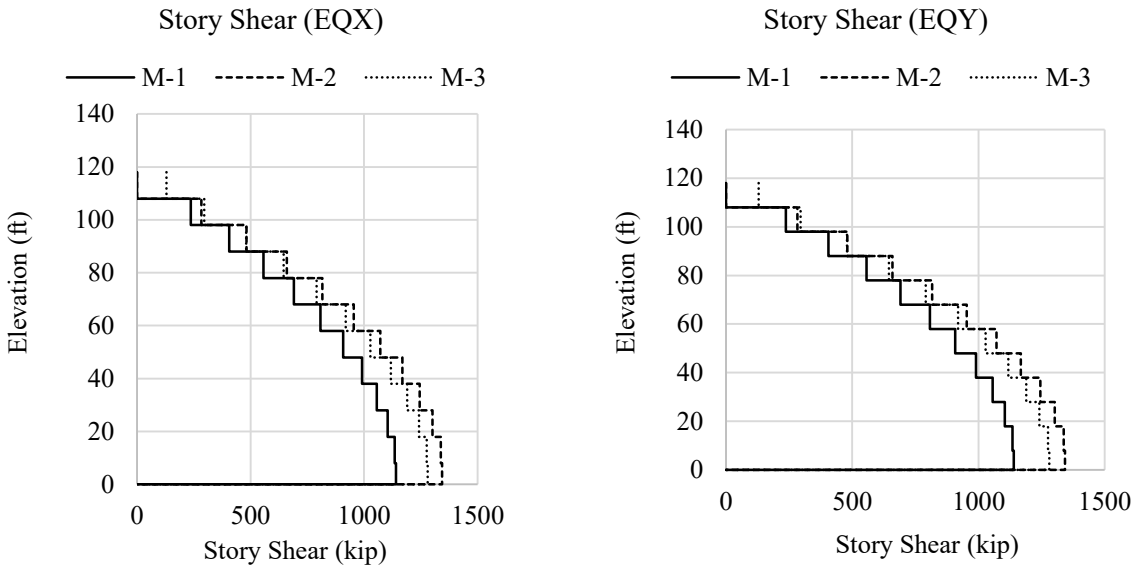

Figure 4.5: Story shear under earthquake loading

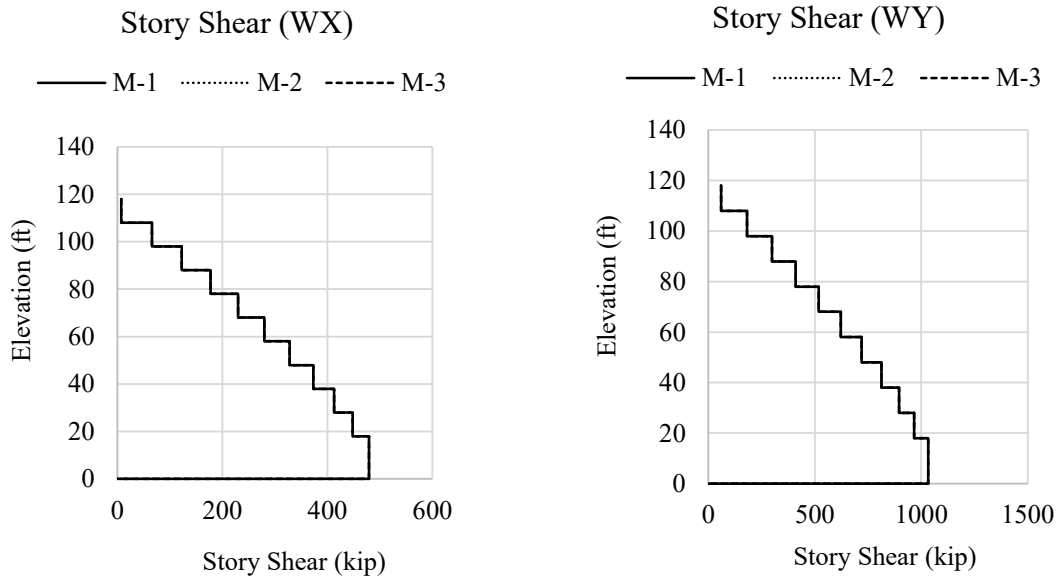

Figure 4.6: Story shear due to wind

Story Shear (figure 4.5 to figure 4.6) due to seismic loads is higher for flat plates (M-2) then wide beam column frames (M-3) and beam column frame structures (M-1). Since the seismic dead load of flat plates is largest among the three, it experiences the highest story shear. Beam column frames are much lighter, as a result experiences a smaller story shear. Since base shear isn't directional, story shears along the x & y – directions are same for a particular system.

On the other hand, the exposed area of the building is larger along the y – direction. As such, the story shear due to wind is higher in the y – direction. Since the exposed area is same for all types of structures, no changes in story shear has been observed among the three types of structures.

d) Story stiffness

Story stiffness (figure 4.7 to figure 4.8) has been observed to be highest for beam column frames (M-1) and lowest for flat plate structures (M-2). Since the diaphragm in a flat plate system cannot transfer the lateral load as efficiently as a beam column frame, flat plates have smaller story stiffness. It can also be seen from the graphs that the story stiffness remains the same along a direction for both earthquake and wind loading. Since the structural arrangement is same for all lateral loads, i.e. to deflect the structures both loads encounter equal moment of inertia, the stiffness stays the same.

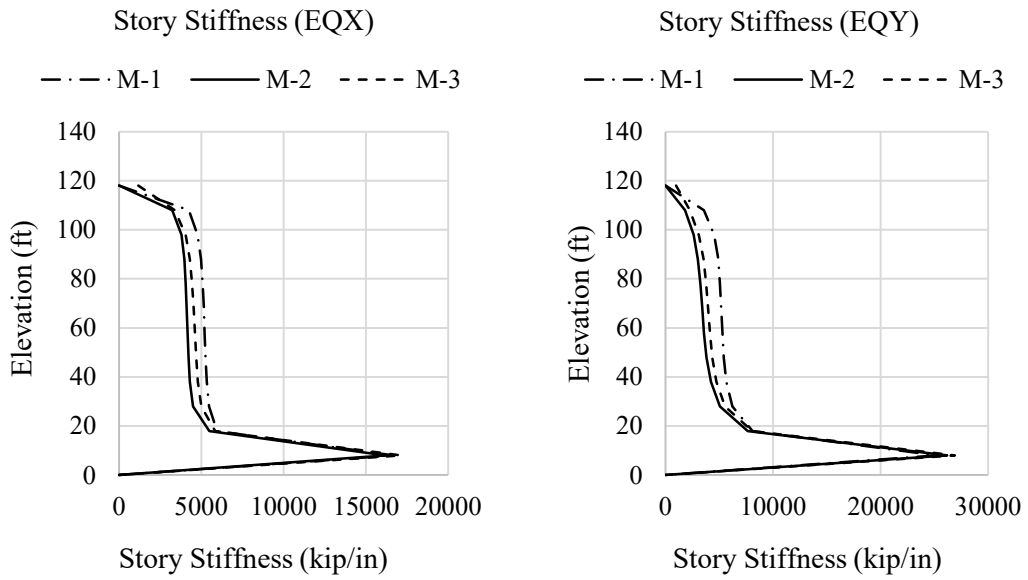

Figure 4.7: Story stiffness under earthquake loading

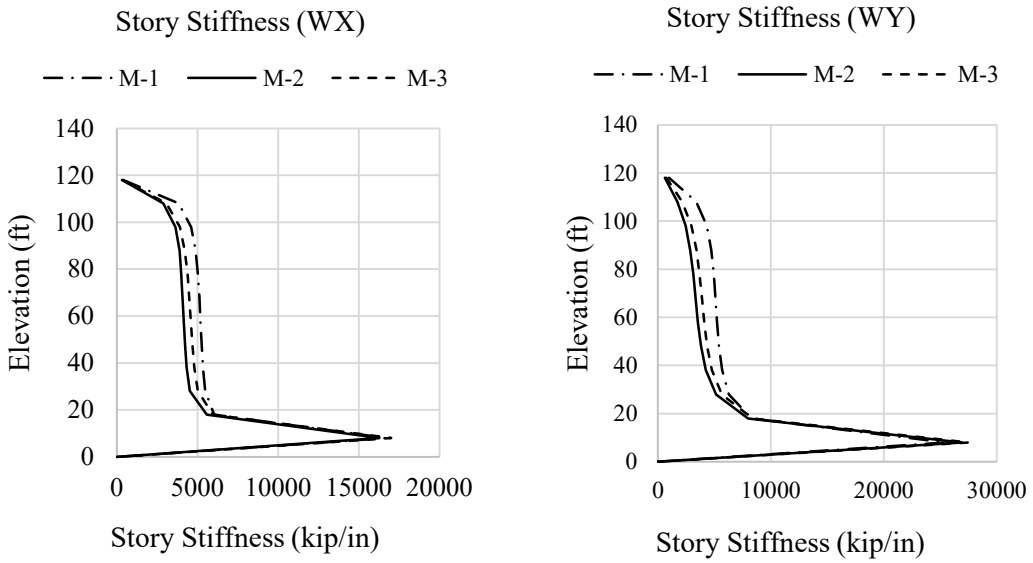

Figure 4.8: Story stiffness due to wind

4.3 Structural Performance from Nonlinear Static Analysis (NLSA)

Comparison of structural performance from NLSA for beam-column frames, flat plates and wide beam frames have been summarized in this section.

4.3.1 Summary of base shear and maximum top displacement

This section summarizes the base shear and corresponding maximum top displacement in two tables (table 4.1 and table 4.2). Base shear and corresponding maximum top displacements are calculated using displacement coefficient method (ASCE 41-13) for serviceability earthquake (SE), design basis earthquake (DBE) and maximum considered earthquake (MCE).

Since the models were designed for DBE, no models exhibited performance point for MCE as per ASCE 41-13. Beam Column frames exhibit performance points regardless of story height and direction for DBE, whereas flat plates of story height 12 ft. fails in the X-direction in most cases. Since stiffness of the models are much higher in the Y-direction all models resist failure in that direction more strongly. Wide Beam Frames do not exhibit performance point for DBE. Moreover, for SE only one wide beam frame exhibited performance point whereas all beam column frames and flat plates exhibit performance point for SE.

Table 4.1: Summary of base shear and maximum top displacement

(*as per BNBC 1993 demand spectrum*)

Model ID	Story Height, h (ft)	EQ Direction	ASCE 41-13 NSP					
			MCE		DBE		SE	
			Base Shear, V(kips)	Top Deflection δ (in)	Base Shear, V(kips)	Top Deflection δ (in)	Base Shear, V(kips)	Top Deflection δ (in)
M- 1.1	10	X	2146	11.8	2149	7.9	2105	5.6
		Y	2654	11.9	2574	7.9	2408	5.6
M- 1.2	12	X	2003	15.6	2003	10.6	1988	7.5
		Y	2338	14.8	2312	10.0	2198	7.0
M- 1.3	10	X	2234	10.7	2221	7.2	2166	5.5
		Y	2786	10.7	2637	7.1	2457	5.0
M- 1.4	12	X	2011	14.0	2024	9.5	2013	6.7
		Y	2421	14.0	2372	9.4	2251	6.6
M- 2.1	10	X	2442	13.4	2520	9.6	2458	6.8
		Y	3141	14.5	3017	9.5	2717	6.7
M- 2.2	12	X	2087	17.4	2087	12.7	2187	9.1
		Y	2667	22.4	2652	14.7	2453	10.2
M- 2.3	10	X	2583	12.8	2581	8.6	2507	6.1
		Y	3237	13.1	3102	8.5	2801	6.0
M- 2.4	12	X	2233	17.0	2242	11.5	2211	8.2
		Y	2745	17.6	2641	11.5	2417	8.1
M- 3.1	10	X	2031	14.4	2031	9.9	1981	7.0
		Y	2307	16.3	2272	10.8	2041	7.4
M- 3.2	12	X	1862	19.3	1862	13.3	1857	9.2
		Y	2026	21.9	2026	14.6	1867	9.5
M- 3.3	10	X	2167	13.0	2170	8.9	2105	6.3
		Y	2581	13.4	2413	8.9	2176	6.2
M- 3.4	12	X	1871	17.5	1871	11.9	1863	8.4
		Y	2187	19.9	2196	13.6	2034	9.4

All the models run satisfy the global acceptance limit as per ASCE 41-13. Measured deflection for beam column frames is well within the immediate occupancy (IO) limit. For flat plates and wide beam frames, deflection do not go beyond the life safety limit, even for MCE.

Table 4.2: Global Acceptance Limit

Model ID	Story Height, h (ft)	EQ Direction	ASCE 41-13 NSP			Global Acceptance Limit		
			MCE	DBE	SE			
			Top Deflection, δ (in)	Top Deflection, δ (in)	Top Deflection, δ (in)	Immediate Occupancy	Life Safety	Structural Stability
M- 1.1	10	X	11.8	7.9	5.6	13.2	26.4	13.9
		Y	11.9	7.9	5.6	13.2	26.4	13.9
M- 1.2	12	X	15.6	10.6	7.5	15.8	31.7	16.7
		Y	14.8	10.0	7.0	15.8	31.7	16.7
M- 1.3	10	X	10.7	7.2	5.5	13.2	26.4	13.9
		Y	10.7	7.1	5.0	13.2	26.4	13.9
M- 1.4	12	X	14.0	9.5	6.7	15.8	31.7	16.7
		Y	14.0	9.4	6.6	15.8	31.7	16.7
M- 2.1	10	X	13.4	9.6	6.8	13.2	26.4	14.1
		Y	14.5	9.5	6.7	13.2	26.4	14.1
M- 2.2	12	X	17.4	12.7	9.1	15.8	31.7	16.9
		Y	22.4	14.7	10.2	15.8	31.7	16.9
M- 2.3	10	X	12.8	8.6	6.1	13.2	26.4	14.1
		Y	13.1	8.5	6.0	13.2	26.4	14.1
M- 2.4	12	X	17.0	11.5	8.2	15.8	31.7	16.9
		Y	17.6	11.5	8.1	15.8	31.7	16.9
M- 3.1	10	X	14.4	9.9	7.0	13.2	26.4	14.0
		Y	16.3	10.8	7.4	13.2	26.4	14.0
M- 3.2	12	X	19.3	13.3	9.2	15.8	31.7	16.8
		Y	21.9	14.6	9.5	15.8	31.7	16.8
M- 3.3	10	X	13.0	8.9	6.3	13.2	26.4	14.0
		Y	13.4	8.9	6.2	13.2	26.4	14.0
M- 3.4	12	X	17.5	11.9	8.4	15.8	31.7	16.8
		Y	19.9	13.6	9.4	15.8	31.7	16.8

4.3.2 Capacity curve (base shear vs top deflection)

From the capacity curves it can be seen that base shear capacity for flat plates are (M-2) are larger than other systems. However when story heights are increased base shear capacity reduces drastically for flat plates and they become weaker than beam column frames. Flat plates (M-2) have a higher base shear capacity than wide beam column frames (M-3). This indicates that wide beam column frames are much less efficient than flat plates in resisting lateral loads, since larger column sizes in flat plate structures lead to higher stiffness.

As story heights are increased, the decrease in base shear capacity is significant. This can be attributed to the decrease in stiffness due to the increased column height. The decrease in stiffness can be as large as fifty percent as heights are increased by one hundred and fifty percent. As material strength is increased the capacity has been observed to increase.

The base shear capacity along the y-direction has been found to be larger as the structures are stiffer in the y-direction due to more favorable orientation of columns.

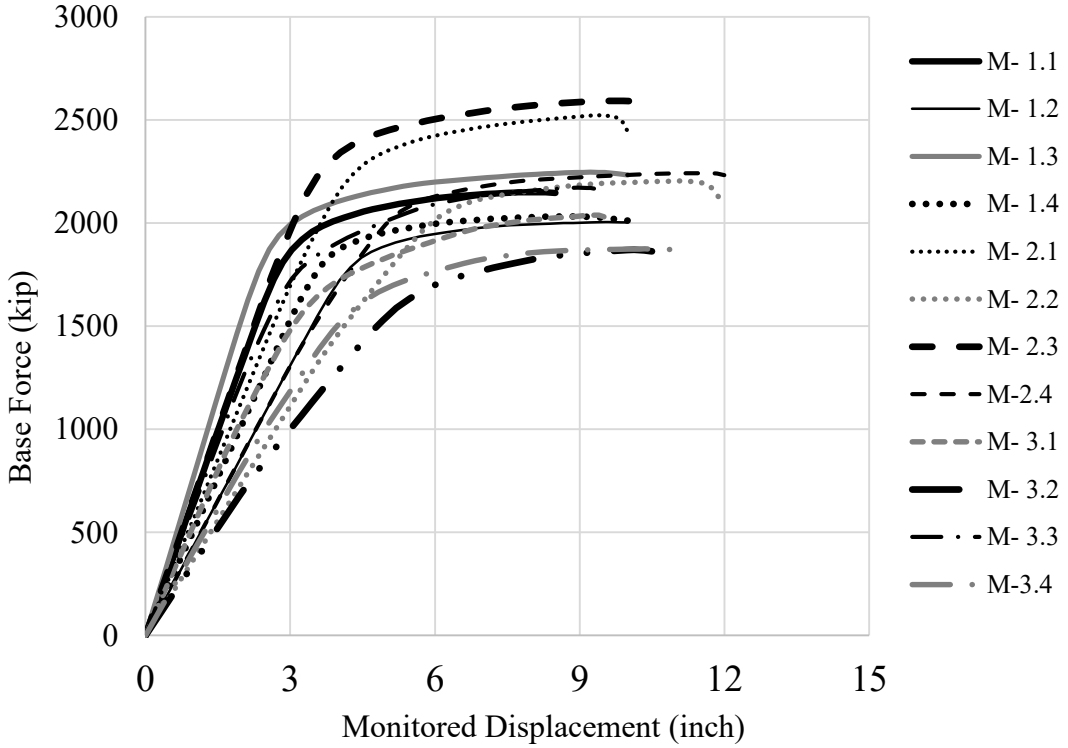

Figure 4.9: Capacity curve x-direction

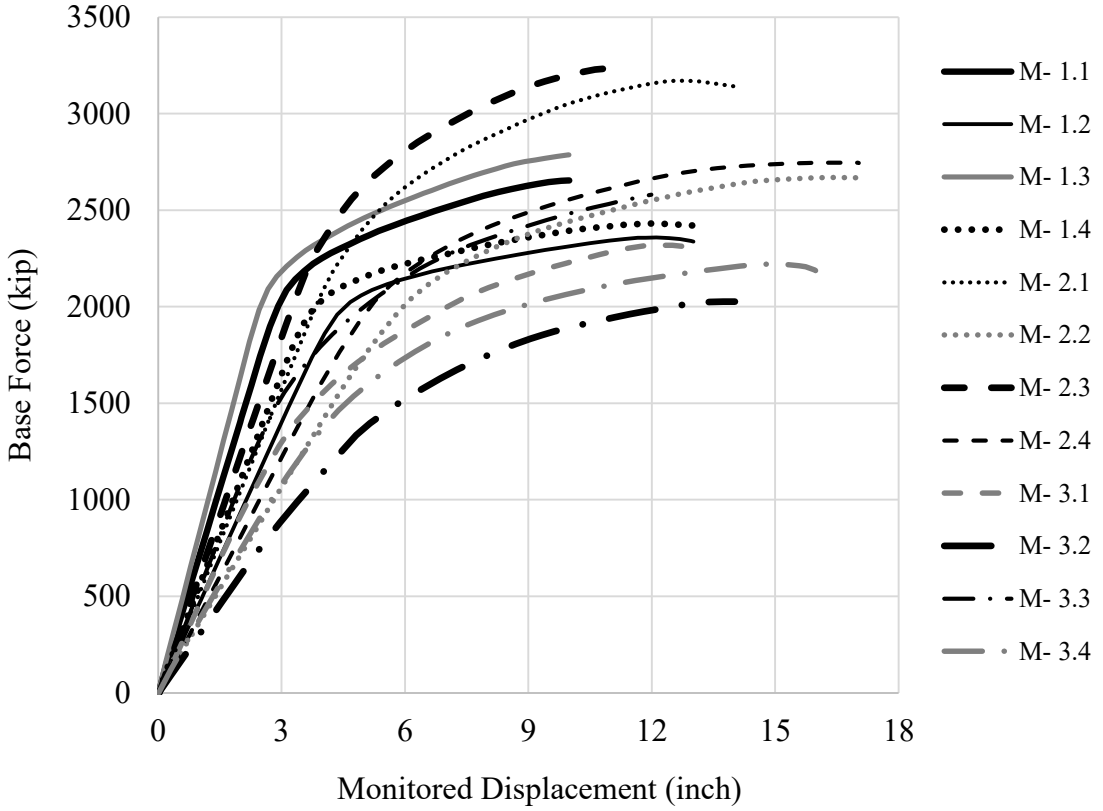

Figure 4.10: Capacity curve y-direction

4.3.3 Plastic hinge state at performance point

The following list presents the states of plastic hinges formed at performance point for all the structural systems under review for both DBE and SE. It can be seen that as story heights are increased the number of plastic hinges with high magnitude of rotational angle increases. Number of plastic hinges at various levels are more in number in wide beam frame structures compared to other structural forms.

For DBE, all hinges in the beam column frames stay within the acceptable (upto LS) limit. One flat plate and two wide beam frame model formed hinges in the LS-CP range, while one wide beam frame model formed hinges beyond the CP (>CP) range.

Table 4.3: Summary table of plastic hinge states at performance point (DBE)

Model ID	Direction	Target Displacement	Base Force	A-IO	IO-LS	LS-CP	>CP	Total Hinges
M- 1.1	X	7.9	2149	2661	369	0	0	3030
	Y	7.9	2574	2639	391	0	0	3030
M- 1.2	X	10.6	2003	2693	337	0	0	3030
	Y	10.0	2312	2629	401	0	0	3030
M- 1.3	X	7.2	2221	2678	352	0	0	3030
	Y	7.1	2637	2706	324	0	0	3030
M- 1.4	X	9.5	2024	2755	275	0	0	3030
	Y	9.4	2372	2678	352	0	0	3030
M- 2.1	X	9.6	2520	2560	470	0	0	3030
	Y	9.5	3017	2425	605	0	0	3030
M- 2.2	X	12.7	2087	2805	225	0	0	3030
	Y	14.7	2652	2355	657	18	0	3030
M- 2.3	X	8.6	2581	2554	476	0	0	3030
	Y	8.5	3102	2511	519	0	0	3030
M- 2.4	X	11.5	2242	2550	480	0	0	3030
	Y	11.5	2641	2414	616	0	0	3030
M- 3.1	X	9.9	2031	2669	361	0	0	3030
	Y	10.8	2272	2556	474	0	0	3030
M- 3.2	X	13.3	1862	2717	313	0	0	3030
	Y	14.6	2026	2573	423	34	0	3030
M- 3.3	X	8.9	2170	2671	357	2	0	3030
	Y	8.9	2413	2648	380	0	2	3030
M- 3.4	X	11.9	1871	2739	291	0	0	3030
	Y	13.6	2196	2540	490	0	0	3030

While all the models run should have formed hinges within the IO range, hinges formed upto LS limit for SE, but number of hinges in IO-LS range has dropped significantly from DBE.

Table 4.4: Summary table of plastic hinge states at performance point (SE)

Model ID	Direction	Target Displacement	Base Force	A-IO	IO-LS	LS-CP	>CP	Total Hinges
M- 1.1	X	5.6	2105	2811	219	0	0	3030
	Y	5.6	2408	2917	113	0	0	3030
M- 1.2	X	7.5	1988	2764	266	0	0	3030
	Y	7.0	2198	2959	71	0	0	3030
M- 1.3	X	5.5	2166	2887	143	0	0	3030
	Y	5.0	2457	3000	30	0	0	3030
M- 1.4	X	6.7	2013	2854	176	0	0	3030
	Y	6.6	2251	2958	72	0	0	3030
M- 2.1	X	6.8	2458	2668	362	0	0	3030
	Y	6.7	2717	2653	377	0	0	3030
M- 2.2	X	9.1	2187	2626	404	0	0	3030
	Y	10.2	2453	2502	528	0	0	3030
M- 2.3	X	6.1	2507	2675	355	0	0	3030
	Y	6.0	2801	2671	359	0	0	3030
M- 2.4	X	8.2	2211	2651	379	0	0	3030
	Y	8.1	2417	2602	428	0	0	3030
M- 3.1	X	7.0	1981	2726	304	0	0	3030
	Y	7.4	2041	2733	297	0	0	3030
M- 3.2	X	9.2	1857	2733	297	0	0	3030
	Y	9.5	1867	2731	299	0	0	3030
M- 3.3	X	6.3	2105	2790	240	0	0	3030
	Y	6.2	2176	2756	274	0	0	3030
M- 3.4	X	8.4	1863	2759	271	0	0	3030
	Y	9.4	2034	2725	305	0	0	3030

The following figures (figure 4.13-4.24) presents the states of plastic hinges formed at performance point for model M-1.1, model M-2.1 and model M-3.1 under pushover cases in both x and y-directions.

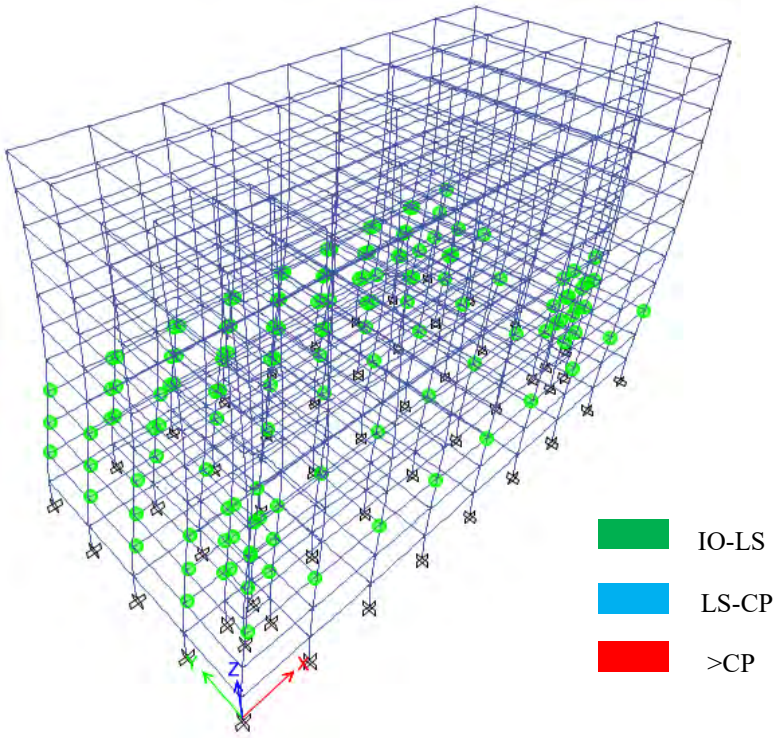

Figure 4.11: plastic hinges formed at performance point for model M-1.1 (3D view) in x-direction

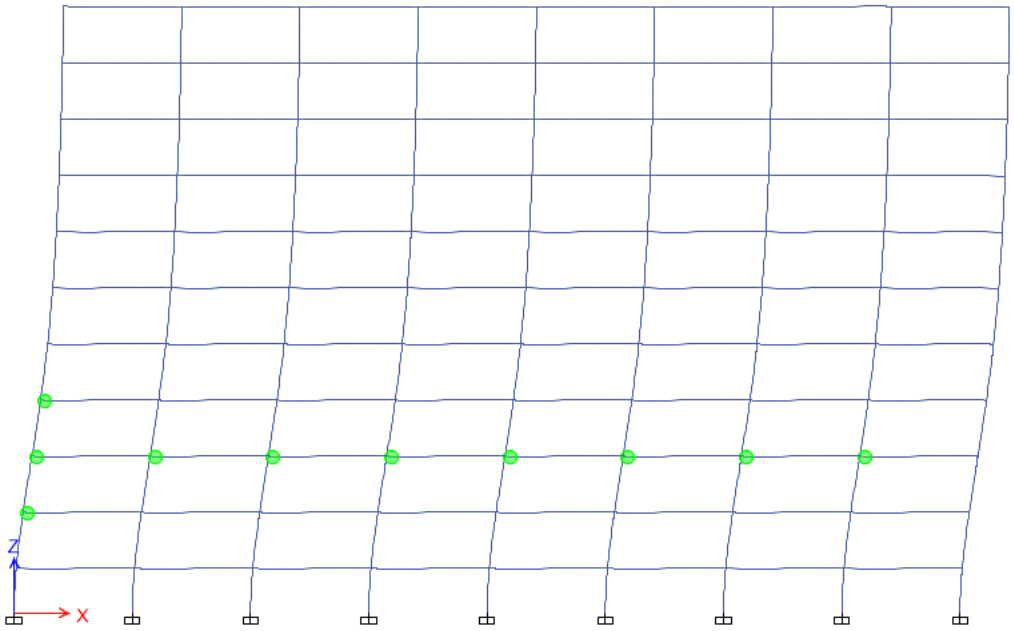

Figure 4.12: plastic hinges formed at performance point for model M-1.1 (elevation 3) in x-direction

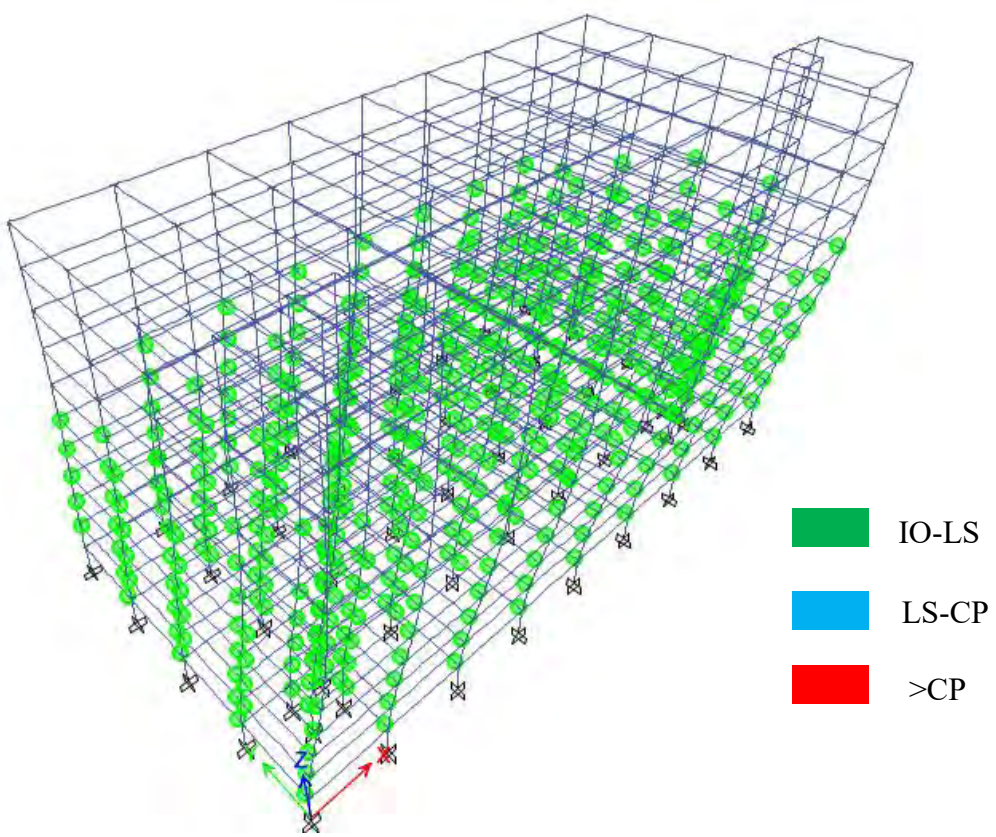

Figure 4.13: plastic hinges formed at performance point for model M-1.1 (3D view) in y-direction

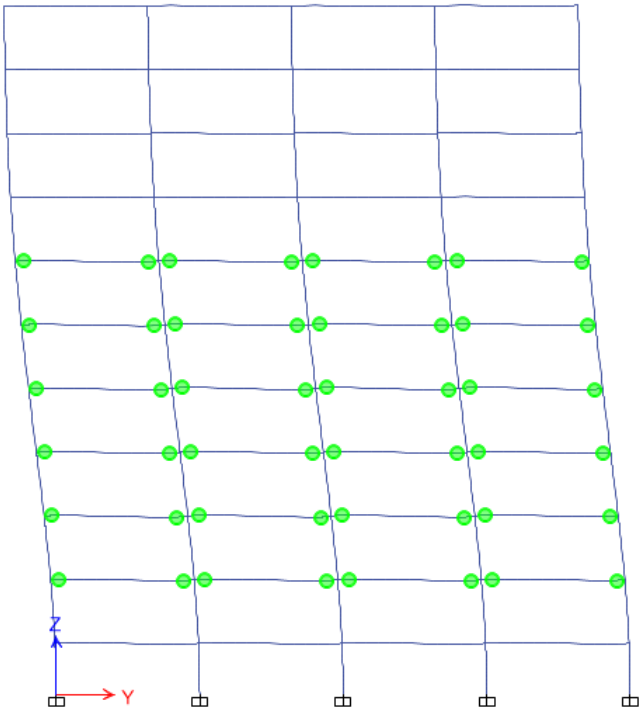

Figure 4.14: plastic hinges formed at performance point for model M-1.1 (elevation C) in y-direction

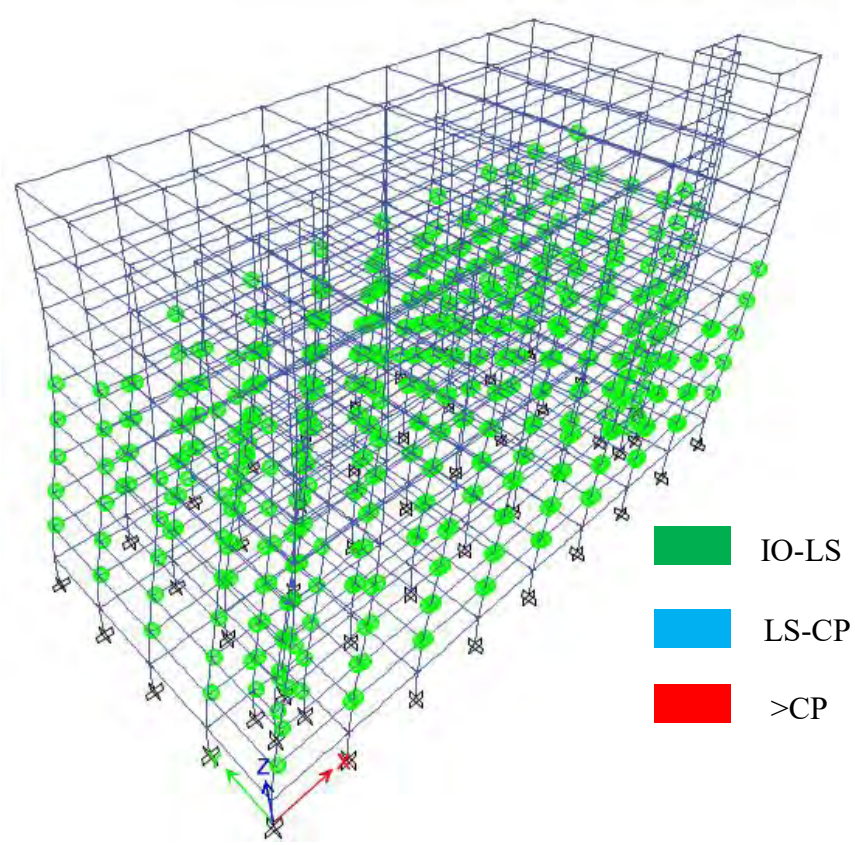

Figure 4.15: plastic hinges formed at performance point for model M-2.1 (3D view) in x-direction

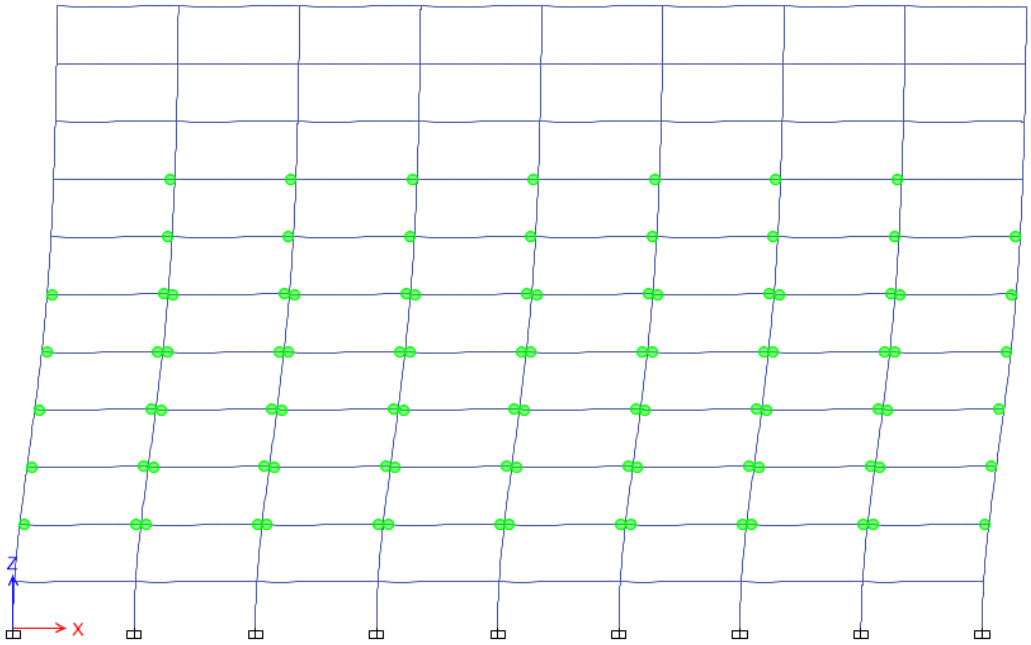

Figure 4.16: plastic hinges formed at performance point for model M-2.1 (elevation C) in x-direction

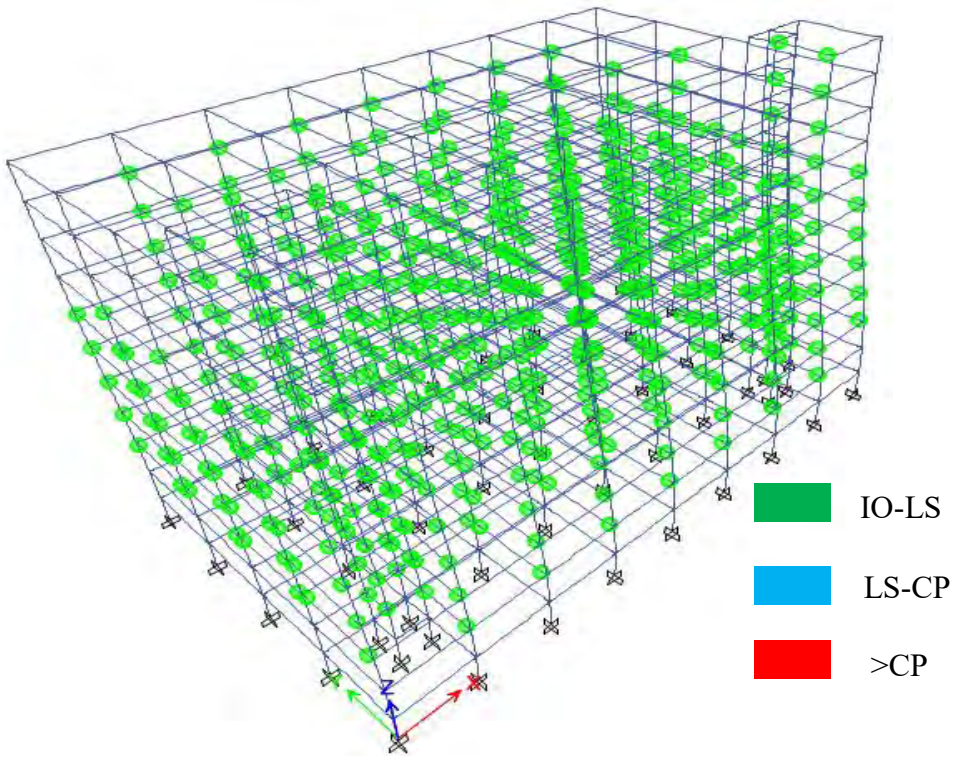

Figure 4.17: plastic hinges formed at performance point for model M-2.1 (3D view) in y-direction

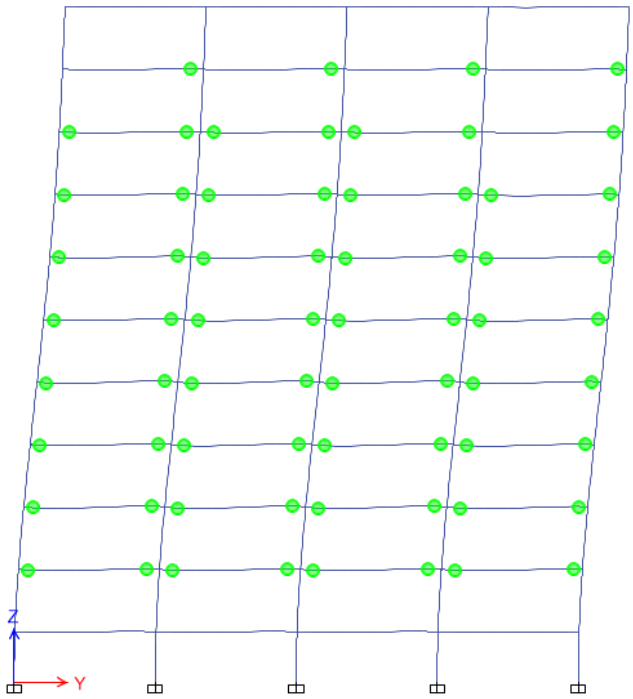

Figure 4.18: plastic hinges formed at performance point for model M-2.1 (elevation C) in y-direction

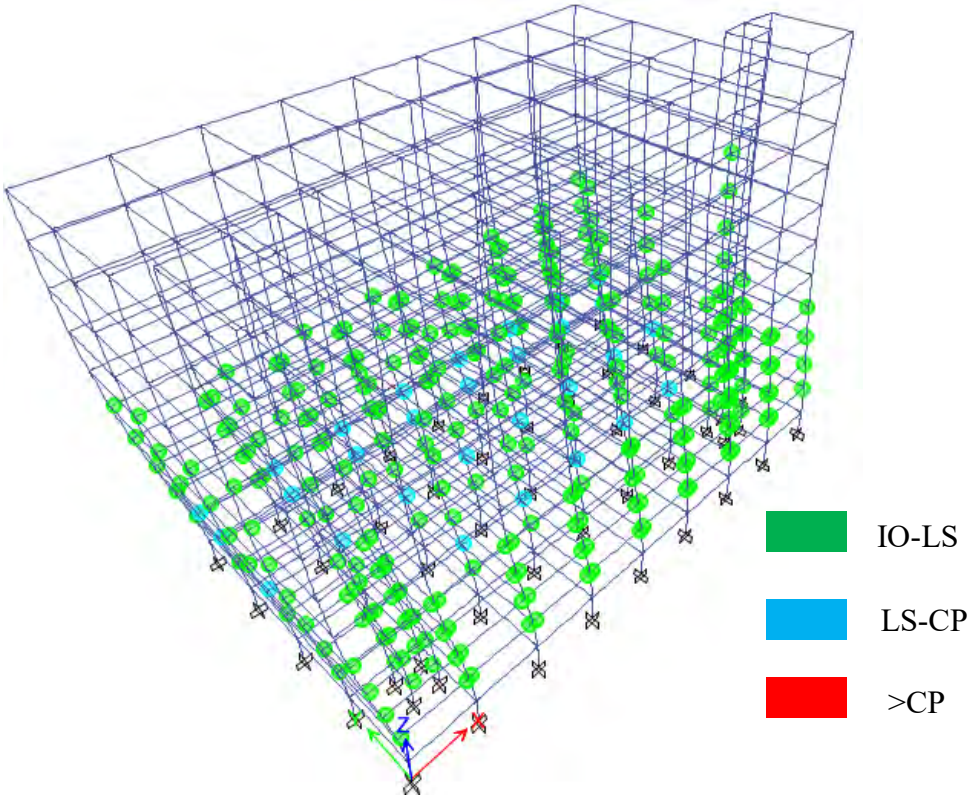

Figure 4.19: plastic hinges formed at performance point for model M-3.1 (3D view) in x-direction

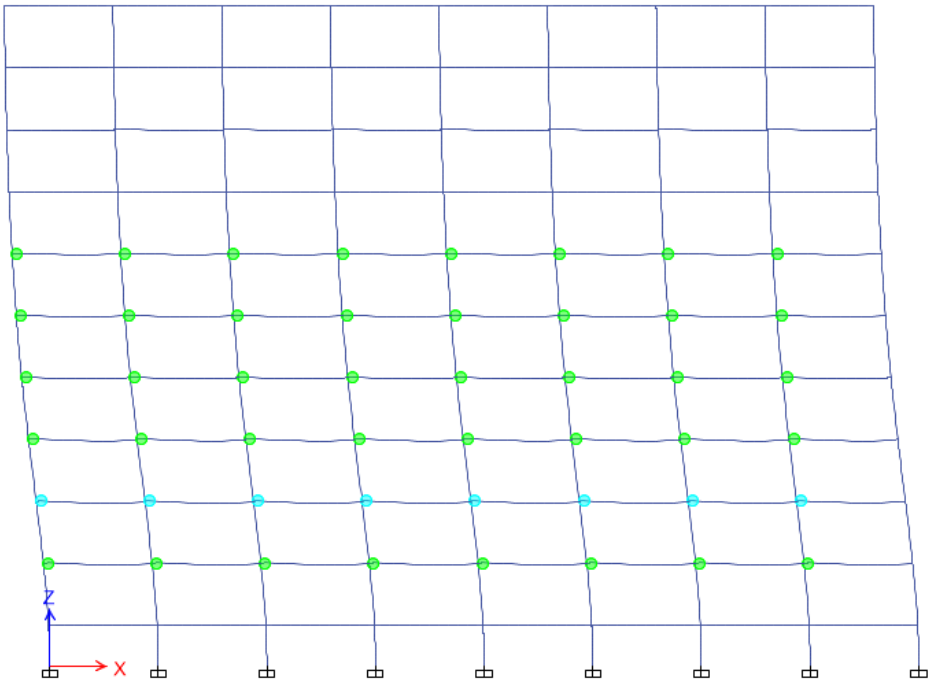

Figure 4.20: plastic hinges formed at performance point for model M-3.1 (elevation C) in x-direction

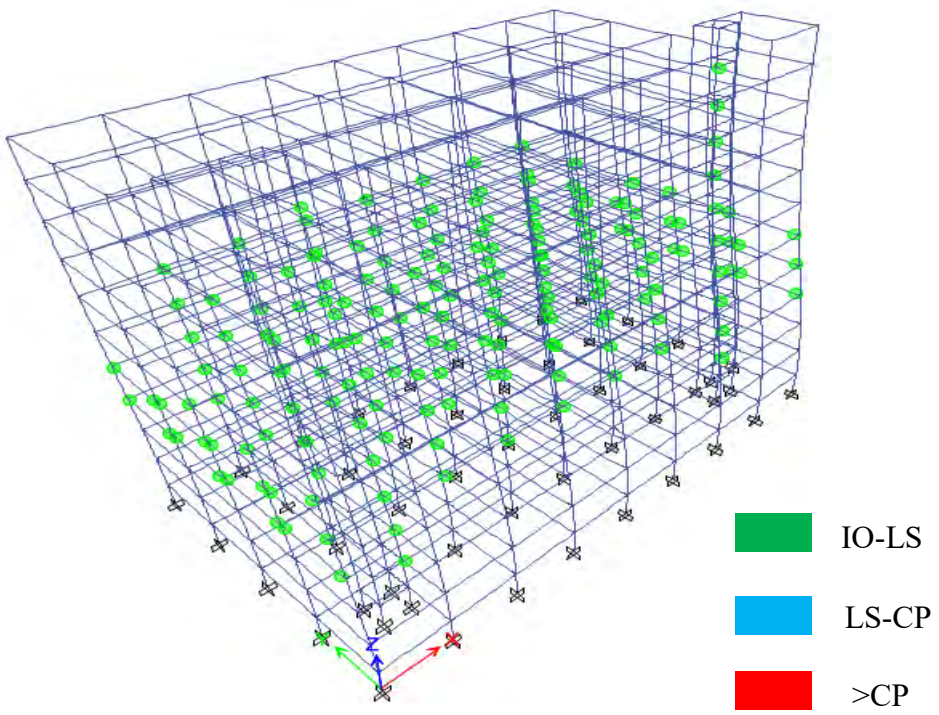

Figure 4.21: plastic hinges formed at performance point for model M-3.1 (3D view) in y-direction

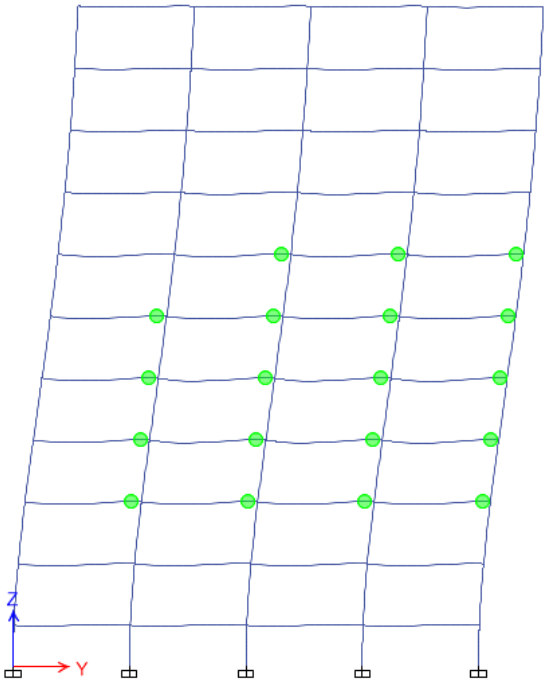

Figure 4.22: plastic hinges formed at performance point for model M-3.1 (elevation C) in y-direction

4.3.4 Base shear capacity chart (DBE)

As story heights are increased it can be seen from the charts (figure-4.29 to figure-4.32) below that base shear capacity gets reduced. Base shear capacity is higher in flat plates than other systems, owing to the larger weight of the flat plate structures. Since stiffness of the structures are higher along the Y-direction, base shear capacity has also been found to be higher. As material strength is increased, the base shear capacity increases for all models. However increasing the story height reduces base shear capacity.

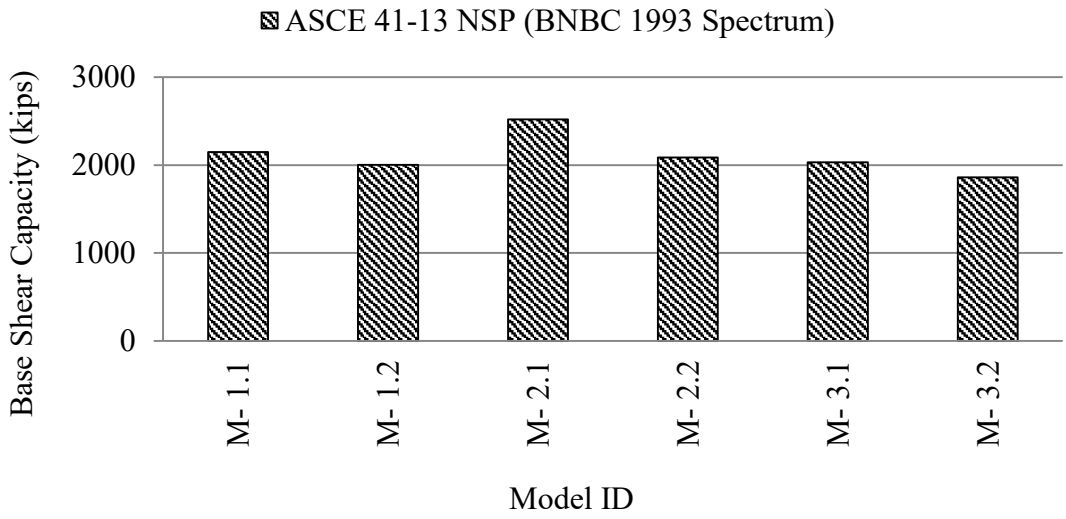

Figure 4.23: Base shear capacity (x-direction) chart (f'c= 3 ksi, fy= 60 ksi)

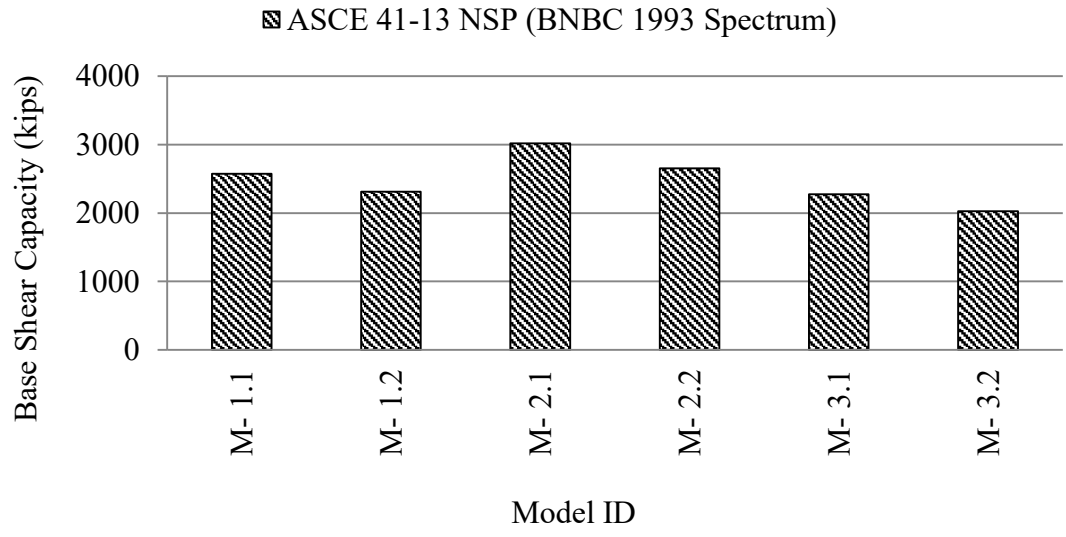

Figure 4.24: Base shear capacity (y-direction) chart (f'c= 3 ksi, fy= 60 ksi)

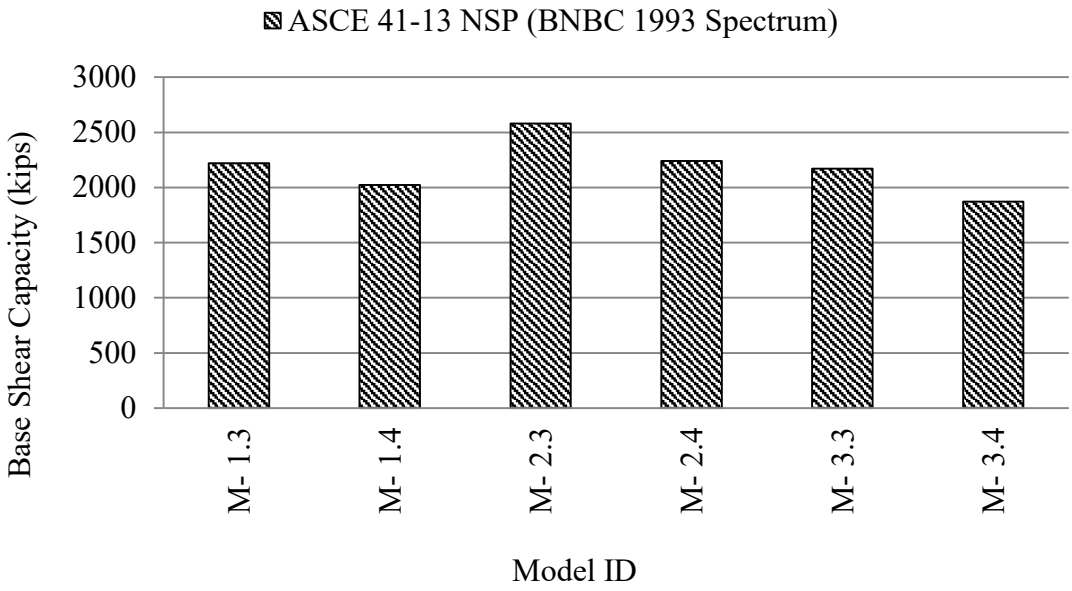

Figure 4.25: Base shear capacity (x-direction) chart (f'c= 4 ksi, fy= 60 ksi)

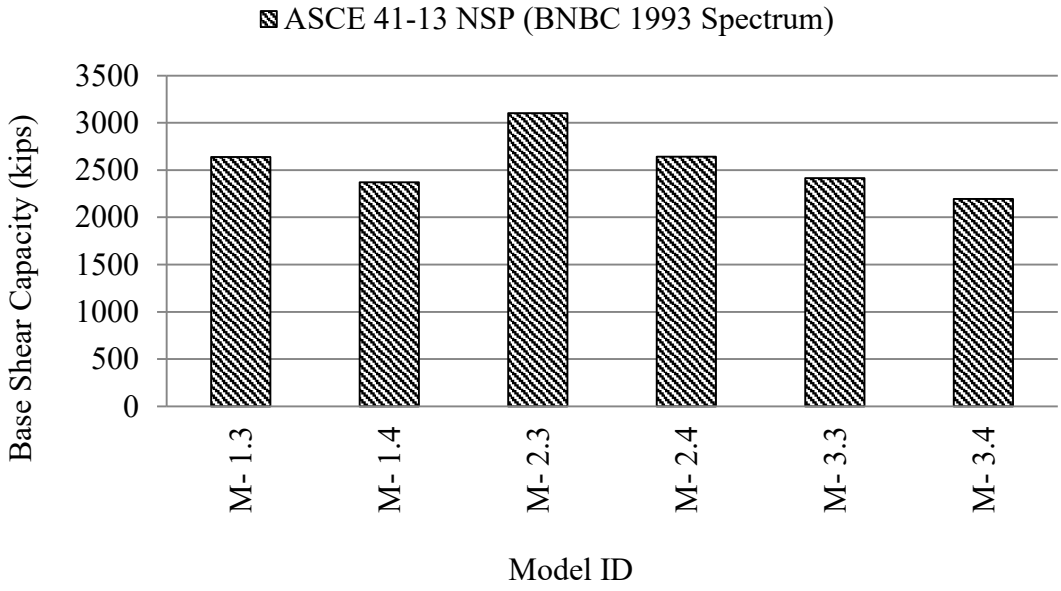

Figure 4.26: Base shear capacity (y-direction) chart (f'c= 4 ksi, fy= 60 ksi)

4.3.5 Maximum top deflection chart (DBE)

Story height greatly influences the top deflection of structures. As story heights are increased top deflection increases for all four models. Top deflection is higher in wide beam frames compared to flat plates and beam column frames. Higher stiffness along the Y-direction resulted in lower deflection along that direction.

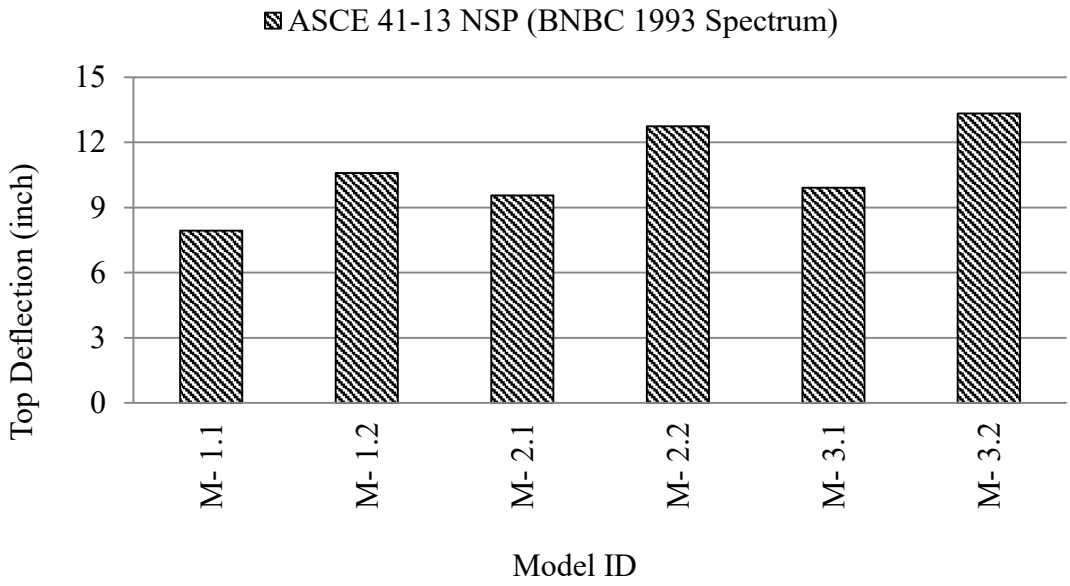

Figure 4.27: Top deflection (x-direction) chart (f'c = 3 ksi, fy = 60 ksi)

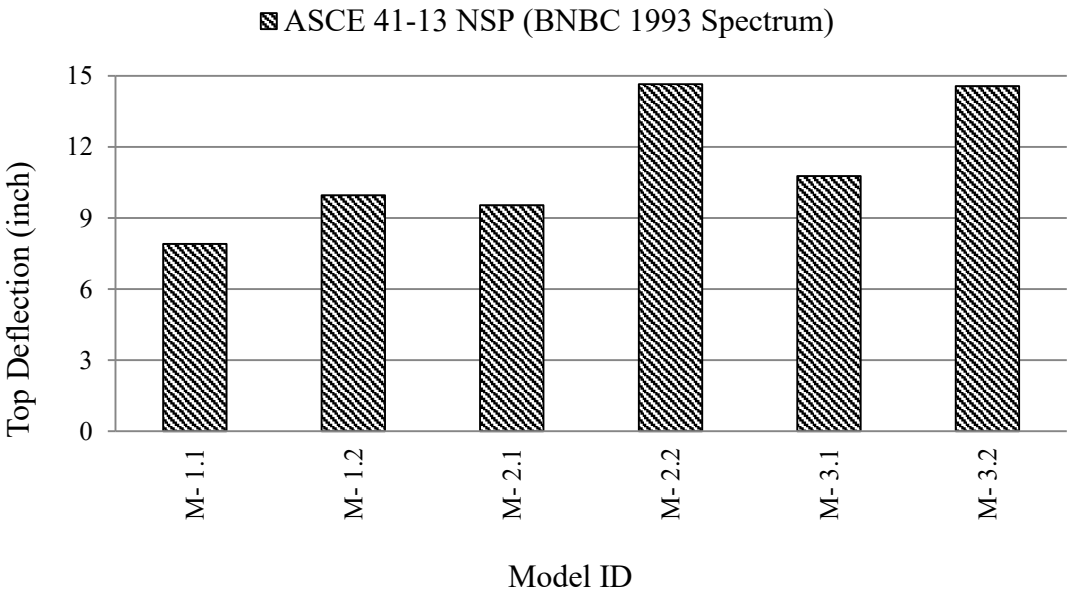

Figure 4.28: Top deflection (y-direction) chart (f'c = 3 ksi, fy = 60 ksi)

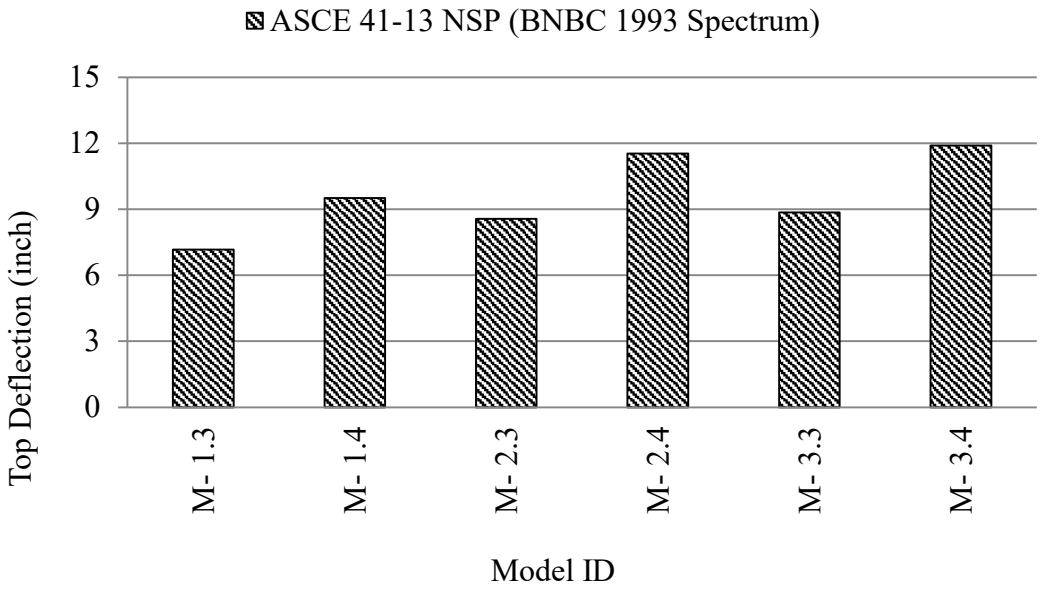

Figure 4.29: Top deflection (x-direction) chart (f'c = 4 ksi, fy = 60 ksi)

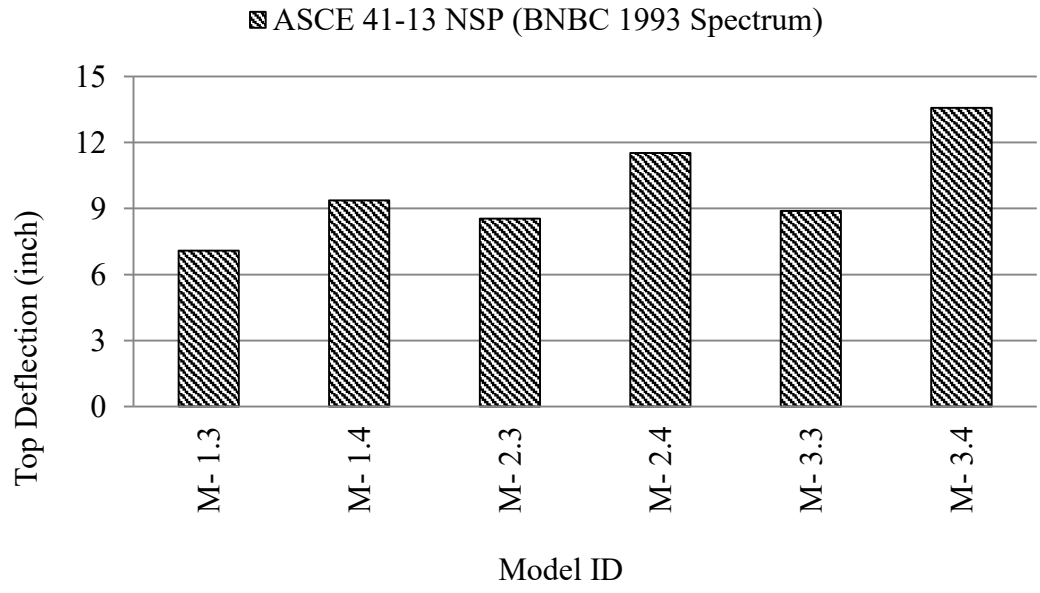

Figure 4.30: Top deflection (y-direction) chart (f'c = 4 ksi, fy = 60 ksi)

4.4 Comparison of Costs of Super Structures

Construction cost of structural elements of superstructures (beam, column and slab) for beam-column frame (M-1), flat plate (M-2) and wide beam frame (M-3) structures have been summarized and compared among one another in this part. From the charts (table 4.6 to table 4.8) shown below it can be seen that the beam column framing system is the cheapest followed closely by wide beam column frames. It can also be seen from

the charts that wide beam frames use up slightly more concrete and steel compared to beam column frames but saves up on cost of shuttering and labor. Except for the savings on shuttering and labor, flat plates have been found to be much more expensive due to the large amount of materials required.

Overall cost of a flat plat structure is 18% and 20% higher compared to wide beam column and beam-column frame structures respectively. Also cost of wide beam column structure is 2% higher compared to beam column frame structure.

Table 4.5: Construction cost of structural part (without foundation) of M-1

Items	Levels	Quantity (cft)	Unit Price (BDT)	Total Cost
Concrete	Below GB	7586	280	2,124,151
	Level-1	19272	294	5,666,035
	Level-2	19272	309	5,949,337
	Level-3	19272	324	6,246,803
	Level-4	19272	340	6,559,144
	Level-5	19272	357	6,887,101
	Level-6	19272	375	7,231,456
	Level-7	19272	394	7,593,029
	Level-8	19272	414	7,972,680
	Level-9	19272	434	8,371,314
	Roof	19272	456	8,789,880
	OHWT	2161	479	1,034,735
	Total			**74,425,664**
	Levels	Quantity (cft)	Unit Price (BDT)	Total Cost
Steel	Below GB	22.24	62000	1,378,880
	Level-1	54.73	62000	3,393,260
	Level-2	51.07	62000	3,166,340
	Level-3	51.07	62000	3,166,340
	Level-4	48.55	62000	3,010,100
	Level-5	48.27	62000	2,992,740
	Level-6	47.14	62000	2,922,680
	Level-7	47.14	62000	2,922,680

	Level-8	47.14	62000	2,922,680
	Level-9	47.14	62000	2,922,680
	Roof	47.14	62000	2,922,680
	OHWT	5.63	62000	349,060
	Total			**32,070,120**
	Levels	Quantity (cft)	Unit Price (BDT)	Total Cost
Shuttering with labour	Below GB	10151	170	1,725,607
	Level-1	24808	179	4,428,298
	Level-2	24808	187	4,649,712
	Level-3	24808	197	4,882,198
	Level-4	24808	207	5,126,308
	Level-5	24808	217	5,382,623
	Level-6	24808	228	5,651,755
	Level-7	24808	239	5,934,342
	Level-8	24808	251	6,231,059
	Level-9	24808	264	6,542,612
	Roof	24808	277	6,869,743
	OHWT	2202	291	640,243
	Total			**58,064,501**
	Grand Total			**164,560,285**

Table 4.6: Construction cost of structural part (without foundation) of M-2

Items	Levels	Quantity (sft)	Unit Price (BDT)	Total Cost
Concrete	Below GB	8043	280	2,252,170
	Level-1	26060	294	7,661,678
	Level-2	26060	309	8,044,762
	Level-3	26060	324	8,447,000
	Level-4	26060	340	8,869,350
	Level-5	26060	357	9,312,818
	Level-6	26060	375	9,778,459
	Level-7	26060	394	10,267,382
	Level-8	26060	414	10,780,751

	Level-9	26060	434	11,319,788
	Roof	26060	456	11,885,778
	OHWT	2540	479	1,216,232
	Total			**99,836,167**
	Levels	Quantity (sft)	Unit Price (BDT)	Total Cost
Steel	Below GB	22.87	62000	1,417,943
	Level-1	75.92	62000	4,707,040
	Level-2	75.92	62000	4,707,040
	Level-3	73.60	62000	4,563,200
	Level-4	71.48	62000	4,431,760
	Level-5	69.75	62000	4,324,500
	Level-6	68.86	62000	4,269,320
	Level-7	68.86	62000	4,269,320
	Level-8	68.86	62000	4,269,320
	Level-9	69.23	62000	4,292,260
	Roof	68.86	62000	4,269,320
	OHWT	4.31	62000	267,220
	Total			**45,788,243**
	Levels	Quantity (sft)	Unit Price (BDT)	Total Cost
Shuttering with labour	Below GB	10322	170	1,754,672
	Level-1	22138	179	3,951,575
	Level-2	22138	187	4,149,154
	Level-3	22138	197	4,356,612
	Level-4	22138	207	4,574,442
	Level-5	22138	217	4,803,164
	Level-6	22138	228	5,043,322
	Level-7	22138	239	5,295,489
	Level-8	22138	251	5,560,263
	Level-9	22138	264	5,838,276
	Roof	22138	277	6,130,190
	OHWT	1925	291	559,826
	Total			**52,016,985**
	Grand Total			**197,641,396**

Table 4.7: Construction cost of structural part (without foundation) of M-3

Items	Levels	Quantity (cft)	Unit Price (BDT)	Total Cost
Concrete	Below GB	8037	280	2,250,416
	Level-1	19956	294	5,867,082
	Level-2	19956	309	6,160,436
	Level-3	19956	324	6,468,458
	Level-4	19956	340	6,791,880
	Level-5	19956	357	7,131,474
	Level-6	19956	375	7,488,048
	Level-7	19956	394	7,862,451
	Level-8	19956	414	8,255,573
	Level-9	19956	434	8,668,352
	Roof	19956	456	9,101,769
	OHWT	2319	479	1,110,783
	Total			**77,156,721**
	Levels	Quantity (cft)	Unit Price (BDT)	Total Cost
Steel	Below GB	22.35	62000	1,385,824
	Level-1	61.31	62000	3,801,220
	Level-2	61.18	62000	3,793,160
	Level-3	57.92	62000	3,591,040
	Level-4	55.79	62000	3,458,980
	Level-5	55.45	62000	3,437,900
	Level-6	53.15	62000	3,295,300
	Level-7	53.15	62000	3,295,300
	Level-8	53.15	62000	3,295,300
	Level-9	53.49	62000	3,316,380
	Roof	53.15	62000	3,295,300
	OHWT	5.86	62000	363,320
	Total			**36,329,024**
	Levels	Quantity (cft)	Unit Price (BDT)	Total Cost
Shuttering with labour	Below GB	10386	170	1,765,698
	Level-1	23065	179	4,117,019

	Level-2	23065	187	4,322,870
	Level-3	23065	197	4,539,013
	Level-4	23065	207	4,765,964
	Level-5	23065	217	5,004,262
	Level-6	23065	228	5,254,475
	Level-7	23065	239	5,517,199
	Level-8	23065	251	5,793,059
	Level-9	23065	264	6,082,712
	Roof	23065	277	6,386,847
	OHWT	2345	291	681,702
	Total			**54,230,818**
	Grand Total			**167,716,563**

CHAPTER 5
CONCLUSIONS AND SUGGESTIONS

5.1 Introduction

In this study the suitability of flat plates and wide beam column frame structures have been discussed at length in terms of cost and seismic performance. Numerical modelling of the structures has been conducted using ETABS and nonlinear behaviors have been assessed. In modelling the ten-story RMG building, the effect of soft stories have been ignored, a thorough approach should include soft stories. This building had no vertical or plan irregularity. A side–by–side comparison of the same structure with irregularities would have been extremely insightful.

When nonlinear static or pushover analyses (NLSA) were performed the joints of the building were assumed to be rigid, as such no hinges formed at the joints. The joints in that case have to be detailed not permitting the formation of hinges. The foundations of the building were modelled as fixed supports, which is not the true representation of the actual conditions.

Although nonlinear static or pushover analysis (NLSA) generates very reliable results, there can exist structural deficiencies that can only be figured out when nonlinear time history analysis (NLTHA) is performed. This study has been conducted on the basis of the assumptions stated above. Further refinement of the results will require a more thorough analysis minimizing the effects of the limitations during modelling.

5.2 Findings

Following conclusion were drawn based on the study:

I. From static linear analysis it can be seen that maximum top displacement is the largest for flat plates and smallest for beam column frames. The Similar trend holds for base shear, story shear and story drift - flat plates exhibit the weakest response.

II. Flat plate structures are stronger in lateral load compared to wide beam column frame structures. Nonlinear static or pushover analysis based on ASCE 41 overturns the findings of LSA – wide beam frames exhibit the weakest response.

III. While traditional beam column frames are cheaper than all other systems, wide beam column frames have been found to be much cheaper than flat plates.

5.3 Suggestions

I. Performance of other common structural systems, such as flat plate shear wall system and dual system need to be compared with alongside the ones focused on in this study.

II. The building under consideration had no vertical or plan irregularities. How such irregularities may affect the seismic performance of buildings need to be studied

III. In order to get more reliable results and finding out latent structural deficiencies Non Linear Time History Analysis (NLTHA) should be performed.

IV. Modelling should take into account the effect of soft stories.

V. The effect of foundation flexibility or soil structure interaction should be considered.

VI. Since seismic performance of the structures in question have been assessed, the structures should have been designed for earthquake load only. However, in this case, the structures had been designed following the 26 load combinations prescribed by BNBC 1993, of which 12 involves wind loads. In some of the models run, wind load has governed the design. For accurate estimation of seismic performance, design should have been guided by earthquake load combinations only.

REFERENCES

ACI 318 (2008): “Building code requirements for structural concrete and commentary”, American Concrete Institute, Michigan.

ACI 318 (2014): “Building code requirements for structural concrete and commentary”, American Concrete Institute, Michigan.

ACI 356.1R (2012): “Guide for design of slab-column connections in monolithic concrete structure”, American Concrete Institute, Michigan.

Almansa F. L., Domínguez D. and Benavent C. A. (2013), “Vulnerability analysis of RC buildings with wide beams located in moderate seismicity regions”, Elseveir Journal of Engineering Structures, Vol. 46, pp. 687-702.

Altug E. and Elnashai A. S. (2003), “Seismic vulnerability of flat-slab structures”, University of Illinois at Urbana-Champaign, Tech. Rep. DS-9 Project.

Apostolska R. P., Necevska C. G. S., Cvetanovska J. P. and Mircic N. (2008), “Seismic performance of flat-slab building structural systems”, *The 14th World Conference on Earthquake Engineering*, Beijing, China.

ASCE/SEI 41 (2013): “Seismic evaluation and retrofit of existing buildings”, American Society of Civil Engineers, Virginia.

ATC-40 (1996): “Seismic evaluation & retrofit of concrete buildings”, Applied Technology Council, California.

Benavent C. A. (2007), “Seismic behavior of RC wide beam-column connections under dynamic loading”, Journal of Earthquake Engineering, Vol.11, pp. 493-511.

Benavent C. A., Cahís X. and Zahran R. (2009), "Reinforced Concrete exterior wide beam-column connections in existing RC frames subjected to lateral earthquake loads", ASCE Journal of Structural Engineering, Vol. 31, pp. 1414-1424.

Corentin C., Johannes T. B., Luuk A. L., Katia B. and Martin V. H. (2015), "Discontinuous Buckling of Wide Beams and Metabeams", APS Physical Review Letters, Vol. 115, pp. 1-5.

Donmez C. (2015), "Seismic performance of wide-beam infill-joist block RC frames in Turkey", ASCE Journal of Performance of Constructed Facilities, Vol. 29, pp. 102-117.

Erberik M. A. and Elnashai A. S. (2004), "Vulnerability analysis of flat slab structures", in *13th World conference on earthquake engineering*, Vol. 5, pp. 3102.

Eurocode 2 (2004): "Design of concrete structures", European Committee for Standardization, Belgium.

Eurocode 8 (2004): "Design of Structures for Earthquake Resistance", European Committee for Standardization, Belgium.

FEMA 356 (2000): "Prestandard and commentary for the seismic rehabilitation of buildings", Federal Emergency Management Agency, Washington, D.C.

FEMA 440 (2005): "Improvement of nonlinear static seismic analysis procedures", Federal Emergency Management Agency, Washington, D.C.

Gagan K. R. R. and Nethravathi S. M. (2015), "Pushover analysis of framed structure with flat plate and flat slab for different structural systems" in *International Journal of Innovative Research and Creative Technology*, Vol. 2, pp. 54-59.

Gasparini D. A. (2002)," Contribution of C.A.P. turner to development of RC flat slabs 1905-1909", ASCE Journal of Structural Engineering, Vol.128, pp. 728-746.

Gasparini D. A. (2005), "Discussion of Contributions of C. A. P. Turner to Development of Reinforced Concrete Flat Slabs 1905–1909" ASCE Journal of Structural Engineering, Vol. 131, pp. 524-525.

Gentry T. R. and Wight J. K. (1994), "Wide beam-column connections under earthquake-type loading", EERI Journal of Earthquake Spectra, Vol. 10, pp. 675-703.

Goel R. K. (2008), "Evaluation of current nonlinear static procedures for reinforced concrete buildings", *The 14th World Conference on Earthquake Engineering*, Beijing, China.

Harras O. A. (2015), "*Seismic behaviour and nonlinear modeling of reinforced concrete flat slab-column connections*" M. Sc. Engg. Thesis, University of British Columbia, Canada.

Hatamoto H., Bessho S. and Matsuzaki Y. (1991), "Reinforced concrete wide-beam-to-column sub-assemblages subjected to lateral load", ACI Special Publication, Vol. 123, pp. 291-316.

Helou S. H. and Awad R. (2014), "Performance based analysis of hidden beams in reinforced concrete structures", MATEC Web conference, Vol. 16, pp. 1-5.

James M. L. and James K. W. (1999) , "Reinforced concrete exterior wide beam-column-slab connections subjected to lateral earthquake loading", ACI Structural Journal, Vol.96, pp. 577-585.

James M. L. and James K. W. (2001), "Behavior and design of reinforced concrete beam-column connections with wide beams", EERI Journal of Earthquake Spectra, Vol. 17, pp. 479-505.

James M. L. and James K. W. (2001), "Reinforced concrete wide beam-column connections vs. conventional construction: Resistance to lateral earthquake loads", EERI Journal of Earthquake Spectra, Vol. 10, pp. 479-505.

James M. L. (April, 2012), “Behavior and design of reinforced concrete beam-column connections with wide beams”, ASCE Structures Congress 2001, pp. 1-2.

Kang T. H. K., Wallace J. W. and Elwood K. J. (2009), “Nonlinear Modeling of flat-plate systems”, ASCE Journal of Structural Engineering, Vol. 135, pp. 135-147.

Kim J. and Kim T. (2008), “Seismic performance evaluation of non-seismic designed flat-plate structures”, ASCE Journal of Performance of Constructed Facilities, Vol. 22, pp. 356-363.

Li B. and Kulkarni S. A. (2010), “Seismic behavior of reinforced concrete exterior wide beam-column joints”, ASCE Journal of Structural Engineering, Vol. 136, pp. 26-36.

Lubell A. S., Bentz E. C. and Collins M. P. (2008), “One-Way shear in wide concrete beams with narrow supports”, ASCE Structures Congress 2008, pp. 1-10.

NZS 3101 (2006): “Concrete structures standard”, New Zealand Standards, Wellington.

Popov E. P., Cohen J. M., Koso T. K. and Kasai K. (1992), “Behavior of interior narrow and wide beams”, ACI Structural Journal, Vol. 89, pp. 607-616.

Shuraim A. B. (2012), “Transverse stirrup configurations in RC wide shallow beams supported on narrow columns”, Journal of Structural Engineering, Vol. 138, pp. 416-424.

Song J.W., Song J.G., Lee Y.W. and Kim G.W. (2012), “Seismic performance of flat plate system with shear reinforcements”, *The 15th World Conference on Earthquake Engineering*, Lisbon.

Stehle J. S., Abdouk K., Goldsworthy H. and Mendis P. (2002), “The seismic performance of reinforced concrete wide band beam construction”, *The 12th World Conference on Earthquake Engineering*, Auckland, New Zealand.

Taqieddin Z. N. (2014), “Deflection of wide hidden beams in one-way slab systems: a nonlinear finite element study”, The International Conference on Advances in Civil and Structural Engineering, Kuala Lumpur, Malaysia.

Tian Y., Jirsa J. O. and Bayrak O. (2009), “Nonlinear modeling of slab-column connections under cyclic loading”, ACI structural journal, Vol. 106, pp. 30-38.

Wang W. and Teng S. (2008), “Finite-element analysis of reinforced concrete flat plate structures by layered shell element”, ASCE Journal of Structural Engineering, Vol. 134, pp. 1862-1872.

Zaidee S. R. and Awad A. K. (2017), “Validation of finite element modeling for wide & shallow reinforced concrete beams”, International Journal of Science and Research, Vol. 6, pp. 1890-1896.

APPENDIX A

DESIGN OUTPUT FROM LINEAR STATIC ANALYSIS

Annexure A1: Model-1 Design Outputs

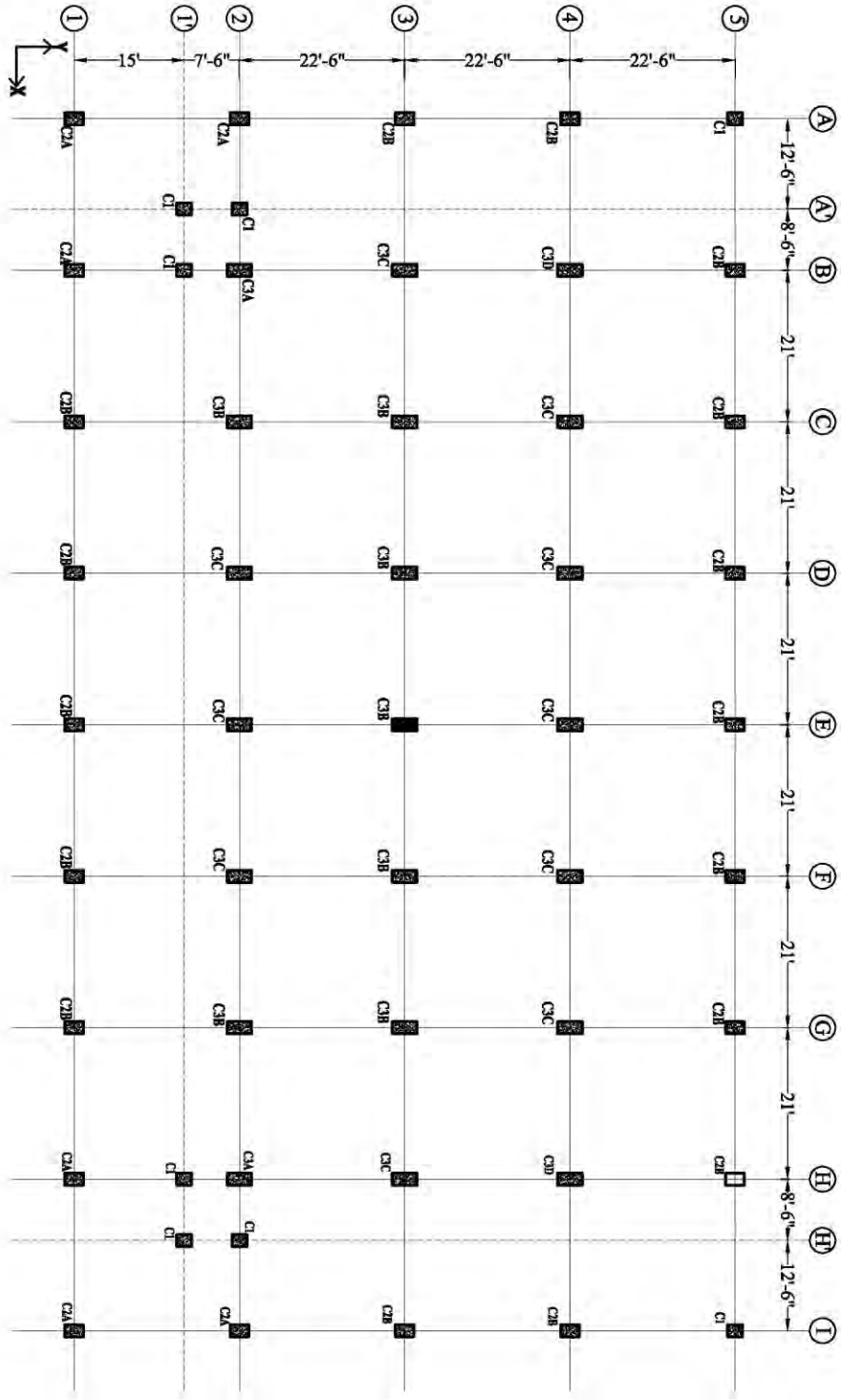

Figure A-3.1: Grid and column layout of Model-1

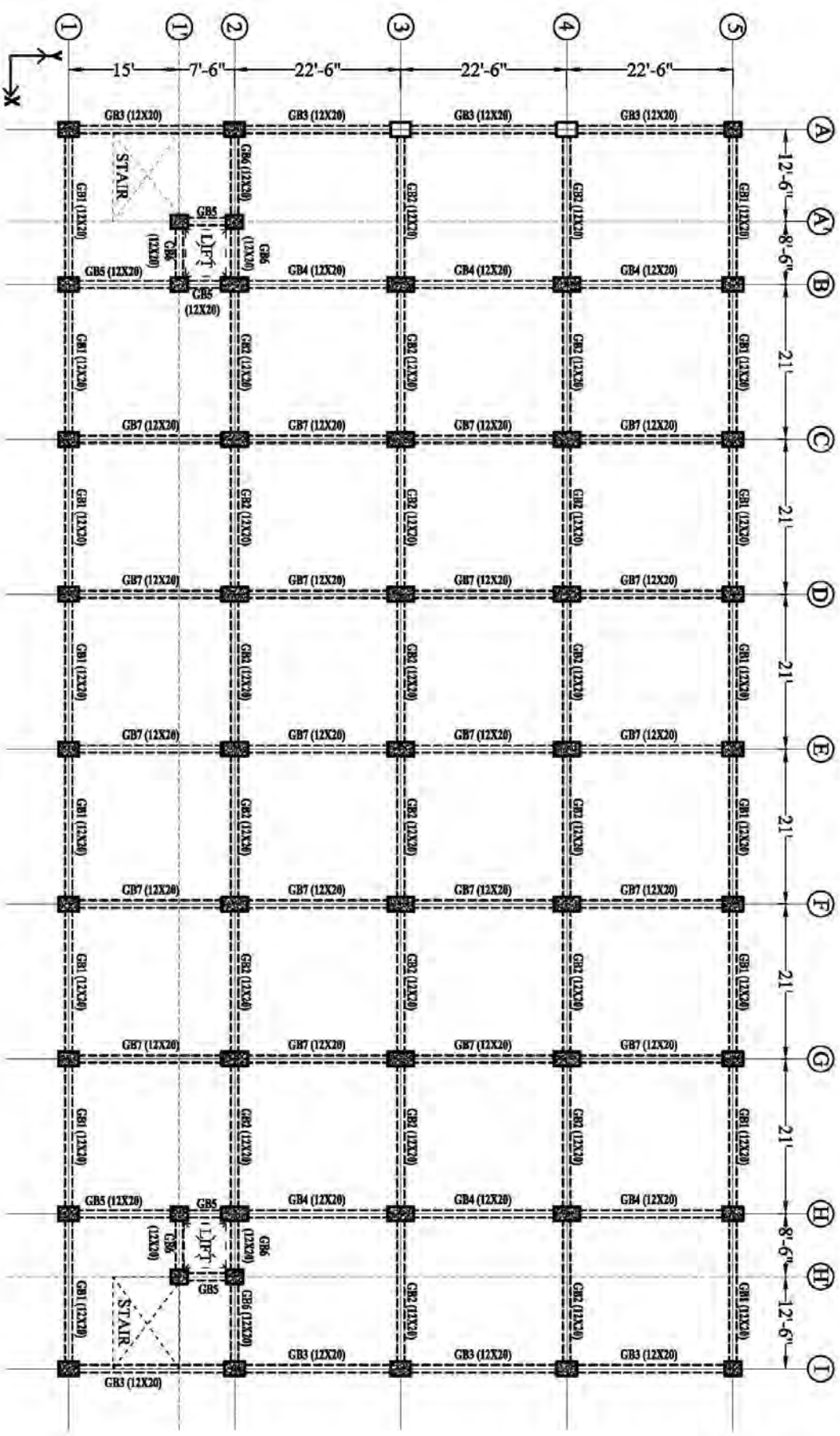

Figure A-3.2: Grade beam layout of Model-1

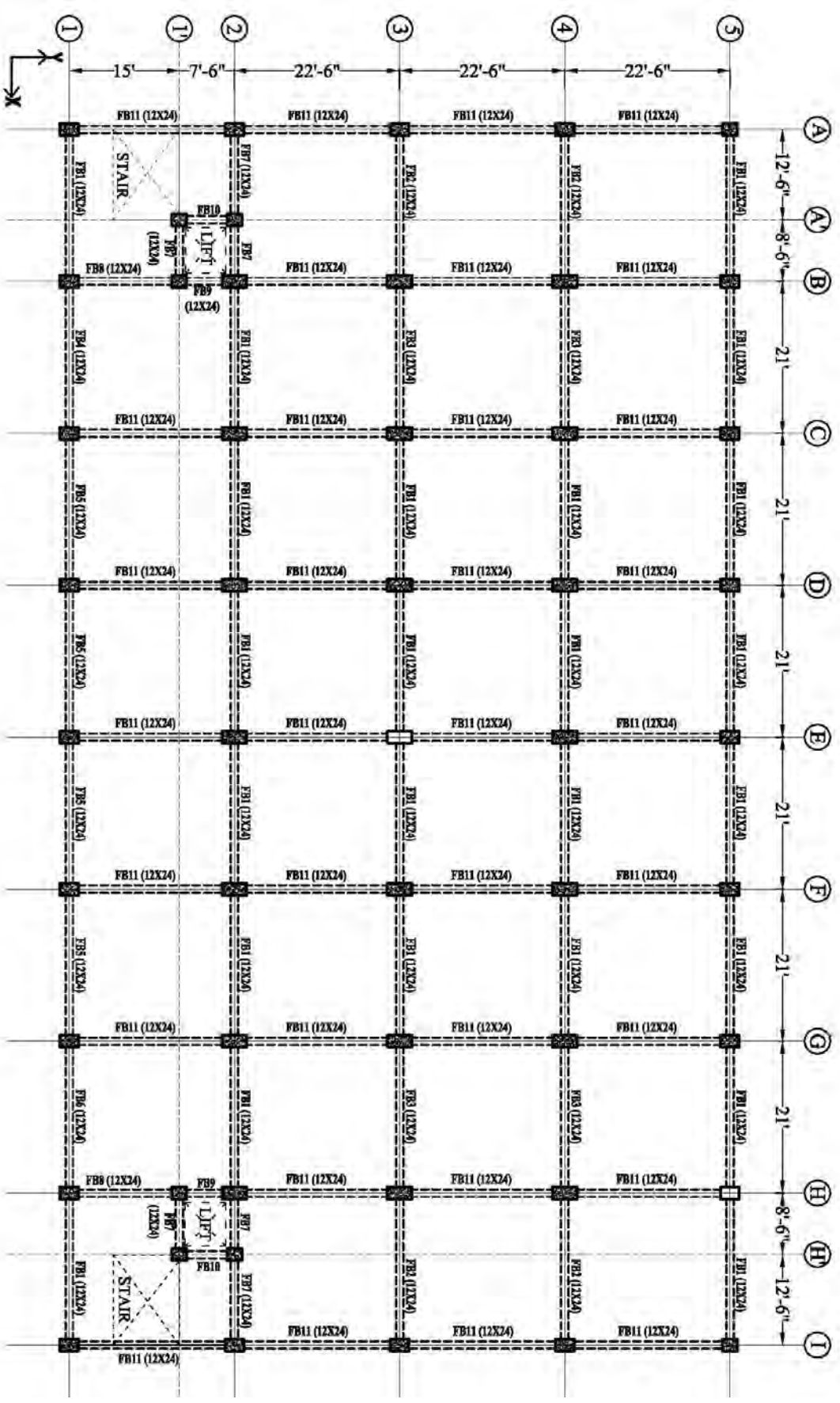

Figure A-3.3: Floor beam layout of Model-1 (1F to 5F)

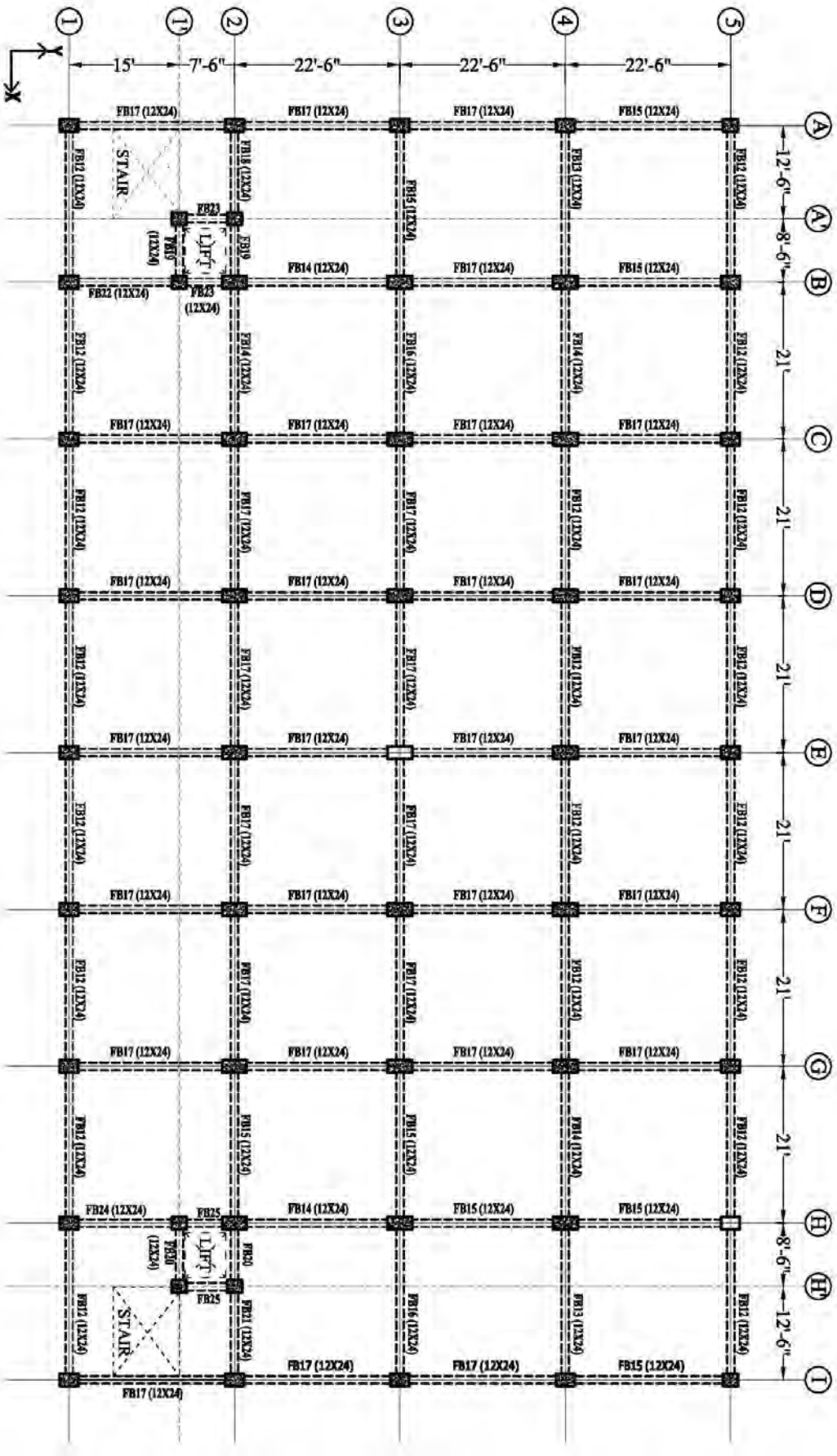

Figure A-3.4: Floor beam layout of Model-1 (6F to Roof)

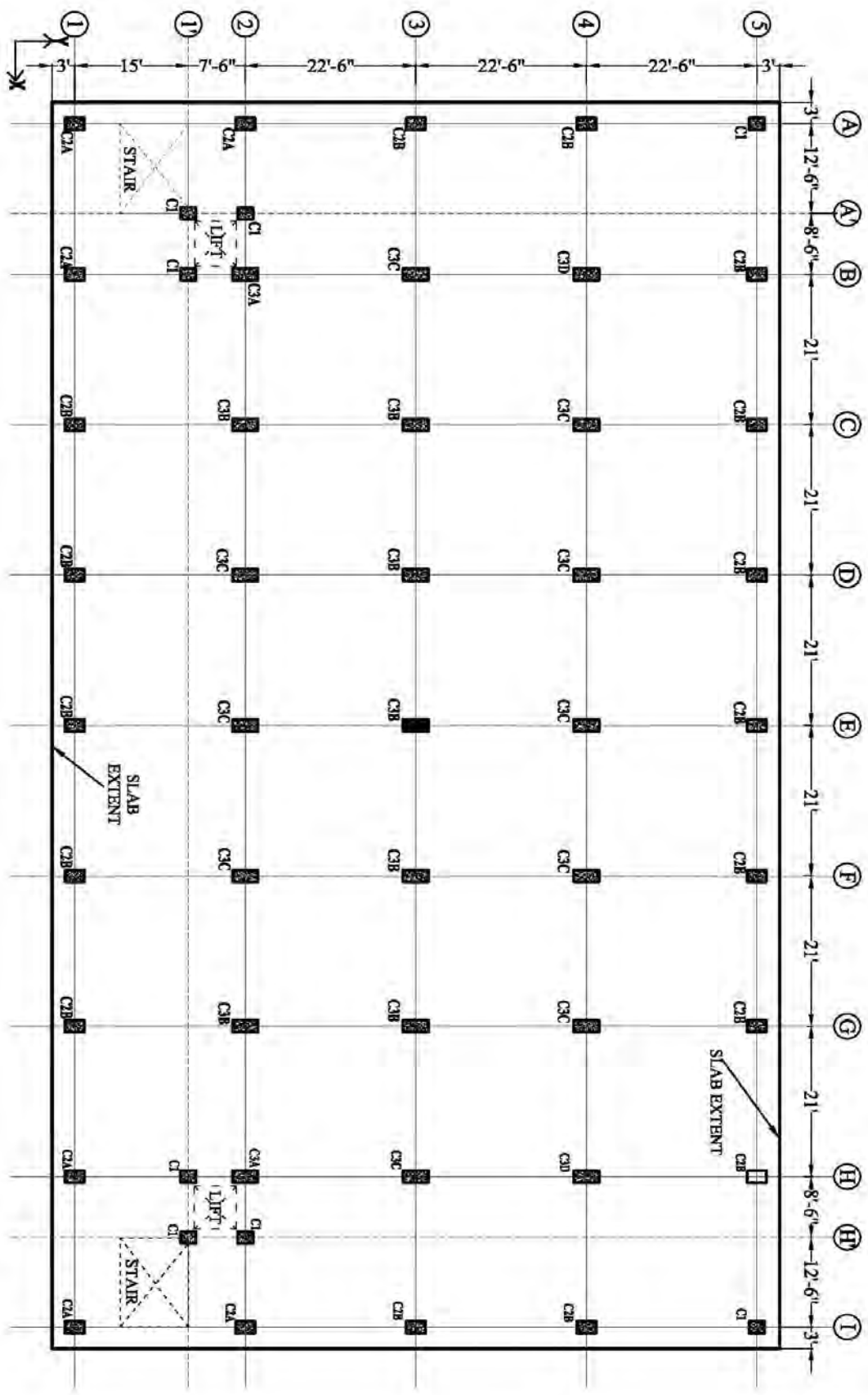

Figure A-3.5: Slab layout of Model-1

Table A-3.1: Column details (Model-1)

Column ID	Below Ground level		Level-1		Level-2 & Level-3		Level-4 to UP	
	Column Size	Reinforcement	Column Size	Reinforcement	Column Size	Reinforcement	Column Size	Reinforcement
C1	23"×27"	20-20mm	20"x24"	20-20mm	20"x24"	16-20mm	20"x24"	12-20mm
C2A	23"×33"	22-20mm	20"x30"	22-20mm	20"x30"	16-20mm	20"x30"	14-20mm
C2B	23"×33"	22-25mm	20"x30"	22-25mm	20"x30"	16-25mm	20"x30"	10-25mm
C3A	23"×43"	22-20mm	20"x40"	22-20mm	20"x40"	18-20mm	20"x40"	18-20mm
C3B	23"×43"	24-25mm	20"x40"	24-25mm	20"x40"	16-25mm	20"x40"	12-25mm
C3C	23"×43"	26-25mm	20"x40"	26-25mm	20"x40"	18-25mm	20"x40"	12-25mm
C3D	23"×43"	28-25mm	20"x40"	28-25mm	20"x40"	20-25mm	20"x40"	12-25mm

Table A-3.2: Beam details (Model-1)

Story: 1F to 5F				
Frame Property	Top Area I-end	Top Area J-end	Bottom Area I-end	Bottom Area J-end
	in²	in²	in²	in²
FB01.12×24	11-16 mm	11-16 mm	6-16 mm	6-16 mm
FB02.12×24	11-16 mm	12-16 mm	6-16 mm	6-16 mm
FB03.12×24	12-16 mm	11-16 mm	6-16 mm	6-16 mm
FB04.12×24	11-16 mm	10-16 mm	6-16 mm	6-16 mm
FB05.12×24	10-16 mm	10-16 mm	6-16 mm	6-16 mm
FB06.12×24	10-16 mm	11-16 mm	6-16 mm	6-16 mm
FB07.12×24	9-16 mm	9-16 mm	9-16 mm	9-16 mm
FB08.12×24	9-16 mm	5-20 mm	6-16 mm	7-16 mm
FB09.12×24	6-16 mm	9-16 mm	6-16 mm	6-16 mm
FB10.12×24	6-16 mm	6-16 mm	6-16 mm	6-16 mm
FB11.12×24	10-16 mm	10-16 mm	6-16 mm	6-16 mm

Story: 6F to Roof				
Frame Property	**Top Area I-end**	**Top Area J-end**	**Bottom Area I-end**	**Bottom Area J-end**
FB12.12×24	9-16 mm	9-16 mm	6-16 mm	6-16 mm
FB13.12×24	9-16 mm	10-16 mm	5-16 mm	5-16 mm
FB14.12×24	10-16 mm	10-16 mm	6-16 mm	6-16 mm
FB15.12×24	10-16 mm	10-16 mm	6-16 mm	6-16 mm
FB16.12×24	10-16 mm	9-16 mm	6-16 mm	6-16 mm
FB17.12×24	9-16 mm	9-16 mm	6-16 mm	6-16 mm
FB18.12×24	5-16 mm	7-16 mm	6-16 mm	5-16 mm
FB19.12×24	7-16 mm	5-16 mm	5-16 mm	3-16 mm
FB20.12×24	3-16 mm	3-16 mm	3-16 mm	3-16 mm
FB21.12×24	7-16 mm	5-16 mm	4-16 mm	6-16 mm
FB22.12×24	5-20 mm	5-16 mm	5-16 mm	6-16 mm
FB23.12×24	3-16 mm	5-20 mm	3-16 mm	5-16 mm
FB24.12×24	5-20 mm	5-16 mm	4-16 mm	6-16 mm
FB25.12×24	3-16 mm	3-16 mm	3-16 mm	3-16 mm

Story: GF				
Frame Property	**Top Area I-end**	**Top Area J-end**	**Bottom Area I-end**	**Bottom Area J-end**
GB1.12×20	6-16 mm	6-16 mm	3-16 mm	3-16 mm
GB2.12×20	5-16 mm	5-16 mm	4-16 mm	4-16 mm
GB3.12×20	5-16 mm	5-16 mm	3-16 mm	3-16 mm
GB4.12×20	3-16 mm	3-16 mm	3-16 mm	3-16 mm
GB5.12×20	4-16 mm	4-16 mm	4-16 mm	4-16 mm
GB6.12×20	6-16 mm	6-16 mm	6-16 mm	6-16 mm
GB7.12×20	3-16 mm	3-16 mm	3-16 mm	3-16 mm

NOTE: Co-ordinate of J-end > I-end in Global X, Y Co-ordinate System at the plan of a member.

Table A-3.3: Slab details (Model-1)

Slab Thickness (inch)	Top Reinforcement at both Direction		Bottom Reinforcement at both Direction	
	Column Strip	**Middle Strip**	**Column Strip**	**Middle Strip**
6	12mm @ 6 in c/c	12mm @ 6 in c/c	10mm @ 6 in c/c	10mm @ 6 in c/c

Annexure A2: Model-2 Design Outputs

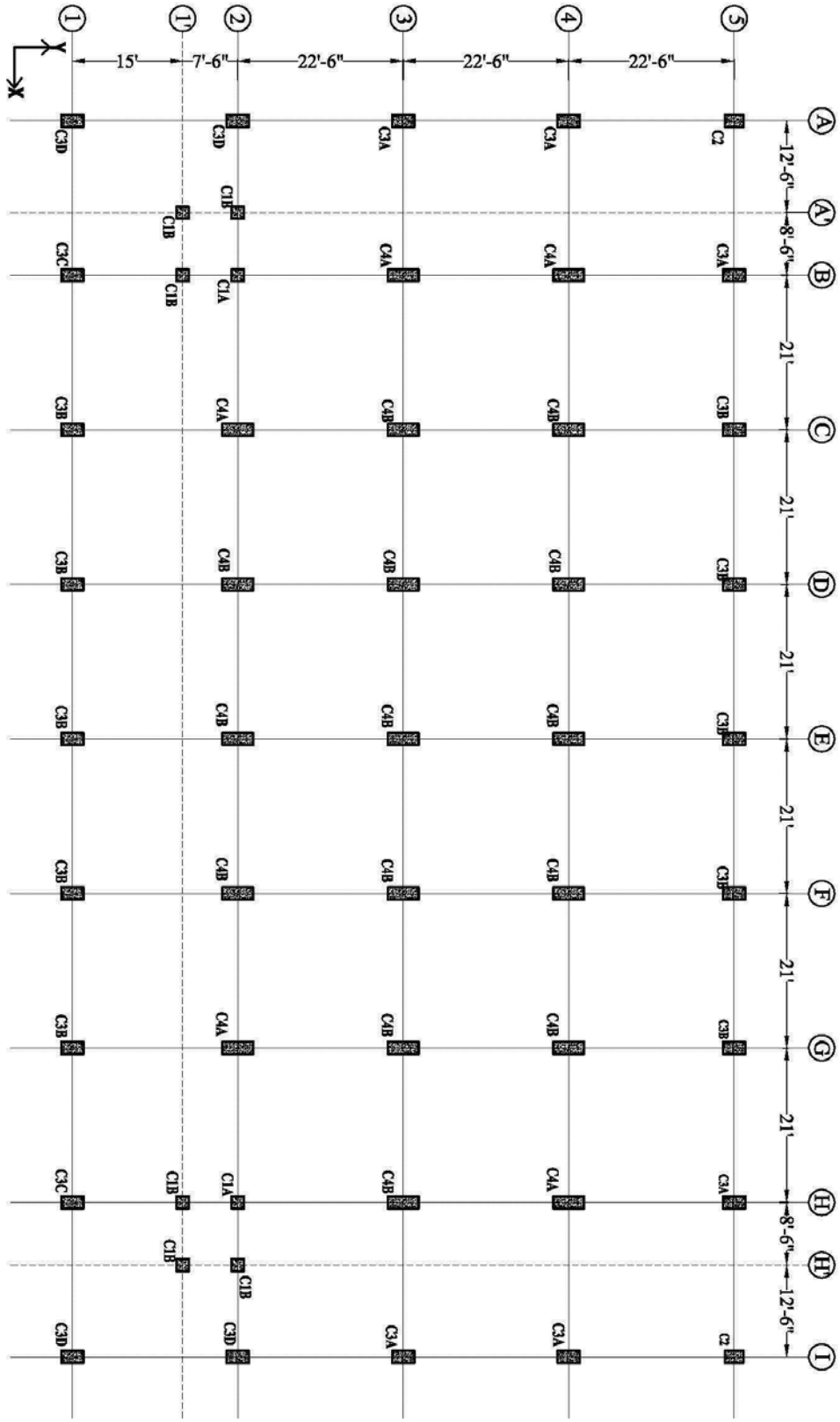

Figure A-3.6: Grid and column layout of Model-2

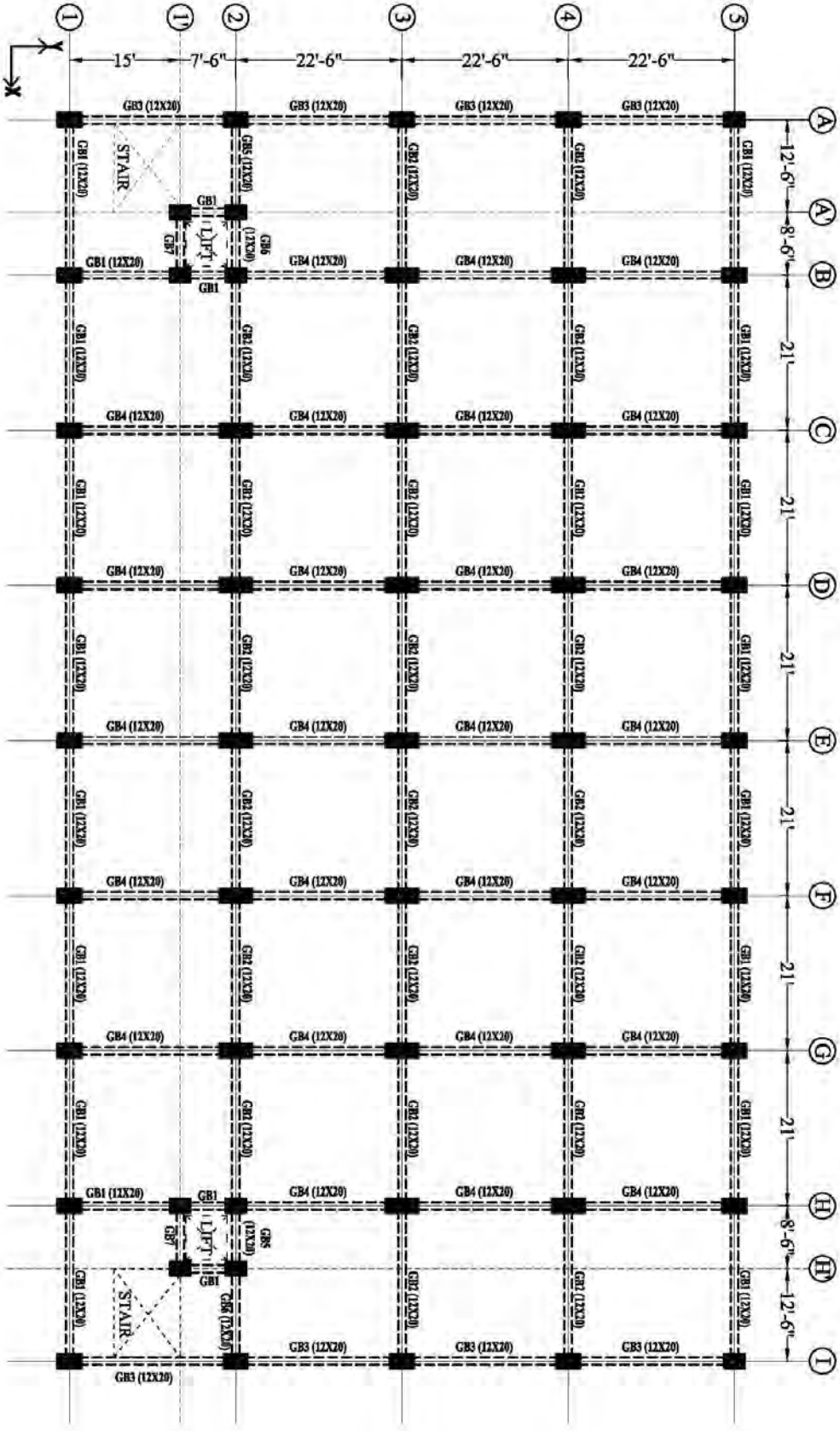

Figure A-3.7: Grade beam layout of Model-2

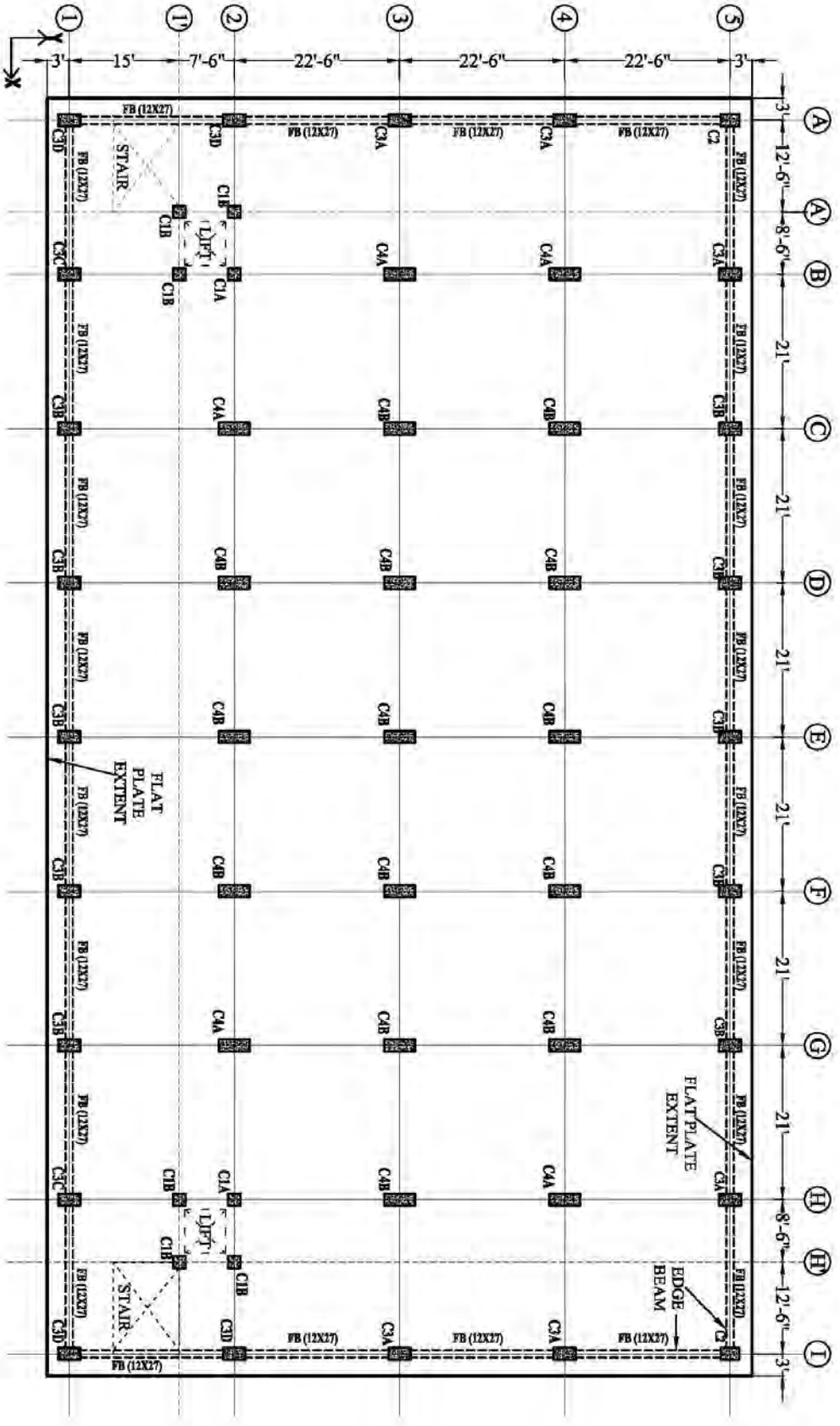

Figure A-3.8: Edge beam and slab layout of Model-2

Table A-3.4: Column details (Model-2)

Column ID	Column Size	Reinforcement	Column Size	Reinforcement			
		Below GB		Level-1	Level-2	Level-3	Level-4 to Top
C1-A	23×23	22-25mm	20X20	22-25mm	16-25mm	10-25mm	6-25mm
C1-B	23×23	18-25mm	20X20	18-25mm	12-25mm	8-25mm	6-25mm
C2	23×33	18-25mm	20X30	18-25mm	18-25mm	12-25mm	8-25mm
C3-A	23×39	22-25mm	20X36	22-25mm	22-25mm	16-25mm	10-25mm
C3-B	23×39	20-25mm	20X36	20-25mm	20-25mm	14-25mm	10-25mm
C3-C	23×39	18-25mm	20X36	18-25mm	18-25mm	10-25mm	10-25mm
C3-D	23×39	16-25mm	20X36	16-25mm	16-25mm	10-25mm	10-25mm
C4-A	23×53	24-25mm	20X50	24-25mm	18-25mm	14-25mm	14-25mm
C4-B	23×53	22-25mm	20X50	22-25mm	14-25mm	14-25mm	14-25mm

Table A-3.5: Beam details (Model-2)

Story: 1F to 5F				
Frame Property	**Top Area I-end**	**Top Area J-end**	**Bottom Area I-end**	**Bottom Area J-end**
FB1.12×27	11-20 mm	11-20 mm	7-20 mm	7-20 mm
FB2.12×27	10-20 mm	10-20 mm	7-20 mm	7-20 mm
FB3.12×27	11-20 mm	11-20 mm	8-20 mm	8-20 mm
FB6.12×24	6-20 mm	6-20 mm	6-20 mm	6-20 mm
FB7.12×24	5-20 mm	5-20 mm	5-20 mm	5-20 mm

Story: 6F to Roof				
Frame Property	**Top Area I-end**	**Top Area J-end**	**Bottom Area I-end**	**Bottom Area J-end**
FB4.12×27	11-20 mm	11-20 mm	6-20 mm	6-20 mm
FB5.12×27	12-20 mm	12-20 mm	6-20 mm	6-20 mm
FB8.12×24	3-20 mm	3-20 mm	3-20 mm	3-20 mm
Story: GF				

Frame Property	Top Area I-end	Top Area J-end	Bottom Area I-end	Bottom Area J-end
GB1.12×20	5-20 mm	5-20 mm	2-20 mm	2-20 mm
GB2.12×20	5-16 mm	5-16 mm	5-16 mm	5-16 mm
GB3.12×20	4-16 mm	4-16 mm	3-16 mm	3-16 mm
GB4.12×20	3-16 mm	3-16 mm	3-16 mm	3-16 mm
GB5.12×20	7-16 mm	6-16 mm	5-20 mm	7-16 mm
GB6.12×20	6-16 mm	7-16 mm	7-16 mm	5-20 mm
GB7.12×20	7-16 mm	7-16 mm	5-20 mm	5-20 mm

NOTE: Co-ordinate of J-end > I-end in Global X, Y Co-ordinate System at the plan of a member.

Table A-3.6: Slab details (Model-2)

Slab Thickness (inch)	Top Reinforcement at both Direction		Bottom Reinforcement at both Direction	
	Column Strip	Middle Strip	Column Strip	Middle Strip
10	16mm @ 5 in c/c	12mm @ 5 in c/c	10mm @ 5 in c/c	10mm @ 5 in c/c

Annexure A3: Model-3 Design Outputs

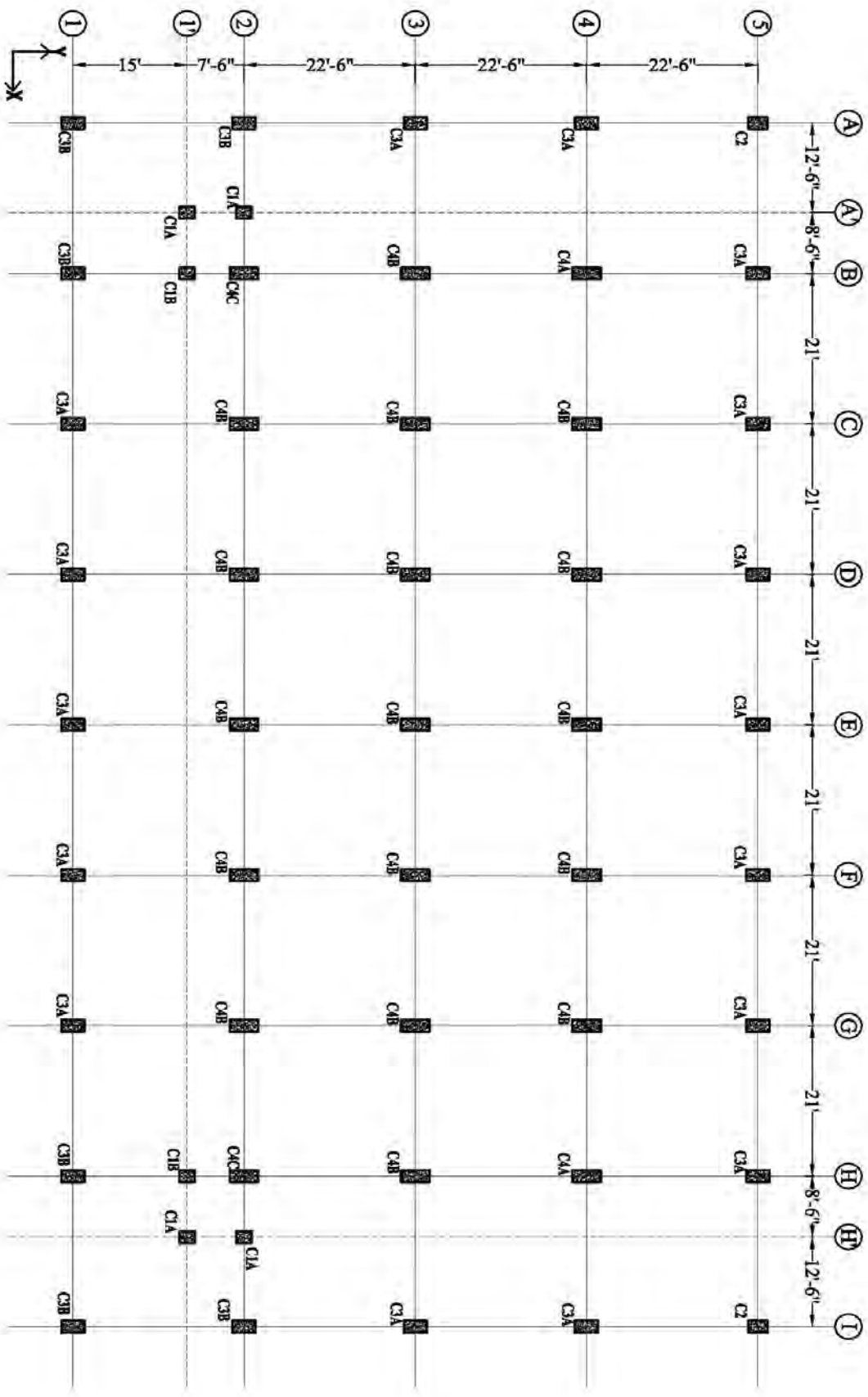

Figure A-3.9: Grid and column layout of Model-3

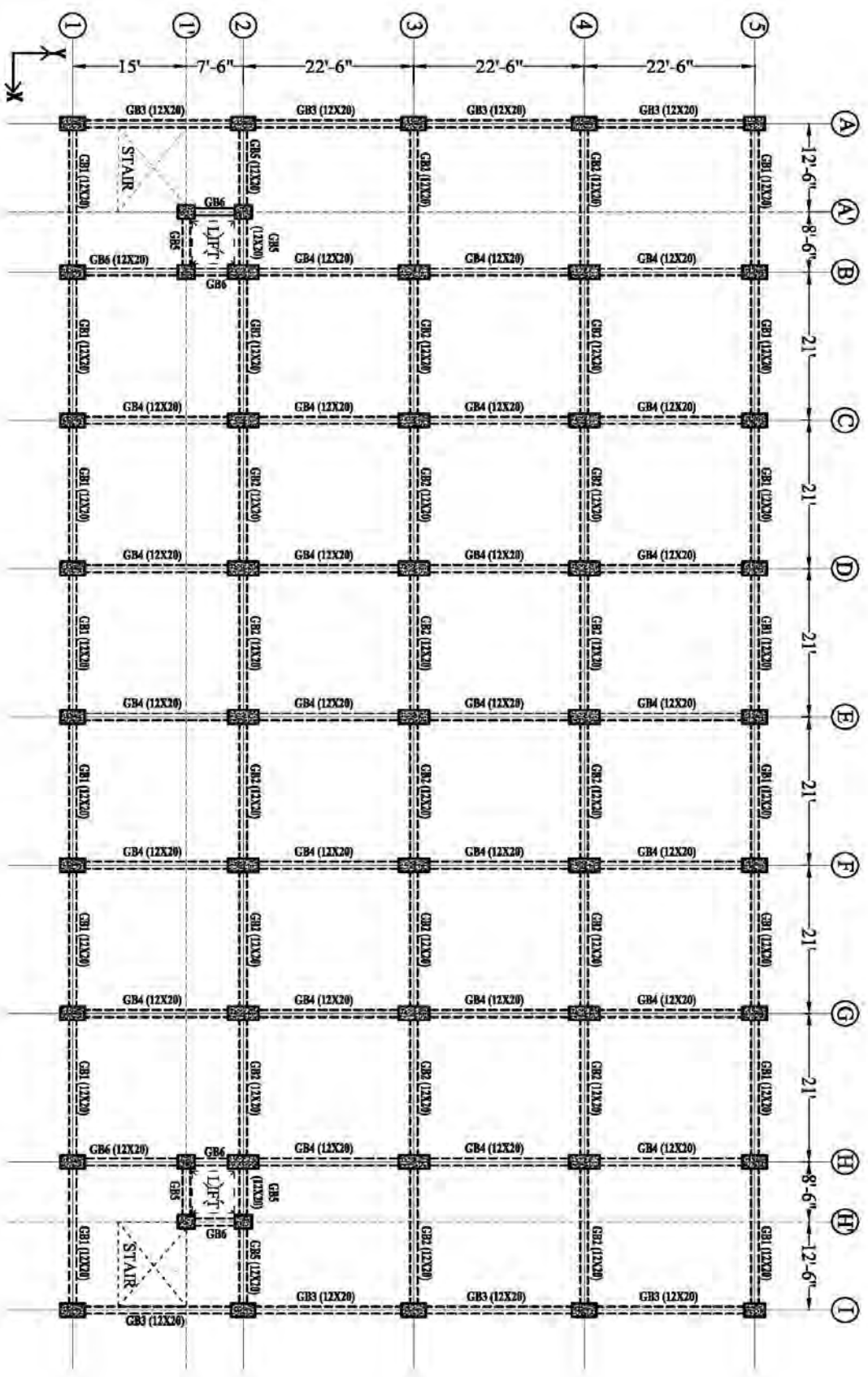

Figure A-3.10: Grade beam layout of Model-3

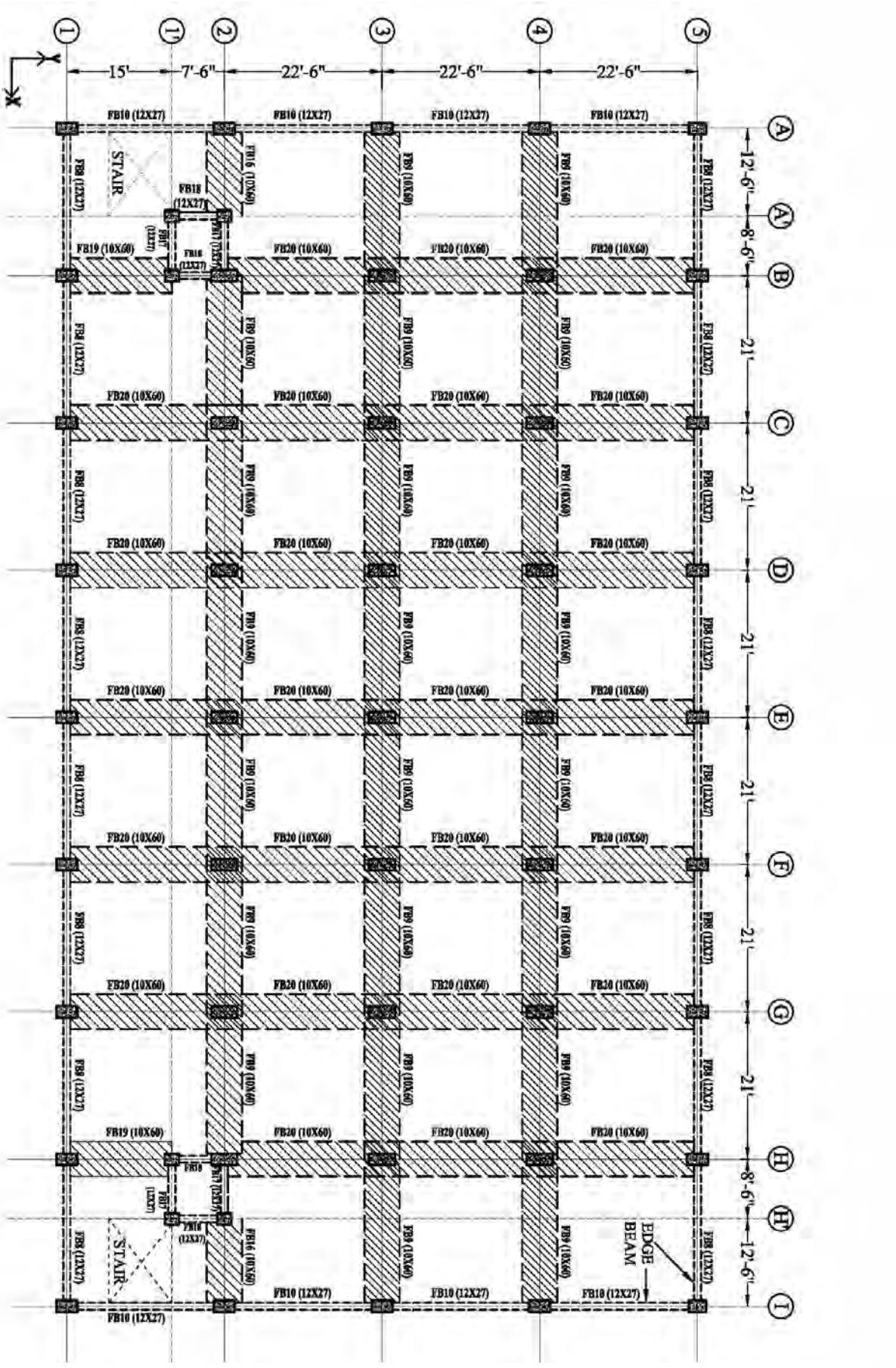

Figure A-3.11: Floor beam layout of Model-3 (1F to 5F)

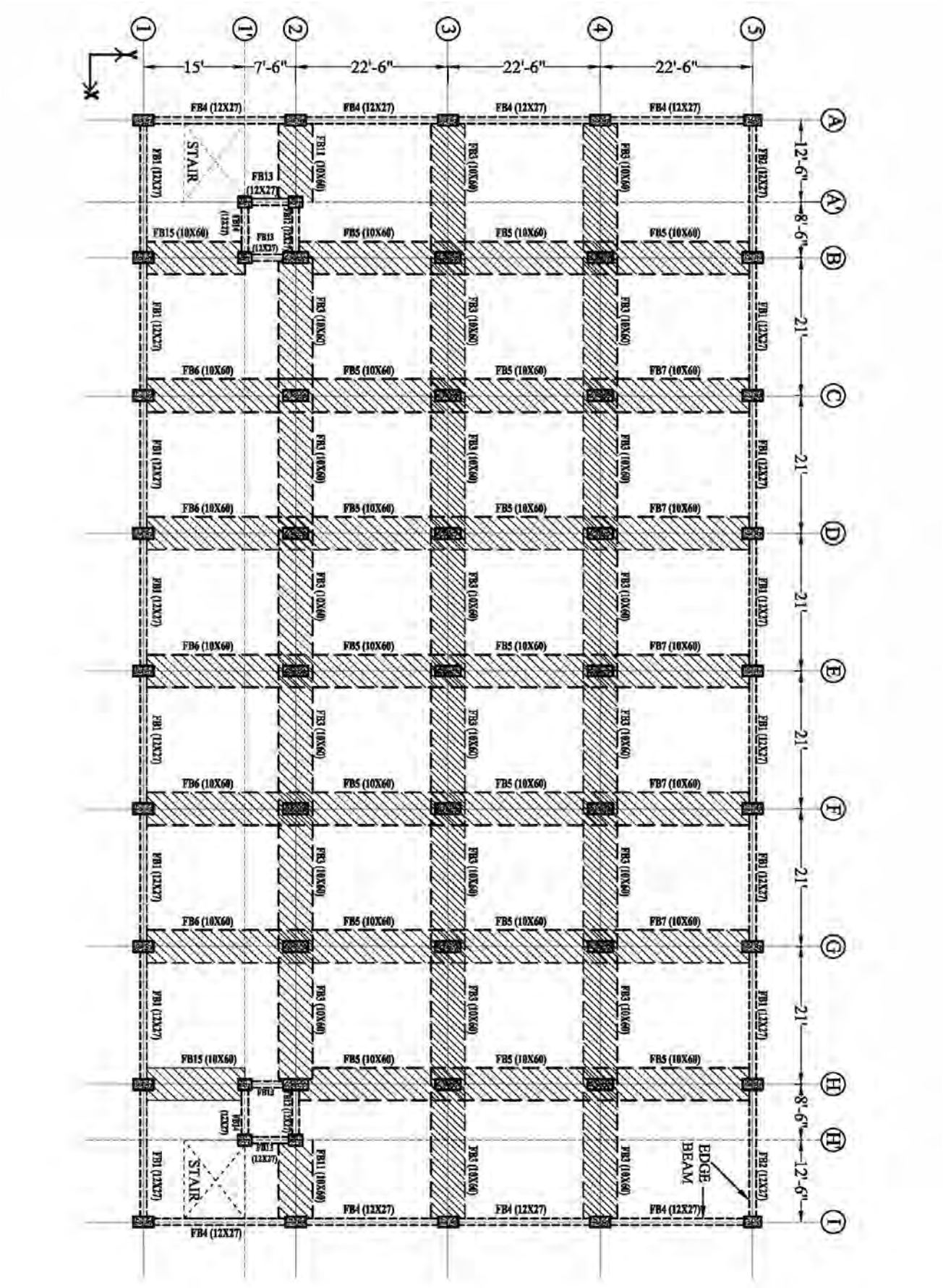

Figure A-3.12: Floor beam layout of Model-3 (6F to Roof)

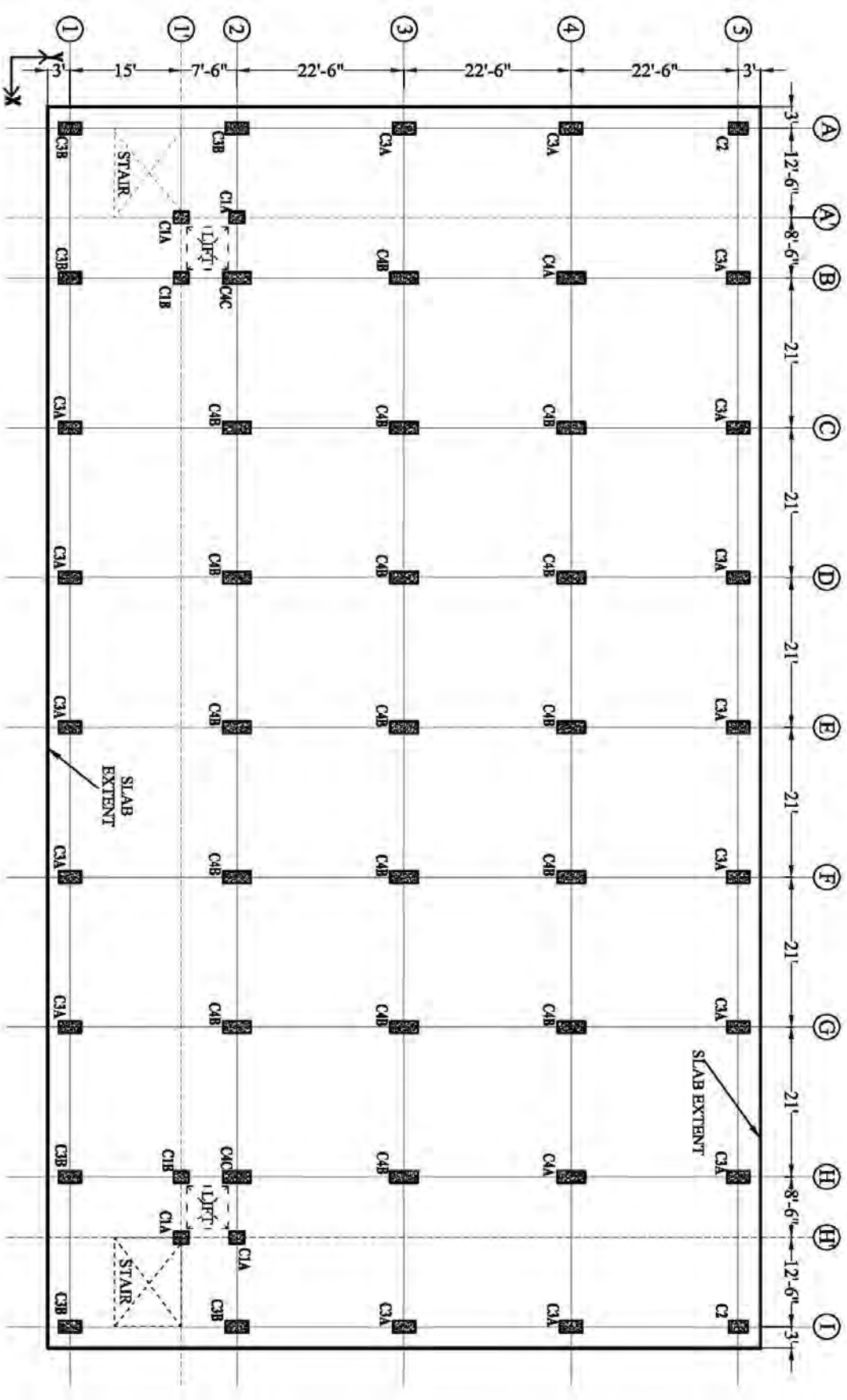

Figure A-3.13: Slab layout of Model-3

Table A-3.7: Column details (Model-3)

Column ID	Size (in×in)	Reinforcement	Size	Reinforcement		
		Below GB		Level-1	Level-2	Level-3 to Top
C1-A	23×27	12-25mm	20X24	12-25mm	12-25mm	8-25mm
C1-B	23×27	10-25mm	20X24	10-25mm	10-25mm	10-25mm
C2	23×33	16-20mm	20X30	14-20mm	14-20mm	14-20mm
C3-A	23×39	18-25mm	20X36	18-25mm	12-25mm	10-25mm
C3-B	23×39	12-25mm	20X36	12-25mm	10-25mm	10-25mm
C4-A	23×48	30-25mm	20X45	30-25mm	20-25mm	12-25mm
C4-B	23×48	28-25mm	20X45	28-25mm	20-25mm	12-25mm
C4-C	23×48	16-25mm	20X45	12-25mm	12-25mm	12-25mm

Table A-3.8: Beam details (Model-3)

Story: 1F to 5F				
Frame Property	Top Area I-end	Top Area J-end	Bottom Area I-end	Bottom Area J-end
FB1.12×27	9-20 mm	9-20 mm	5-20 mm	5-20 mm
FB2.12×27	9-20 mm	9-20 mm	6-20 mm	5-20 mm
FB3.10×60	13-20 mm	13-20 mm	7-20 mm	7-20 mm
FB4.12×27	9-20 mm	9-20 mm	6-20 mm	6-20 mm
FB5.10×60	10-20 mm	10-20 mm	8-20 mm	8-20 mm
FB6.10×60	11-20 mm	10-20 mm	8-20 mm	8-20 mm
FB7.10×60	10-20 mm	11-20 mm	8-20 mm	8-20 mm
FB11.10×60	10-20 mm	10-20 mm	8-20 mm	6-20 mm
FB12.12×27	7-20 mm	9-20 mm	7-20 mm	8-20 mm
FB13.12×27	5-20 mm	5-20 mm	5-20 mm	5-20 mm
FB14.12×27	6-20 mm	6-20 mm	6-20 mm	6-20 mm
FB15.10×60	9-20 mm	11-20 mm	7-20 mm	5-20 mm

Story: 6F to Roof				
Frame Property	**Top Area I-end**	**Top Area J-end**	**Bottom Area I-end**	**Bottom Area J-end**
FB8.12×27	7-20 mm	7-20 mm	4-20 mm	4-20 mm
FB9.10×60	11-20 mm	11-20 mm	6-20 mm	6-20 mm
FB10.12×27	9-20 mm	9-20 mm	5-20 mm	5-20 mm
FB16.10×60	7-20 mm	9-20 mm	6-20 mm	6-20 mm
FB17.12×27	4-20 mm	4-20 mm	3-20 mm	3-20 mm
FB18.12×27	3-20 mm	3-20 mm	3-20 mm	3-20 mm
FB19.12×27	10-20 mm	10-20 mm	6-20 mm	6-20 mm
FB20.10×60	10-20 mm	10-20 mm	8-20 mm	8-20 mm

Story: GF				
Frame Property	**Top Area I-end**	**Top Area J-end**	**Bottom Area I-end**	**Bottom Area J-end**
GB1.12×20	5-20 mm	5-20 mm	4-16 mm	4-16 mm
GB2.12×20	5-16 mm	5-16 mm	5-16 mm	5-16 mm
GB3.12×20	5-16 mm	5-16 mm	3-16 mm	3-16 mm
GB4.12×20	3-16 mm	3-16 mm	3-16 mm	3-16 mm
GB5.12×20	5-20 mm	5-20 mm	5-20 mm	5-20 mm
GB6.12×20	5-16 mm	5-16 mm	5-16 mm	5-16 mm

NOTE: Co-ordinate of J-end > I-end in Global X, Y Co-ordinate System at the plan of a member.

Table A-3.9: Slab details (Model-3)

Slab Thickness (inch)	**Top Reinforcement at both Direction**		**Bottom Reinforcement at both Direction**	
	Column Strip	**Middle Strip**	**Column Strip**	**Middle Strip**
6	12mm @ 6 in c/c	10mm @ 5 in c/c	10mm @ 6 in c/c	10mm @ 6 in c/c

APPENDIX B
MODELING PARAMETERS FOR NON-LINEAR STATIC ANALYSIS

Annexure B1: Models Layouts Used in NLSA

Model 1 and Model 3 layout and details are described in Appendix A. Model 2 and Model 4 Effective beam width (Equivalent to flat plate) are discussed in this section and other relevant information is discussed in appendix A. Model 4 column details are same as Model 1 and flat plate details are same as Model 2.

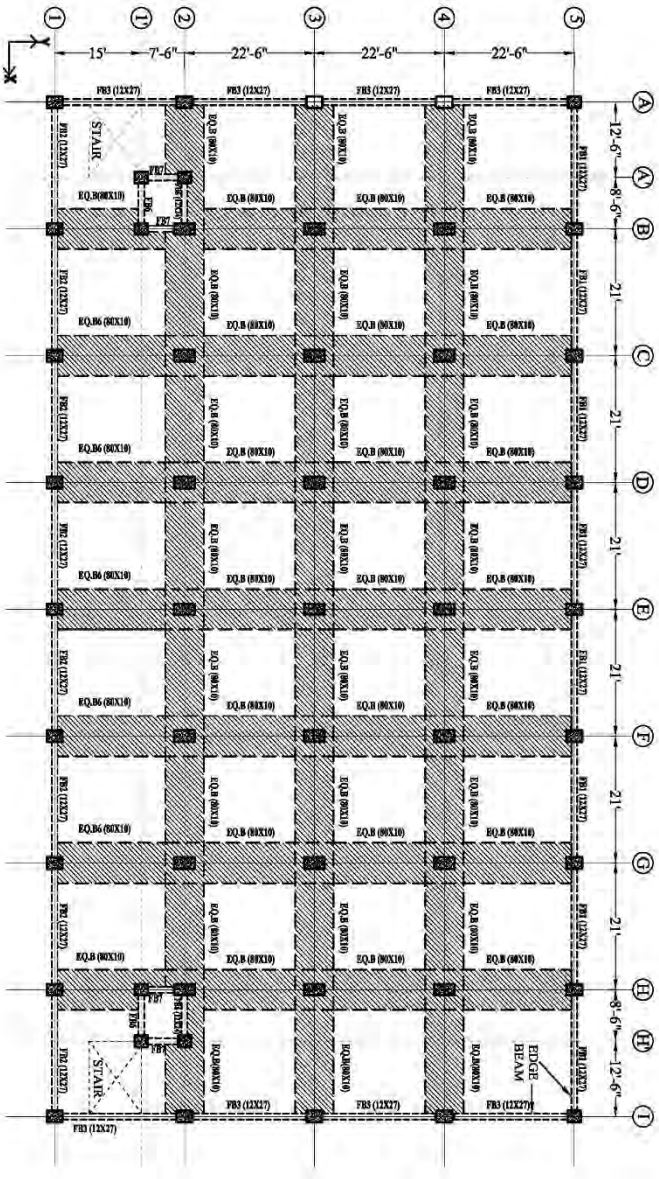

Figure B-3.1: Model 2 effective beam width (eqt to flat plate) layout (F1-F5)

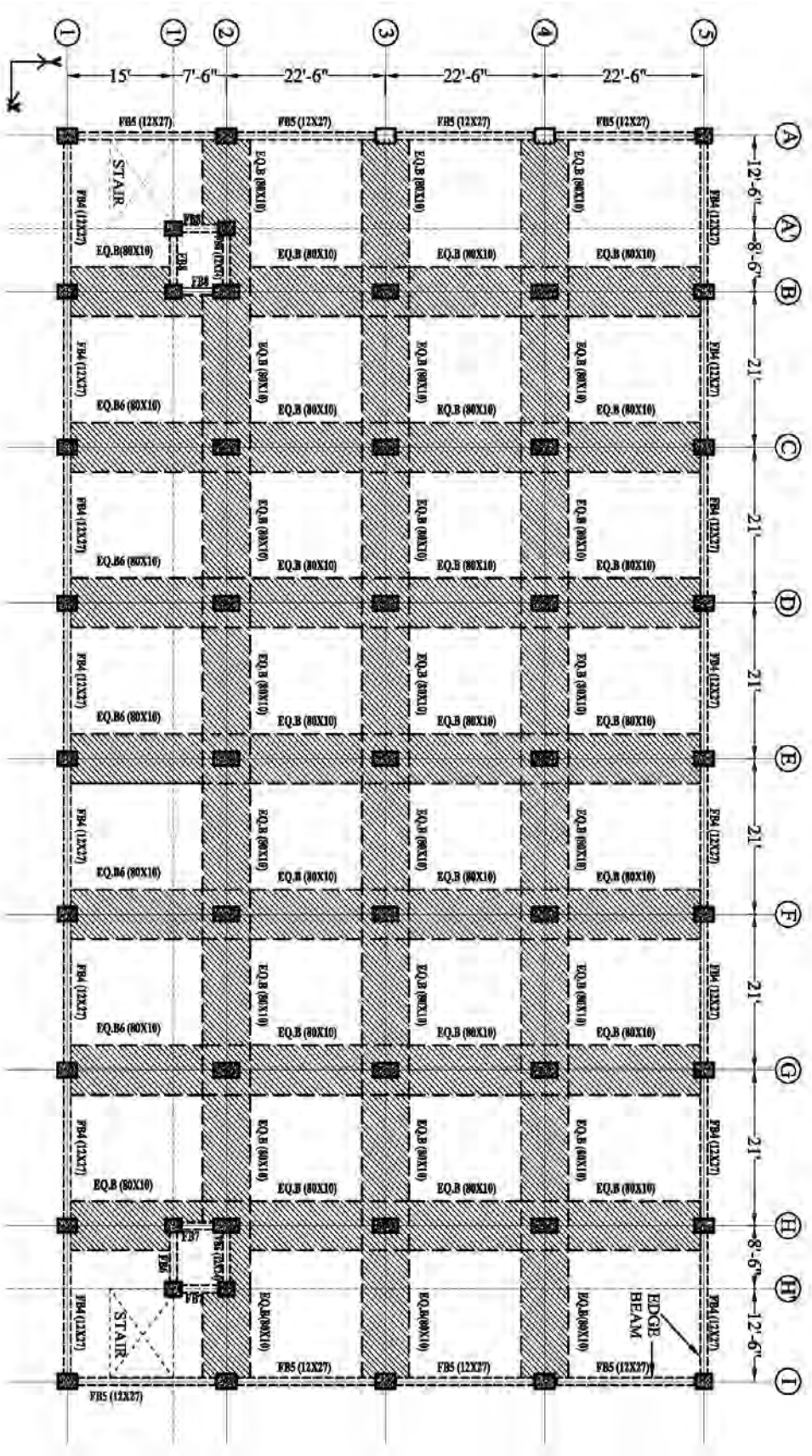

Figure B-3.2: Model 2 effective beam width (eqt to flat plate) layout (F6-Roof)

Annexure B2: Effective Beam Width (Equivalent to flat plate) Details of Model 2

Table B-3.1: Model 2 effective beam width (eq^t to flat plate) details

Story: 1F to 5F				
Frame Property	**Top Area I-end**	**Top Area J-end**	**Bottom Area I-end**	**Bottom Area J-end**
EQ.B80X10	16 mm @ 5 in c/c"	16 mm @ 5 in c/c"	12 mm @ 5 in c/c	12 mm @ 5 in c/c

NOTE: Co-ordinate of J-end > I-end in Global X, Y Co-ordinate System at the plan of a member

Annexure B3: Modeling Parameters and Acceptance Criteria for Non-Linear Static Analysis.

Table B-3.2: Modeling parameters and numerical acceptance criteria for nonlinear procedures—reinforced concrete beams

Conditions			Modeling Parameters[a]			Acceptance Criteria[a]		
			Plastic Rotation Angle (Radians)		Residual Strength Ratio	Plastic Rotations Angle (Radians)		
						Performance Level		
			a	b	c	IO	LS	CP
Condition i. Beams controlled by flexure[b]								
(ρ-ρ')/ρbal	Transverse Reinforcement[c]	$V/(b_w d\sqrt{fc'})$[d]						
≤ 0.0	C	≤ 3 (0.25)	0.025	0.050	0.20	0.010	0.025	0.050
≤ 0.0	C	≥ 6 (0.5)	0.020	0.040	0.20	0.005	0.020	0.040
≥ 0.5	C	≤ 3 (0.25)	0.020	0.030	0.20	0.005	0.020	0.030
≥ 0.5	C	≥ 6 (0.5)	0.015	0.020	0.20	0.005	0.015	0.020
≤ 0.0	NC	≤ 3 (0.25)	0.020	0.030	0.20	0.005	0.020	0.030
≤ 0.0	NC	≥ 6 (0.5)	0.010	0.015	0.20	0.002	0.010	0.015
≥ 0.5	NC	≤ 3 (0.25)	0.010	0.015	0.20	0.005	0.010	0.015
≥ 0.5	NC	≥ 6 (0.5)	0.005	0.010	0.20	0.002	0.005	0.010
Condition ii. Beams controlled by shear[b]								
Stirrup spacing ≤ d /2			0.003	0.020	0.20	0.0015	0.010	0.020
Stirrup spacing ≥ d /2			0.003	0.010	0.20	0.0015	0.005	0.010
Condition iii. Beams controlled by inadequate development or splicing along the span[b]								
Stirrup spacing ≤ d /2			0.003	0.020	0.00	0.0015	0.010	0.020
Stirrup spacing ≥ d /2			0.003	0.010	0.00	0.0015	0.005	0.010
Condition iv. Beams controlled by inadequate embedment into beam–column joint[b]								
			0.015	0.030	0.20	0.010	0.0200	0.030

NOTE: fc′ in lb/in.^{2} (MPa) units.

[a]Values between those listed in the table should be determined by linear interpolation.

[b]Where more than one of conditions i, ii, iii, and iv occur for a given component, use the minimum appropriate numerical value from the table.

[c]"C" and "NC" are abbreviations for conforming and nonconforming transverse reinforcement, respectively. Transverse reinforcement is conforming if, within the flexural plastic hinge region, hoops are spaced at ≤ d/3, and if, for components of moderate and high ductility demand, the strength provided by the hoops (Vs) is at least 3/4 of the design shear. Otherwise, the transverse reinforcement is considered nonconforming.

[d]V is the design shear force from NSP or NDP.

Table B-3.3: Modeling parameters and numerical acceptance criteria for nonlinear procedures—reinforced concrete columns

Conditions			Modeling Parameters[a]			Acceptance Criteria[a]		
			Plastic Rotation Angle (Radians)		Residual Strength Ratio	Plastic Rotations Angle (Radians)		
						Performance Level		
			a	b	c	IO	LS	CP
Condition i[b]								
$P/(A_g f'_c)$[c]	$\rho=(A_v/b_w s)$							
≤ 0.1	≥ 0.006		0.035	0.060	0.20	0.005	0.045	0.060
≥ 0.6	≥ 0.006		0.010	0.100	0.00	0.003	0.009	0.010
≤ 0.1	= 0.002		0.027	0.034	0.20	0.005	0.027	0.034
≥ 0.6	= 0.002		0.005	0.005	0.00	0.002	0.004	0.005
Condition ii[b]								
$P/(A_g f'_c)$[c]	$\rho=(A_v/b_w s)$	$V/(b_w d\sqrt{fc'})$[d]						
≤ 0.1	≥ 0.006	≤ 3 (0.25)	0.032	0.060	0.20	0.005	0.045	0.060
≤ 0.1	≥ 0.006	≥ 6 (0.5)	0.025	0.060	0.20	0.005	0.045	0.060
≥ 0.6	≥ 0.006	≤ 3 (0.25)	0.010	0.010	0.00	0.003	0.009	0.010
≥ 0.6	≥ 0.006	≥ 6 (0.5)	0.008	0.008	0.00	0.003	0.007	0.008
≤ 0.1	≤ 0.0005	≤ 3 (0.25)	0.012	0.012	0.20	0.005	0.010	0.012
≤ 0.1	≤ 0.0005	≥ 6 (0.5)	0.006	0.006	0.20	0.004	0.005	0.006
≥ 0.6	≤ 0.0005	≤ 3 (0.25)	0.004	0.004	0.00	0.002	0.003	0.004
≥ 0.6	≤ 0.0005	≥ 6 (0.5)	0.000	0.000	0.00	0.000	0.000	0.000
Condition iii[b]								
$P/(A_g f'_c)$[c]	$\rho=(A_v/b_w s)$							
≤ 0.1	≥ 0.006		0.000	0.060	0.00	0.000	0.045	0.060
≥ 0.6	≥ 0.006		0.000	0.008	0.00	0.000	0.007	0.008
≤ 0.1	≤ 0.0005		0.000	0.006	0.00	0.000	0.005	0.006
≥ 0.6	≤ 0.0005		0.000	0.000	0.00	0.000	0.000	0.000
Condition iv. Columns controlled by inadequate development or splicing along the clear height[b]								
$P/(A_g f'_c)$[c]	$\rho=(A_v/b_w s)$							
≤ 0.1	≥ 0.006		0.000	0.060	0.40	0.000	0.005	0.060
≥ 0.6	≥ 0.006		0.000	0.008	0.40	0.000	0.007	0.008
≤ 0.1	≤ 0.0005		0.000	0.006	0.20	0.000	0.005	0.006
≥ 0.6	≤ 0.0005		0.000	0.000	0.00	0.000	0.000	0.000

NOTE: fc′ in lb/in.^{2} (MPa) units.

[a]Values between those listed in the table should be determined by linear interpolation.

[b]Refer to Section 10.4.2.2.2 of ASCE 41-13 for definition of conditions i, ii, and iii. Columns are considered to be controlled by inadequate development or splices where the calculated steel stress at the splice exceeds the steel stress specified by Eq.(10-2) of ASCE 41-13. Where more than one of conditions i, ii, iii, and iv occurs for a given component, use the minimum appropriate numerical value from the table.

[c]Where P > 0.7Ag f'c, the plastic rotation angles should be taken as zero for all performance levels unless the column has transverse reinforcement consisting of hoops with 135-degree hooks spaced at ≤ d/3 and the strength provided by the hoops (Vs) is at least 3/4 of the design shear. Axial load P should be based
on the maximum expected axial loads caused by gravity and earthquake loads.
[d]V is the design shear force from NSP or NDP.

Table B-3.4: Modeling parameters and numerical acceptance criteria for nonlinear procedures—two-way slabs and slab–column connections

Conditions		Modeling Parameters[a]			Acceptance Criteria[a]		
		Plastic Rotation Angle (Radians)		Residual Strength Ratio	Plastic Rotations Angle (Radians)		
					Performance Level		
						Secondary	
		a	b	c	IO	LS	CP
Condition i. Reinforced concrete slab–column connections[b]							
$(V_g/V_o)^c$	Continuity Reinforcement[d]						
0.0	Yes	0.035	0.050	0.20	0.01	0.035	0.050
0.2	Yes	0.030	0.040	0.20	0.01	0.030	0.040
0.4	Yes	0.020	0.030	0.20	0.00	0.020	0.030
≥ 0.6	Yes	0.000	0.020	0.00	0.00	0.000	0.020
0.0	No	0.025	0.025	0.00	0.01	0.020	0.025
0.2	No	0.020	0.020	0.00	0.01	0.015	0.020
0.4	No	0.010	0.010	0.00	0.00	0.008	0.010
0.6	No	0.000	0.000	0.00	0.00	0.000	0.000
≥ 0.6	No	0.000	0.000	0.00	__e	__e	__e
Condition ii. Posttensioned slab–column connections[b]							
$(V_g/V_o)^c$	Continuity Reinforcement[d]						
0.0	Yes	0.035	0.050	0.40	0.01	0.035	0.050
0.6	Yes	0.005	0.030	0.20	0.00	0.025	0.030
≥ 0.6	Yes	0.000	0.020	0.20	0.00	0.015	0.020
0.0	No	0.025	0.025	0.00	0.01	0.020	0.025
0.6	No	0.000	0.000	0.00	0.00	0.000	0.000
≥ 0.6	No	0.000	0.000	0.00	__e	__e	__e
Condition iii. Slabs controlled by inadequate development or splicing along the span[b]							
		0.000	0.020	0.00	0.00	0.010	0.020
Condition iv. Slabs controlled by inadequate embedment into slab–column joint[b]							
		0.015	0.030	0.20	0.01	0.020	0.030

[a]Values between those listed in the table should be determined by linear interpolation.

[b]Where more than one of conditions i, ii, iii, and iv occur for a given component, use the minimum appropriate numerical value from the table.
[c]Vg is the gravity shear acting on the slab critical section as defined by ACI 318, and Vo is the direct punching shear strength as defined by ACI 318.
[d]"Yes" should be used where the area of effectively continuous main bottom bars passing through the column cage in each direction is greater than or equal to 0.5 Vg /(ϕfy). Where the slab is posttensioned, "Yes" should be used where at least one of the posttensioning tendons in each direction passes through the column cage. Otherwise, "No" should be used.
[e]Action should be treated as force controlled. Action should be treated as force controlled